UNIVERSITÀ DEGLI STUDI DI TRIESTE

XXX CICLO DEL DOTTORATO DI RICERCA IN NANOTECNOLOGIE

TARGETING A SOLITARY FIBROUS TUMOR CELL LINE USING A NOVEL NANOMICELLE FORMULATION TO ENHANCE CURCUMIN ANTITUMOR ACTIVITY

Settore scientifico-disciplinare: BIO/13

DOTTORANDA
SILVIA BRICH

COORDINATORE
PROF. LUCIA PASQUATO

SUPERVISORE DI TESI
PROF. SABRINA PRICL

TUTORE DI TESI
DOTT.SSA ELENA TAMBORINI

ANNO ACCADEMICO 2016/2017

Index

Abstract

Various evidence has shown that curcumin, a natural compound, can induce increased sensitivity to chemotherapy, inhibit tumor growth, metastasis formation and Epithelial-Mesenchymal Transition (EMT).

A solitary fibrous tumor (SFT) cell line treated with curcumin (50μMol) showed a decreased expression of EMT markers. However, this concentration is incompatible with its *in vivo* use. Therefore, it is thought of use curcumin encapsulated by nanomicelles that can deliver curcumin directly to the cells. Nanomicelle treatments, named C_{16}-DAPMA, C_{16}-SPD and C_{16}-SPM, analyzed by means MTT, showed their cytotoxic potential using a significantly lower curcumin concentrations (500nM, 1μM). Moreover, performing biochemical analyses, it was possible to detect a reduction in the expression of EMT-associated markers, particularly significant after treatment with C_{16}-SPD. In addition, invasion assay shed light on the invasive potential of SFT cells that, after treatment with nanomicelles, resulted significantly lower than the untreated control.

Due to its low toxicity, curcumin could be administered in combination with other drugs, such as histonedeacetylase inhibitors (HDACi), which can inhibit migration and tumor growth. Combinations with HDACis and nanomicelles resulted in a decreased expression of HDAC2, especially after treatment with C_{16}-DAPMA, while C_{16}-SPD significantly reduced the expression of metalloproteinase 2(MMP2). In addition, immunofluorescence analysis after HDACi treatments, revealed a loss of spindle-fused SFT tumor cell structure in favor of a more epithelioid-like.

Photodynamic Therapy (PDT) is an innovative minimally invasive technique, which is not subject to resistance, easily manageable, selective, does not involve systemic toxicity such as standard chemotherapy and does not induce resistance phenomena. Recent studies also report that the cytotoxic effect obtained using low concentrations of curcumin, administered in combination with blue light (laser) on tumor cell lines, was particularly significant using nanomicelle-encapsulated with curcumin. In line with studies already published, preliminary MTT analyses, performed on SFT cells irradiated with blue laser and treated with nanomicelles loaded with curcumin, showed a significant reduction in tumor cell viability.

1. Introduction

1.1 Mechanism of carcinogenesis

Cancer was first described by Greek Hippocrates who used the Greek word carcinos (crab or crayfish) to describe it due to its crab-like tenacity. Cancer consists of a variety of diseases characterized by the abnormal development of cells that are uncontrollably divided and capable of infiltrating and destroying normal body tissues. The World Health Organization (WHO) states cancer to be a leading cause of death worldwide accounting for 7.6 millions death (around 13% of all death) and is projected rising to over 11 millions in 2030. The major challenge in cancer treatment is to understand how to block the spread of metastatic cells and to confirm the existence of cancer stem cells that survive all the therapies currently in use, which are involved in metastasis formation and recurrences. As described by Hanahan and Weinberg in 2000, there are six essential physiological alterations, which instruct malignant tumor growth:

Sustaining proliferative signaling. Growth factors are responsible for the proper propagation of normal cells. On the other hand, this dependency is reduced in tumor cells which may send signals to stimulate normal cells within the surrounding stroma to supply cancer cells with growth factors by overexpressing them.

Evading growth suppressor. In a physiological scenario multiple anti-proliferative signals, such as p53 and c-myc, operate to maintain cellular quiescence and tissue homeostasis.

Resisting cell death. Cancer cell are able to evolve many strategies to limit or circumvent apoptosis. Most common is the loss of p53 tumor suppressor function. Tumor cells may increase the expression of anti-

apoptotic factors (Bcl-2, Bcl-xL) and downregulate pro-apoptotic regulators (Bax, Bim, Puma).

Enabling replicative immortality. Untransformed cells are limited in their replicative potential by the length of their telomers.

Sustained angiogenesis. Tumor can activate the angiogenic switch by changing the balance of angiogenesis inducers such as VEGFs and inhibitors like thrombospondin-1.

Tissue invasion and metastasis. Tumor cells can degrade adherens and tight junction proteins. Consequently, cell-cell contact is lost and cancer cells can migrate and metastasize to the distant organs. Migration is possible thanks to activated proteases (such as metalloproteases), which degrade the surrounding extracellular matrix.

In 2011 Hanahan and Weinberg added two more hallmarks:

Reprogramming energy metabolism. In the tumor environment characterized by hypoxia, only cancer cells with altered metabolism can survive and proliferate (Semenza, 2010). Some tumors display two different subpopulations of cancer cells, which differ in their energy-generating pathway. One population consist of glucose dependent cells that secrete lactate, which in turn is used by the other population as energy source (Semenza, 2008).

Evading immune destruction. Immune surveillance is responsible for recognizing and eliminating the majority of cancer cells. By contrast, tumor cell have to omit themselves from immune system: TGF-β is secreted in order to inhibit the anti-tumoral activity of cytotoxic $CD8^+$ T-cell (Thomas and Massague, 2005).

1.2 Epithelial-Mesenchymal Transition (EMT)

To gain migratory and invasive properties, cancer cells undergo EMT, which is a basic cellular process in which epithelial cells lose their epithelial properties, such as polarized organization, cell-cell tight junctions, changes in cytoskeleton and cell shape, and acquire mesenchymal features. EMT can be classified in three different subtypes:

- Type 1 EMT is associated with implantation and embryonic gastrulation and give rise to mesoderm
- Type 2 EMT is involved in wound healing, inflammation and fibrosis
- Type 3 EMT comprises the transformation of epithelium associated with organs into cancer cells which later leads to invasion and metastasis

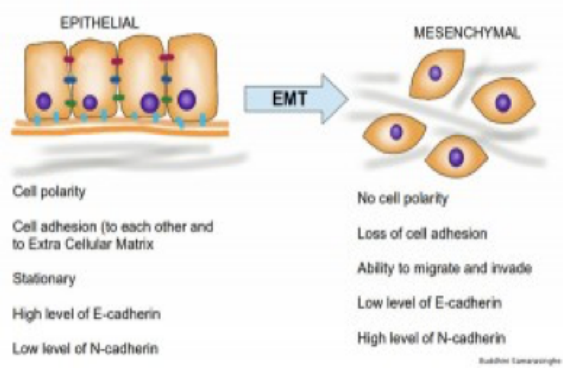

Figure 1. Epithelial to Mesenchymal Transition, with associated characteristics of the two cell types (Credit:The Hallmarks of Cancer 6: Tissue Invasion and Metastasis, Buddhini Samarasinghe).

1.2.1 EMT and E-cadherin

E-cadherin is part of the cadherins family; it is mainly expressed in the epithelium as it is essential and necessary for cell-cell adhesion and its cytoplasmic domain is related to the cytoskeleton (via β and γ cadherins).

The loss of E-cadherin (in this context acting as tumor-suppressor) during the EMT process involves the reduction of cell polarity and also cell-cell adhesions, which allowed the individual cells to stay in contact and resist mobility (Hood and Cheresh, 2002). Indeed, E-cadherin results silenced in many carcinomas and its activation is sufficient to reduce the aggressiveness of tumor cells. Although it is downregulated during EMT, E-cadherin expression is restored in metastatic cells, especially during intravasation and seeding of metastatic cells. Moreover, repression of E-cadherin may be induced by the activation of repressor such as Snail, Zeb1 and Zeb2 (Thiery and Morgan, 2004).

1.2.2 EMT and Vimentin

Traditionally, vimentin, which is expressed in the cytoplasm of mesenchymal cells during their developmental stages, is thought to play a role in the cytoarchitecture and tissues integrity. Moreover, vimentin is involved in the formation of complexes with cell signalling molecules and other adaptor proteins, mediating several pathways and cellular processes important in EMT and tumor progression (Vuoriluoto et al, 2011). Vimentin is also associated with cancer invasion and poor prognosis in several tumor histotypes, including breast, prostate, lung cancer and melanoma (Lehtinen et al, 2013) and serves as a potential target for cancer therapy. Vimentin organization within the cell has pivotal effects on invadopodia and lamellopodia formation during cancer invasion and migration: invadopodia allow the cell to invade the surrounding tissues, then, metastatic cells will form lamellopodia which is the leading edge of the cells (Schoumacher et al, 2010).

During transformation, focal adhesion stability and cytoskeleton distribution are impared. Changes in cytoskeleton organization and focal adhesion turnover are correlated to the changes in cancer cells motility and invasiveness during tumorigenesis.

The Wnt signalling pathway is a conservative EMT-related pathway which is important in the development of several tumors. The β-catenin is the Wnt signalling pathway, which facilitates the transfer of molecules from the cytoplasm into the nucleus in the Wnt pathway.

1.2.3 EMT and transcription factors

Genes that keep epithelial polarity and organization, such as E-cadherin, are under control of potent transcription factors acting as repressors like Snail1/2, Slug, Zeb1/2 and Twist (Zhang et al, 2008). Zeb1 and Zeb2 are subjected to post-translation regulation by Polycomb repressive complex 2 (PRC2), which impairs their repressor activities. Moreover, IDs transcription factors are usually suppressed during EMT by rapid activation of expression of the transcription repressor ATF3 by TGF-β. Loss of Id1 expression is associated with a decrease in E-cadherin expression (Kang et al, 2003).

1.2.4 EMT and metastasis

Metastasis is the major cause of death among cancer patients. Indeed, this process involved the spread of cancer cells from its primary site to distant areas in the body. Cancer are able to invade blood vessels and lymph nodes, finding their way into the bloodstream. Metastasis is a multistage process that consists of i) local invasion, ii) intravasation into the circulation, iii) survival and transport in the circulation, iv) extravasation from the

bloodstream and v) growth in the metastatic site (Condeelis and Segall, 2003). Changes in cellular phenotype such as adhesion molecules expression, antiapoptotic capability, expression of metalloproteases (MMP) in order to invade the extracellular matrix (ECM) are required for metastatic progression. Cancer cells use the lymphatic drainage system to escape from the tumor primary site: this is why for many cancer histotypes lymph nodes are surgically removed to investigate if cancer has spread and oncologists can use this information to determine the "stage" of the disease.

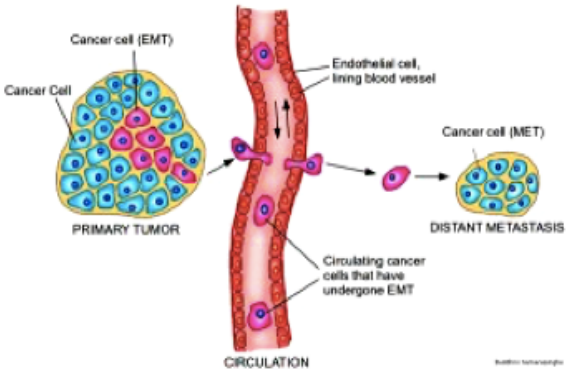

Figure 2. EMT and Metastasis. A tumor will have a population of cells that have undergone EMT. These cells are now able to migrate freely, by entering the circulatory system. Upon reaching their final destination, the cells undergo the reverse MET program and form a secondary tumor at a distant site (Credit: The Hallmarks of Cancer 6: Tissue Invasion and Metastasis, Buddhini Samarasinghe).

1.2.5 EMT and migration

Epithelial, stromal and neuronal cells migrate limited during morphogenesis ceasing with terminal differentiation toward intact tissue to become reactivated only for tissue regeneration or neoplastic processes. For other cell types, such as leukocytes, migration is integral to their function and it is maintained throughout their lifespan. Many molecules are essential for controlling migration: integrin family mediate interaction with the ECM,

MMPs are responsible for ECM degradation, cadherins set stable intercellular adhesions and signaling proteins which regulate the actin cytoskeleton (Friedl and Wolf, 2010).

1.2.6 EMT and cancer stem cell

The tumor mass displays functional heterogeneity with different morphology, differentiation grade, proliferation rate and invasiveness. In literature, many authors reported that the ability of a tumor to propagate and proliferate relies on a small cellular subpopulation characterized by stem-like properties, called cancer stem cells (CSCs). As reported for normal stem cells, CSCs have the ability to perpetually self-renew and produce tumors composed of cells with different features. CSCs show active signaling pathway shared with cancer cells, such as Wnt, Shh and Notch. Moreover, ineffectiveness of chemotherapy to destroy these cells is due to the presence of an ATP-binding cassette transporter, which remove drugs from the cell (Dean et al, 2005). Normal stem cells are under metabolic control and can divide only under specific condition, on the other hand, CSCs have these kind of control anymore and, like cancer cells, they are also able to resist apoptosis. Some authors reported that CSCs may arise from the transformation of their normal counterpart, but, most recent studies suggest that CSCs may originate from fully differentiated cells though an adaptative trans-differentiation program such as EMT (Vesuna et al, 2009). In the EMT context, the trans-differentiation process is considered as a biological event that convert differentiated epithelial cells into CSCs. The balance between these cellular sub-populations is considered a highly dynamic process with important repercussion on therapeutic approaches,

complete eradication of the primary tumor and prevents recurrences (Gupta et al, 2009).

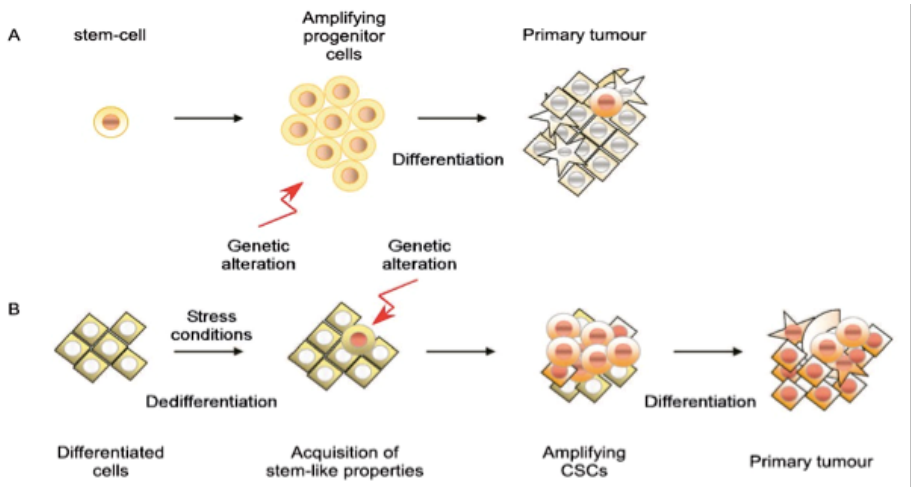

Figure 3. (A) The "cancer stem-cell theory" is based on the assumption that during tissue regeneration, the amplification of progenitor cells opens a window of time suitable for accumulating genetic alterations, leading to the emergence of cancer cell-stems (CSCs). CSCs would thus initiate and sustain tumour growth. (B) Alternatively, under stress conditions, fully differentiated cells reacquire stem-like properties, including self-renewal. This gain of function is influenced by cellular intrinsic properties as well as micro-environmental conditions. These cells could potentially be prone to transformation and give rise to CSCs. Both models are not exclusive. CSCs and cell dedifferentiation would thus constitute the initial and secondary tumour drivers, respectively (Credit:Transcriptional control of Epithelial to Mesenchymal Transition by Regulatory Factors and Epigenetic Mechanisms, Neha Tiwari,thesis, Basel, 2011).

1.2.7 EMT and miRNAs

miRNAs are highly conserved, small non-coding RNA molecules which regulate about the 30% of human genes expression at post-transcriptional level by interacting with specific target mRNA. They are involved in the control of cell differentiation, proliferation, angiogenesis, cell cycle and apoptosis (Esquela-Kerscher and Slack, 2006). miRNAs can act as oncogenes as well as tumor-suppressors: p53 and Myc are targeted by miRNAs and they are involved in tumorigenesis, tumor growth, tumor

angiogenesis and metastasis (Le et al, 2009). miR200 can inhibit metastasis by downregulating Zeb1/2 which in turn, by a double-negative feedback, transcriptionally repress miR200. This directly affects the EMT status of the cancer cells and their migratory potential (Wellner et al, 2009).

1.2.8 EMT and Polycomb

Polycomb comprise Polycomb repressive complex 1 (PRC1) and Polycomb repressive complex 2 (PRC2). Ezh2 is a catalytic subunit of PRC2, particularly studied in cancer , which represent one of the first observed molecules significantly associated with EMT. Indeed, Ezh2 is reported to be overexpressed in metastatic cancer, such as prostate cancer (Berezovska et al, 2006). Moreover, Ezh2 could target and repress E-cadherin expression: this Ezh2-mediated suppression can be inhibited by the histone deacetylase (HDAC) inhibitor SAHA (Vorinostat) (Rhodes et al, 2003). Moreover, Zeb2 and integrinβ4 are PRC2 target: the expression of integrinβ4 is lost during EMT and its loss correlates with active/repressive modification of histone H3. Indeed, reversal of EMT (also called Mesenchymal-Epithelial transition, MET) leads to re-expression of integrinβ4: this evidence underlines the dynamic nature of epigenetic regulation during fate changes of epithelial cell (Yang et al, 2009).

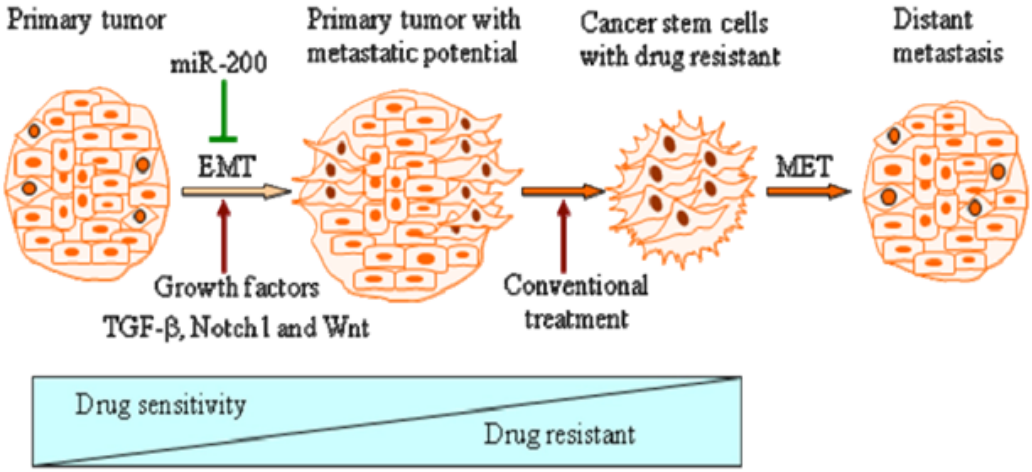

Figure 4. Induction of epithelial-to-mesenchymal transition (EMT)-phenotypic cells produces cancer stem-like cells with drug-resistant characteristics. Growth factors, including FGF, EGF, PDGF-B and PDGF-D as well as factors such as TGF-β, Notch-1 and Wnt, can induce EMT, while miR-200 family inhibits EMT by regulating the expression of transcription repressors ZEB1 and ZEB2. EMT-phenotypic cells acquire stem-like cell signatures characterized by increased metastatic capacity, self-renewal ability and acquired drug resistance. These cells metastasize to distant sites and undergo MET to produce metastatic tumors that are phenotypically similar to the primary tumor (Credit: Cancer Stem Cells and Epithelial-to-Mesenchymal Transition (EMT)-Phenotypic Cells: Are They Cousins or Twins? Dejuan Kong, Yiwei Li, Zhiwei Wang and Fazlul H. Sarkar Cancers 2011, 3(1), 716-729).

1.3 Curcumin

Curcumin ($C_{21}H_{20}O_6$), a hydrophobic polyphenol (mol mass 368.63) derived from the rhizome of the herb Curcuma longa, which belongs to family Zingiberaceae. It has been used for centuries in Chinese traditional and Indian medicine. Traditionally, turmeric has been used as anti-inflammatory, anti-oxidant, anti-microbial, anti-carcinogenic agent. Additionally, the hepato- and nephro-protective, thrombosis suppressing, myocardial infarction protective, hypoglycemic and anti-rheumatic effects of curcumin are also well established (Anand et al, 2007). Not only the FDA in the USA and the Natural Health Products Directorate of Canada, but also by the

Food and Agriculture Organization/World Health Organization (FAO/WHO) has declared turmeric products as safe.

Figure 5. Curcumin and its chemical structure.

Chemical structure of curcumin dictate its biophysical and biochemical activities: curcumin can interact with a large number of molecules through non-covalent and covalent binding. Curcumin is insoluble in water, but it can be dissolved in dimethylsulfoxide (DMSO), acetone and ethanol. In the last ten years, many in vitro and in vivo studies have been performed with the aim to establish the mechanism of action of curcumin and its activities against several pathologies (Schneider et al, 2015). Firstly, curcumin bioavailability has to be determined. The first study performed to determine the biological availability was carried out by Wahlstrom and Blennow in 1978, where curcumin was administered to Sprague-Dawley rats: only a low dose of curcumin was measured in rats blood plasma. Later studies with rats demonstrated that oral bioavailability of curcumin was around 1%, when 3600 to 12000 mg were administered for achieving any beneficial effects (Yang et al, 2007). In relation with the administration form, encapsulation in liposomes, polymeric nanoparticles, cyclodextrin encapsulation, lipid complexes have been investigated. All of them have increased the activity

and bioavailability of curcumin and improved the beneficial effect of curcumin against some pathology such as cancer (Prasad et al, 2014). In particular, many studies have investigated the capacity of curcumin as an adjuvant in anti-tumor therapy or reducing adverse side effects associated with the treatment, rather than as chemotherapeutic agent itself.

1.3.1 Curcumin and epigenetics

Recently, natural compounds as curcumin have been shown to alter epigenetic mechanisms, which may lead to increased sensitivity of cancer cells to standard chemotherapy agents and, thus, inhibition of tumor growth and metastasis formation. The above-mentioned epigenetic mechanisms include changes in DNA methylation, histone modifications and altered miRNA expression (Yoo and Jones, 2006).

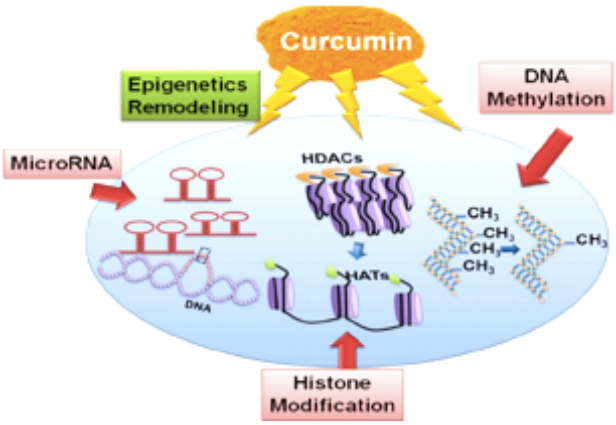

Figure 6. Curcumin-mediated epigenetic mechanisms involving DNA methylation, histone modifications and miRNA based epigenetic processes (Credit: Anuradha Kalani, Pradip K Kamat, Komal Kalani, and Neetu Tyagi. Epigenetic impact of curcumin on stroke prevention. Metab Brain Dis. 2015 Apr; 30(2): 427–435).

Histone acetyltransferases (HATs) and HDACs abnormal activity has been associated with the pathogenesis of cancer. In particular, HDAC inhibitors

are being explored as cancer therapeutic compounds because of their ability to alter different cellular processes (Davis and Ross, 2007). The transcription factor Snail recruits HDAC1 and HDAC2 to the E-cadherin promoter to repress its expression (Peinado et al, 2004). Downregulation or loss of function of E-cadherin has been implicated in the acquisition of invasive potential by carcinomas, and so the aberrant recruitment of HDACs to this promoter may have a crucial role in tumor invasion and metastasis. On the other hand, HDAC2 could be restored after curcumin treatment (Meja et al, 2008): this underlines the different effect of curcumin on different HDAC enzymes. Thus, further researches are required in order to better understand curcumin behaviour on HDACs expression. Moreover, the investigation of curcumin effects on DNA methylation suggests that curcumin could covalently block DNA methyltransferase to exert its inhibitory action on DNA methylation. By contrast, a more recent study (Medina-Franco et al, 2010) showed no curcumin-dependent demethylation: also in this case more research is urgently needed. It is known that curcumin can regulate the expression of genes which are strictly involved in signalling pathways inside the cytoplasm, which are in turn regulated by specific miRNAs. Some of them could regulate the formation of CSCs and also sustain the EMT, making these cancer cells drug resistant (Li et al, 2010). Furthermore, miR200 family has been reported to inhibit EMT, maintaining the epithelial phenotype thanks to the repression of ZEB1 and ZEB2 (Korpal et al,2008). In contrast, miR21, which is an oncomiR overexpressed by tumors, could promote cancer progression and distal metastasis. As reported in literature, curcumin treatment could reduce miR21 promoter activity and expression in primary tumors by inhibiting AP-1 binding to the promoter and finally induce tumor suppressions expression (Mudduluru et al, 2001).

1.3.2 Curcumin and EMT

Recent studies showed that curcumin could suppress EMT and metastasis via FAK-pathway inhibition and E-cadherin upregulation in colorectal and liver cancers (Duan et al, 2014). Curcumin inhibits cancer cell invasion by suppressing NF-kB activation. NF-kB is a structurally conserved family of dimeric transcription factors, which play pivotal roles in both promoting and maintaining an invasive phenotype. NF-kB was identified as the upstream regulator of Snail expression during EMT in human mammary epithelial MCF10A cells. The NF-kB signaling pathway is involved in Snail-mediated EMT, involving an increased expression of NF-kBp65 and Snail proteins, accompanied by a decreased expression of E-cadherin: these effects were blocked by curcumin 20μM for 24 hours treatment. These results underline the ability of curcumin to inhibit cancer invasiveness associated with the EMT process, by decreasing the expression of the important downstream EMT markers (Huang et al, 2012). Moreover, Lee and colleagues (2015) investigated anti-invasive effect of curcumin on EMT markers expression and also MMP-2 as invasiveness hallmark. The authors showed that anti-proliferative effect of curcumin was able to cause more than a 50% decrease in cell viability after 24 hours of 15μM treatment when compared with the untreated sample. As reported by some studies in literature, curcumin also reduced the level of β-catenin gene expression significantly; thus, it has anti-tumor effects though the inhibition of the Wnt signalling pathway (Zhang et al, 2016).

1.3.3 Curcumin and EZH2

Polycomb group proteins, which are involved in gene silencing through post-traslational modification of histone proteins, include two polycomb repressive complexes: Polycomb Repressive complex (PRC) 1 and PRC2.

PRC1 consists of Bmi, Ring1b, CBX4 and PHC subunits; in contrast, PRC2 consists primarily of enhancer of zeste homolog 2 (EZH2), EED, SUZ12 and catalyses the methylation of histone H3 lysine27 (H3K27) to generate H3K27me3. EZH2, the catalytic subunit of PRC2, has been demonstrated to be essential for cancer initiation, development, progression, metastasis and also drug resistance, making EZH2 a promising drug target (Kim and Roberts, 2016). Indeed, EZH2 is frequently overexpressed in many cancer types and its regulators are also critical for cell proliferation, tumorigenesis and stem cell maintenance. Myc binds to EZH2 promoter and activates its transcription. Moreover, Myc upregulates EZH2 expression which in turn can positively regulates c-Myc expression. SOX4, a regulator of stem cells, can directly regulate the expression of EZH2 mRNA, which play a pivotal role in SOX4-mediated EMT. Multiple transcription factors, such as Ying Yang 1 (YY1), interact with PRC2 to recruit it to specific loci cancer related. The interaction between EZH2 and YY1 results in a repression of the tumor suppressor APC, promoting cell growth. Another partner of EZH2, Snail, could form a complex with it via HDAC1/2 and recruit it to E-cadherin promoter in order to suppress E-cadherin expression, soliciting EMT process. Moreover, noncoding RNAs (ncRNAs) interact with EZH2: overexpression of HOTAIR, a described ncRNA, enhances cancer cell invasion and metastasis , while its loss reduces cancer progression. In many cancer types, EZH2 overexpression correlates with higher proliferation, aggressive behavior of cancer cells and poor prognosis. Furthermore, EZH2 could act as a tumor suppressor: inactivating mutation of EZH2 are reported for patient with myeloid malignancies (Makishima et al, 2010). Together, these results suggest that the role of EZH2 is cell-dependent, although it functions as an oncogenic factor in many solid tumors. Given EZH2's central role in proliferation, migration, invasion and stem cell properties, it is

considered a potential drug target. In addiction to DZNep, GSK126 and EPZ6438 (highly selective small molecules inhibitors against EZH2) other compounds have been reported to downregulate EZH2 expression, such as curcumin (Hua et al, 2010; Yamaguchi and Hung, 2014). Hua and colleagues reported that curcumin inhibited cellular proliferation (cells stalled in G_1 phase) and induced the downregulation of EZH2 protein in MDA-MB-435 cells in a dose and time dependent manner, without any change in mRNA levels.

1.3.4 Curcumin and CSCs

Increasing evidence suggests that many cancer types, characterized by chemo-radiation resistance, could be composed of a subset of cancer cells, termed CSCs, with peculiar features, which are distinct from the bulk of the tumor cells. CSCs show tumor initiating potential and can be derived from either self-renewing normal stem cells or from progenitor cells that have acquire the self-renewal ability due to mutation or dedifferentiation of mature cancer cells. CSCs are not synonymous with normal stem cells. Indeed, CSCs can form tumors when transplanted into animals (but normal stem cells cannot) due to their tumorigenicity, they can divide asymmetrically generating a subpopulation of non-tumorigenic cells and show self-renewal capacity and specific markers which separate them from the non-stem cells. Although they represent only a small number in a cancer cells mass (<1%), their responsibility for tumor recurrences, therapy resistance and metastasis, make them a crucial target in the cancer treatment. As reported in literature, in the last few years, curcumin, and its analogues, could provide an effective treatment either as a stand-alone or in combination with other chemotherapeutic drugs, influencing (directly or

indirectly) the CSC self-renewal pathways (Wnt/β-catenin; Shh and Notch) (Ramasamy et al, 2015). Published studies have reported no toxicity with moderate dose of curcumin over few months, showing beneficial effects against different pre-malignant or malignant diseases (Kanai et al, 2013). Moreover, treatments with novel formulations of curcumin and nanotechnology approaches (diflourinated-curcumin, GO-Y030 and curcumin encapsulated in CSO-SA micelles) underline their major efficacy rather than the natural curcumin. They could inhibit colorectal CSCs maybe due to their superior stability, better accumulation and enhanced therapeutic effect in vivo (Ramasamy et al, 2015). Thus, curcumin treatment allows to administer a lower dose of the chemotherapeutic agent, reducing drug toxicity and side effects.

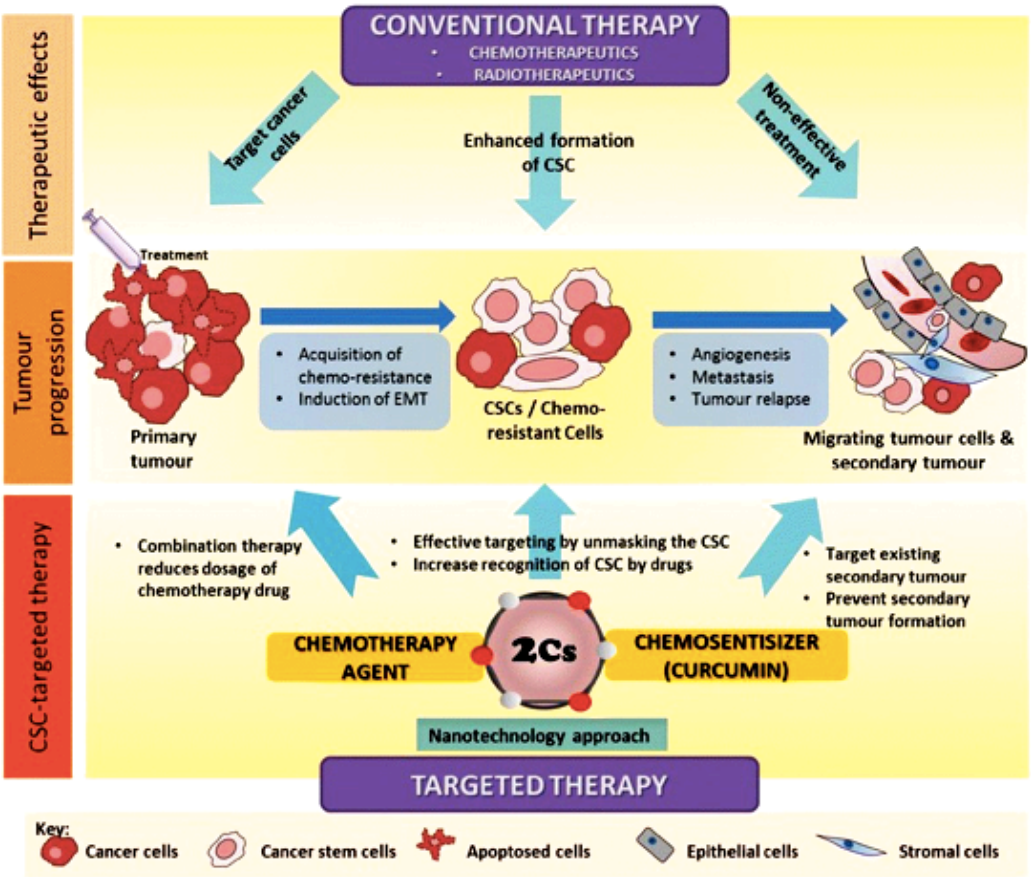

Figure 7. Schematic diagram of the outlook of advanced therapy for targeting cancer and resistant CSC incorporating nanotechnology approaches to improve the formulation of curcumin and its analogues to achieve better therapeutic effects. The top panel shows the typical effects of conventional therapy in relation to tumour progression (middle panel), noting that CSC typically escapes the treatment, thus causing tumour recurrence and metastasis. The bottom panel shows the future effect of targeting the CSC population using curcumin and its analogues and the future perspective of using a nanotechnology approach to improve drug formulation (Credit: Ramasamy TS, Ayob AZ, Myint HH, Thiagarajah S, Amini F. Targeting colorectal cancer stem cells using curcumin and curcumin analogues: insights into the mechanism of the therapeutic efficacy. Cancer Cell Int. 2015 Oct 9;15:96.)

1.3.5 Curcumin and cancer-associated fibroblast (CAFs)

Carcinogenesis depends on the dynamic interactions between cancer cells and the surrounding microenviroment, where CAFs are localized. CAFs can regulate many aspect of tumor mass, including growth, survival, metastatis, angiogenesis and immune surveillance. They can be identified as active when vimentin and α-smooth muscle actin are expressed. Nevertheless, cancer cells can also transform into fibroblast-like cells via EMT, acquiring higher invasiveness and metastasis ability. Buhrmann and colleagues (2014) investigated the role of tumor microenvironment in tumor progression via the interaction of colorectal cancer cells in the stromal fibroblast (CAFs) and the effect of curcumin treatments. Treatment with 5-Fluoracil (5-FU) not only increased the crosstalk between cancer cells and CAFs but also their metastatic activity. However, curcumin was shown to strongly inhibit these activities and sensitized them to 5-FU. Moreover, curcumin is also reported to inhibit the migration and metastasis of pancreatic cancer cells by reducing the mesenchymal features of CAFs, which, in turn, reverse the EMT process in pancreatic cancer cells (Wang et al, 2017).

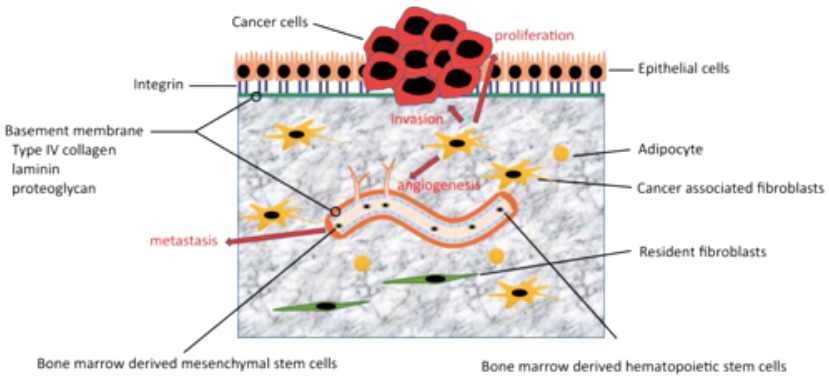

Figure 8. Tumor-stroma interactions and the role of CAFs. CAFs contribute to cancer proliferation, invasion, metastasis, and angiogenesis through several factors (Credit: Kazuyoshi Shiga, Masayasu Hara, Takaya Nagasaki, Takafumi Sato, Hiroki Takahashi, Hiromitsu Takeyama. Cancer-Associated Fibroblasts: Their Characteristics and Their Roles in Tumor Growth. Cancers (Basel) 2015 Dec; 7(4): 2443–2458. Published online 2015 Dec 11).

1.3.6 Curcumin and nanotechnology

Curcumin low solubility in water (0.0004mg/ml at pH 7.3) is the major problem when it is orally administered. Moreover, rapid metabolism, poor absorption, fast degradation and systemic elimination are crucial factors that lead to the poor bioavailability that characterize curcumin treatments.

Furthermore, curcumin must be administered to patients at high concentration, which, in turn, exert intolerance and serious side effects. Recently, new drug delivery systems, which increase curcumin bioavailability, can make curcumin a promising anticancer drug: this is possible with the advent of nanotechnology. It has become possible to design curcumin-encapsulated nanoparticles or nanocurcumin by compressing its bulky size to less than 100nm:

- Liposomes are closed, spherical, phospholipids vesicles in which drugs are incorporated into their aqueous interior (Sak, 2012).

- Polymer nanoparticles are small, nano-sized molecules , highly biocompatible and easy circulate in the bloodstream for long time. The widely used synthetic polymer conjugates include chitosan, D,L-lactide-co-glycolide (PLGA), poly-ethylene (PEG), silk fibroin and N-iso-propyl acrylamide (Yallapu et al, 2012).

- Solid lipid nanoparticless (SLNs) consist of natural lipidis like lecithins or triglycerides that are solid at 37°C. This kind of nanoparticle protect not stable compounds from degradation, improving their bioavailability, such as curcumin (Pandit et al, 2015).

- Magnetic nanoparticles loaded with drug can be targeted to the tumor site by an external magnetic field. It is reported that Fe_3O_4 loaded with curcumin, conjugated with oleic acid or chitosan resulted in the formation of nanosized, fluorescent-magnetic and water-dispersible nanoparticles capable to increase curcumin bioavailability and cellular uptake (Yallapu (A) et al, 2012).

- Polymer micelles represent another drug delivery system used for enhancing drug-loading capacity, increasing water solubility, decreasing toxicity and degradation (Wang et al, 2011).

- Microspheres and microcapsules composed of rutin, andrographolide and camptothecin can store curcumin in their inner core, increasing efficacy, stability, drug bioactivities and organ-targeted bioavailability (Wang et al, 2011).

- Microemulsions consist of small-droplet dispersion of mixture of oil and water stabilized by interfacial films of surfactant molecules. This kind of drug-delivery system is ideal for hydrophobic molecules like curcumin. Moreover, microemulsions (e.g. Tween20 and

triacylglycerol) are characterized by thermodynamic stability, high drug dissolution and solubility (Wang et al, 2011).

- Inclusion complexes such as β-cyclodextrins are widely used as they are easily accessible and cost-effective. They increase curcumin stability, water solubility and its bioavailability (Serri et al, 2017).

- Nanogels, due to their 3D-polymer networks and high drug-loading capacity, represent one of the efficient drug-delivery procedures that allow high dispersion stability, targeted drug-delivery efficacy across the cellular barriers and fast drug-releasing (Bisht et al, 2007).

- Nanocurcumin is made of pure curcumin without any carriers. Curcumin is dissolved with ethanol and homogenized at high pressure (Bisht et al, 2007).

- Solid dispersion consists of an inert carrier/matrix at solid state in which molecules, such as curcumin, can be dissolved by melting (fusion). Curcumin physicochemical and pharmacokinetic activities result improved using crystal and amorphous solid dispersions (Bisht et al, 2007).

1.4 Nanomicelles

Nanomicelles can abrogate many of the negative aspects of standard chemotherapy, such as high systemic toxicity and low therapeutic efficacy due to the limited bioavailability of the drug, its reduced stability, solubility and nonspecificity. Moreover, these new nanodrugs, due to their specific properties, can prevent drug resistance by increasing the drug accessibility and sensitivity. Furthermore, high local drug concentration at the tumor site can be achieved via enhanced permeation and retention (EPR) effect, firstly

reported by Matsumura and Maeda in 1986. Their investigations showed that most solid tumors exhibit blood vessels with defective architecture which involved enhanced vascular permeability, ensuring a supply of nutrients and oxygen to tumor tissues for rapid growth. The EPR effect is based on this specific vascular feature that facilitates macromolecules (larger that 40 KDa) transportation into the tumor mass. On the other hand, normal structure of capillares and vessels in normal tissues doesn't allow the EPR effect. This unique phenomenon, as well as other various barriers to drug delivery, has to be considered in tumor-targeted chemotherapy. The first barrier is represented by vessels, but, in a tumor scenario, drugs could easily reach tumor interstitium through leaky vascular walls, instead they facilitate selective delivery of macromolecules to tumor mass. The second barrier is the matrix that surrounding target tumoral cells: macromolecules could diffuse across it for a sizable distance. The third one is the cell membrane: macromolecules could be conjugated with antibody in order to obtain a better endocytosis, but also macropinocytosis seems to work. The last barrier to effective macromolecular anticancer therapy is the release rate of the active principle of the drug from liposomes, micelles or drug-polymer conjugates.

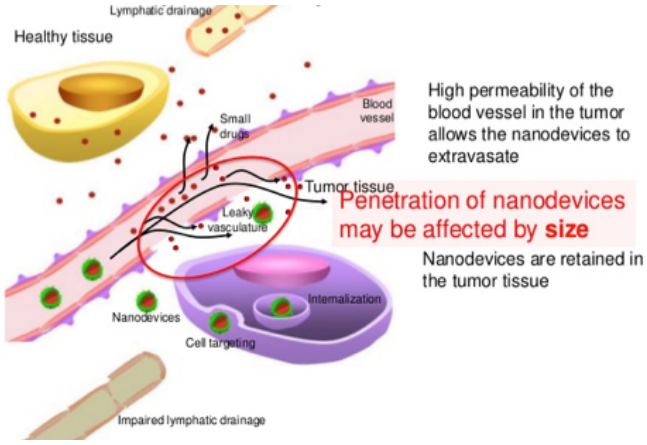

Figure 9. Schematic representation of the EPR effect.

Among various nanotechnology-based drug delivery systems, nanomicelles have gained interest in cancer therapy due to their intriguing advantages such as high drug loading and small size (<30nm). Nanomicelles are usually produced using lipids and amphiphilic polymers. Unfortunately, lipid-based nanomicelles are characterized by limited stability and polymers are penalized by dispersed molecular weight distribution. The best formulation would include a nanomicelles-based delivery system in which the combination of the benefits of lipids and polymers can overcome their shortcomings. The novel nanomicellar drug delivery platform based on amphiphilic dendrimers (Wei et al,2015), is represented by hybrid molecules composed of a hydrophobic lipid entity entailing molecular self-assembly in water environment, and a hydrophilic dendritic polymer component. These nano-assemblies are able to combine in a single entity the stability and mechanical strength of dendrimeric polymers and the micelle-forming feature of lipids. Moreover, this kind of nanomicelles shows a large void space within their inner core, which can be exploited for achieving high drug-loading efficiency.

1.4.1 C_{16}-DAPMA, C_{16}-SPD and C_{16}-SPM

Self-Assembled Multivalent ligand display (SAMul), is a tunable strategy because it only requires the synthesis of small molecules (e.g. anphiphilic molecules) with different ligands which could self-assemble into micelles characterized by cation ligand surfaces. C_{16}-DAPMA, C_{16}-SPD and C_{16}-SPM were obtained by Fechner et al. (2016) using palmitic acid (C_{16}) as hydrophobe. C_{16}-DAPMA had good aqueous solubility, spermidine-based

C16-SPD was slightly less soluble and spermine-derived C_{16}-SPM was more difficult to dissolve. Critical micelle concentrations (CMCs) were evaluated by means of Nile Red Assay which supported the macroscopic solubility observations, with C_{16}-DAPMA having the lowest CMC and C_{16}-SPM the highest. Moreover, isothermal tritation calorimetry (ITC) evidenced (data not shown) that resulting CMCs were in agreement with those from the Nile Red assay and dynamic light scattering (DLS) revealed that all three compounds formed similar-sized assemblies.

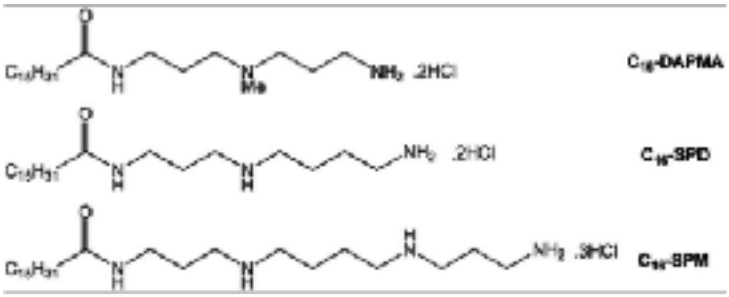

Figure 10. Compound investigated

	C_{16}-DAPMA	C_{16}-SPD	C_{16}-SPM
CMC (μM)	40±1	51±2	65±20
Diameter (nm)	6.2±1.3	6.6±0.2	6.2±0.1

Table 1. CMCs determined by Nile Red assay and diameter parameters from DLS.

To further understand self-assembly, a multiscale molecular simulation evidenced that spherical micelles were obtained in all cases. Interestingly, simulation indicated that the compounds formed micelles with different packing densities. Specifically, the aggregation number (N_{agg}) suggests that C_{16}-DAPMA (N_{agg}=16±2) forms more tightly packed micelles than C_{16}-SPD (N_{agg}=13±1), which in turn is more densely packed than C_{16}-SPM

(N_{agg}=10±1). As suggested from experiment, the hydrophobic C_{16} chain struggles to bring together the more highly charged SPM ligands.

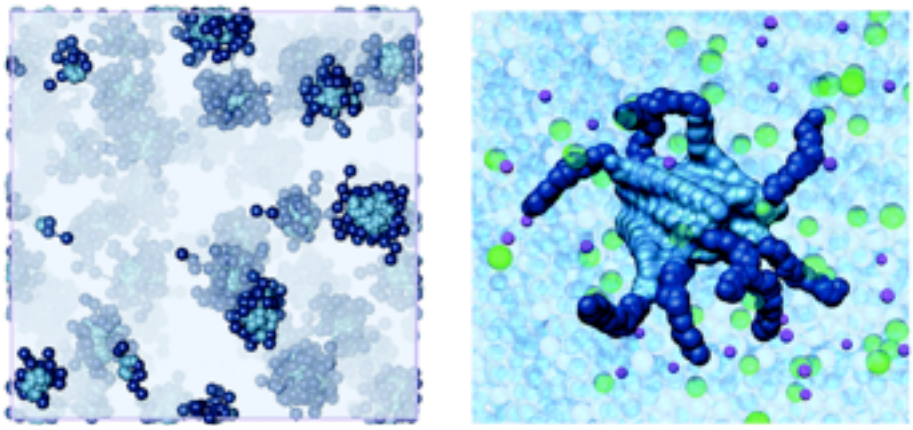

Figure 11. Mesoscopic (left) and atomistic (right) simulations of C_{16}-SPM self-assembling into micelles. The C_{16} hydrophobic portion is shown as steel blue spheres whereas the SPM residues are portrayed as navy blue spheres. In the left panel, water, ions and counterions are shown as light grey field; in the right panel, water molecules are depicted as transparent light blue spheres, some Na^+ and Cl^- ions are shown as purple and green spheres, respectively.

Furthermore, the self-assembled nanostructures formed by these ligands were visualized by means of transmission electron microscopy (TEM).

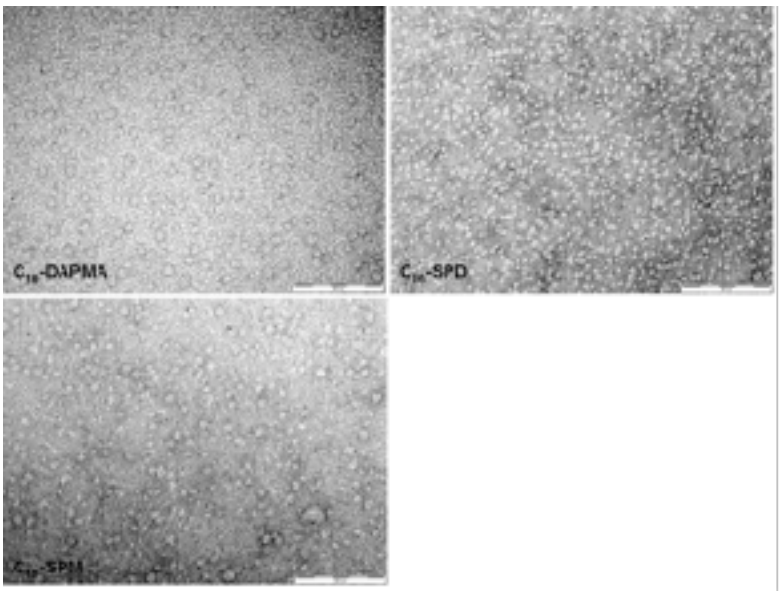

Figure 12. TEM images of nanomicelles.

1.5 Photodynamic therapy (PDT)

The combinations of dyes and light to treat diseases dates back to ancient Egypt, where psoriasis and vitiligo were treated with natural compounds and sunlight (Spikes, 1985). However, it was only in the 20th century with the discoveries of O. Rabb and von Tappeiner (Raab, 1900). and Jesionek that modern photodynamic therapy (PDT) was conceived for the first time. Nowadays, PDT is considered a promising treatment against many types of cancer. The combination of PDT and chemotherapy is reported to be significantly efficient in eliminating cancer cells as shown by Szacilowsky et al in 2005.

1.5.1 PDT and cancer

PDT was carried on in the field of microbiology but since the introduction of antibiotics in the 1940s, PDT was severely cutback. On the contrary, it is being revisited in the last decades because of the increasing of bacterial drug-resistance (Khan et al, 2017). In PDT there are three specific actors: photosensitizer (PS), light source (laser or LED) and oxygen. Clinical PDT protocols which include a standard dose of drug, a light source and a PS, unfortunately lead to different outcomes, probably due to poor light delivery to the target tissue, drug resistance and the rapid metabolism of the PS (Allison et al, 2013). In particular, the choice of the right PS plays a pivotal role for successful PDT treatment. PS must be non-toxic to cell in the dark (without laser/LED irradiation), cancer cells must selectively capture it and it should stimulate immunogenic cell death (Mroz et al, 2011). PDT displays some advantages over standard chemotherapy or radiotherapy: i) PDT has no long-term side effects; ii) PDT is less invasive than standard

surgical procedures; iii) the light source can destroy the vasculature associated with the tumor which contributed to cancer mass death; iv) PDT is very selective because the tumor mass irradiated by the light is the only area which contains also the PS (because of this selectivity PDT does not cause damage to normal structures like nerves, collagen fibers and large blood vessels); v) it can be repeated at the same localization several times unlike radiations; vi) PDT doesn't leave scars after treatment (cancer cells are eliminated via apoptosis/necrosis maintaining the scaffold supplied by the extracellular matrix) and lastly; vii) PDT costs less than any other cancer treatment. However PDT also shows some drawback: i) it is impossible to use PDT in disseminated metastasis; ii) PDT requires tumor oxygenation: tumor surrounded by necrotic tissues or characterized by a dense tumor mass lead to an impaired PDT; iii) deep tumor masses that can't be reached without a surgical procedure are difficult to treat due to the low penetration of visible light.

Three PDT death pathways were described: apoptosis, autophagy and necrosis. The apoptosis remains unclear and complex to understand. The mechanisms and roles of autophagy following PDT could differ markedly in different cell types: some cell types undergo apoptosis first and by contrast other cell types can produce different types or locations of damage thus leading to more resistance (organelle turnover) or cell death (Kessel and Oleinick, 2009). When the PS is excited by the light source with a specific wavelength, its interactions with the surroundings can lead to react with biomolecules (transferring hydrogen atoms via the radical mechanism). This, in turn, generates free radicals and radical ions that react with oxygen resulting in reactive oxygen species (ROS) generation. ROS have high

reactivity but a short half-life. PDT directly affects those biological substrates that are close to the region where ROS are generated (about 20 nm radius).

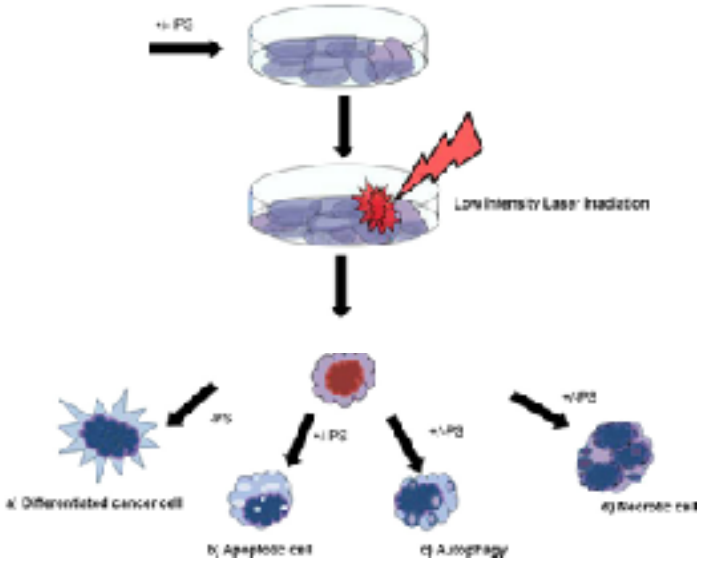

Figure 13. Possible effects of low-intensity laser irradiation and PDT on cancer cells (Credit: Anine M Crous and Heidi Abrahamse, Lung cancer stem cells and low-intensity laser irradiation: A potential future therapy? Stem Cell Research & Therapy 2013, 4:129)

1.5.2 Curcumin-mediated PDT

In 1994, curcumin was proven to lead to production of ROS in mammalian cells upon irradiation with visible light (Dahl et al, 1994). Moreover, curcumin cytotoxicity against several tumoral cells could be strongly enhanced irradiating with blue light (Bernd, 2014): low doses of curcumin exert amplified cytotoxicity with irradiation with wavelengths near the absorbance maximum of curcumin (420nm). Blue light irradiation (480nm) induced a strong reduction of IC_{50} and the needed interaction time of cells with curcumin could be shortened significantly.

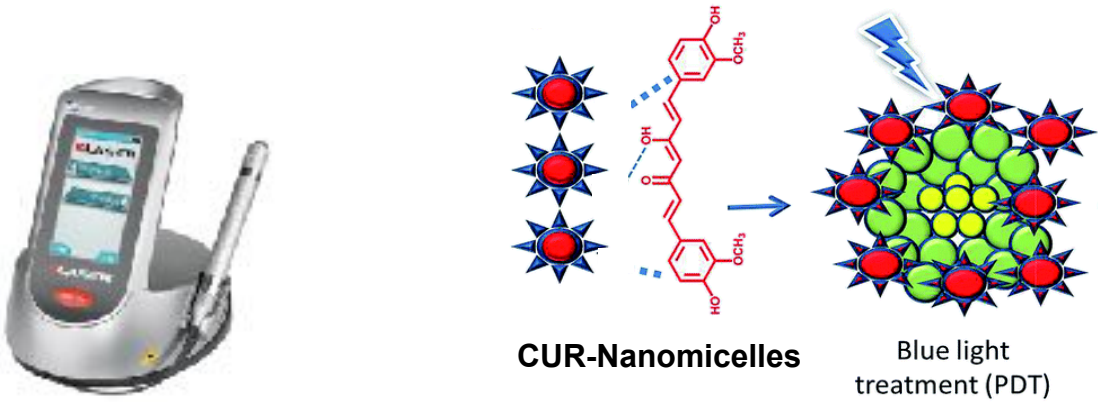

Figure 14. Laser device and schematic representation of PDT with nanomicelles on cancer cells.

1.6 Solitary Fibrous Tumor (SFT)

Although curcumin has been used for long time to treat inflammatory diseases, its efficacy in cancer treatment is reduced because of its limited bioavailability. Furthermore, to be effective in cancer therapy, curcumin should be administered in a high concentration that induces serious side effects in patients. However, recent in vitro and in vivo experiments, that underline the chemopreventive and therapeutic effects of curcumin, have let to the beginning of a number of clinical trials which have the aim to approve the pharmacokinetics, safety and efficacy of curcumin in different types of cancer. The first clinical trial started in 1987 by Kuttan and colleagues in patients with external cancerous lesions. In the last years, the most successful results were obtained in pancreatic cancer, external cancer lesions and postsurgery inflammation. Moreover, recent clinical trial have also reported antitumor activities in neoplastic diseases such as colon cancer, myeloma and gastric cancer. Current clinical trials are focusing on ovarian, breast and oral cancer (www.clinicaltrials.gov). Little, or nothing, is reported for rare cancers and sarcomas (Thway et al, 2016).

Solitary fibrous tumors (SFTs) are fibroblastic mesenchymal tumors that are ubiquitous but rare soft tissue sarcomas. SFT shows circumscribed proliferation of bland spindle to ovoid cells within prominent collagenous stroma characterized by CD34 expression. In the last decades, fibroblastic mesenchymal neoplasms with the above-mentioned features were described as hemangiopericytoma, but they are now subsumed into the category of SFTs. SFTs have an higher incidence in middle-aged adults (20-70 years), affect both sexes equally and can arise within the deep soft tissues in the whole body. Lesions tend to grow slowly and painlessly, they may generate symptoms because of the mass or pressure effect on the adjacent anatomic structures. Radiologically, SFTs are large, well-defined, lobulated, solid and vascular masses. The tumor mass, the heterogeneous intensity of the radiologic signal correlate with malignancy as well as, a tumor size bigger than 10cm, and characterized by an high mitotic rate has been reported as predictive of a higher incidence of metastasis disease (Jo and Fletcher, 2013). SFTs are associated with *NAB2-STAT6* gene fusion, which arised from the intrachromosomal rearrangements on 12q13. This genetic fusion leads to nuclear expression of the C-terminal portion of *STAT6* and to an altered function of the transcriptional corepressor *NAB2*. Like other members of the STAT family of transcription factors, when phosphorylated by receptor-associated kinases, STAT6 translocates to the cell nucleus. The discovery of the NAB2/STAT6 fusion made it possible to diagnose solitary fibrous tumor molecularly using reverse-transcription polymerase chain reaction. Moreover, the overexpression and phosphorylation-independent nuclear translocation of the STAT6 C-terminus can be readily identified by means of STAT6 immunohistochemistry, a sensitive, specific and more widely available means of accurate diagnosis. However, although the presence of the NAB2/

STAT6 rearrangement is pathognomonic for solitary fibrous tumors, it does not provide any known insights into the biological basis of the spectrum, prognosis or progression of the tumors.

SFTs are characterised by a spectrum of "usual/benign", "malignant" and "dedifferentiated" variants. Most SFTs fall into the so-called "usual/benign" category and can be cured by means of complete surgical resection, which remains the gold standard treatment for localized disease; 10–15% behave aggressively and lead to local recurrences and/or distant metastases.

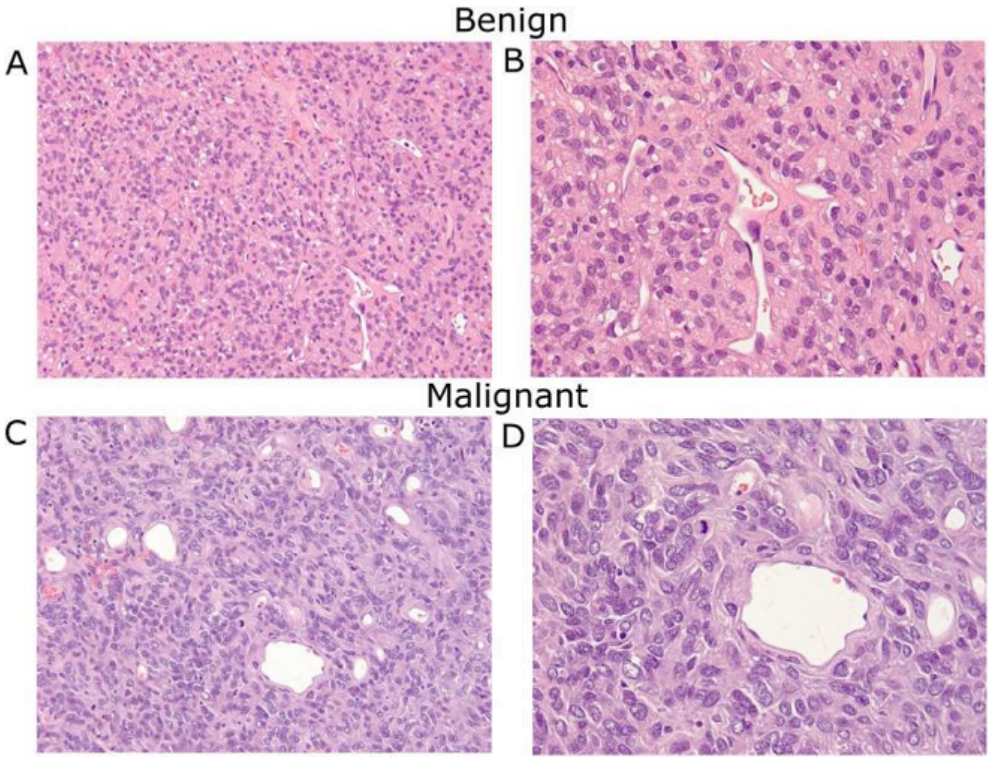

Figure 15. A: Benign SFT. The tumor shows a patternless architecture composed of spindle cells with hyalinized stroma and thin-walled branching vessels (H&E stain; x200 magnification). B: Benign SFT. The spindle tumor cells have vesicular nuclei without significant cytological atypia, mitosis, and necrosis (H&E stain; x400 magnification). C: Malignant SFT. The tumor has similar architecture; however, cells exhibit marked cytological atypia, including nuclear pleomorphism and increased mitotic activity (H&E stain; x200 magnification). D: Malignant SFT showing atypical mitotic tumor (H&E stain; x400 magnification) (Credit: DeVito N,Henderson E, Han G, Reed D, Bui MM, Lavey R, Robinson L, Zager JS, Gonzales RJ, Sondak VK, Letson GD, Conley A. Clinical Characteristics and Outcomes for Solitary Fibrous Tumor (SFT): A Single Center Experience, PLoS One. 2015; 10(10): e0140362. Published online 2015 Oct 15).

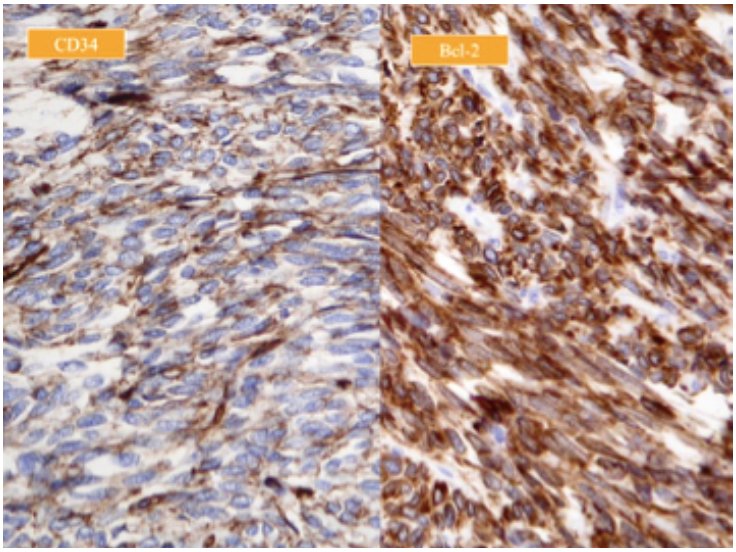

Figure 16. CD34 and Bcl-2 are positive in the tumor. (X 400) (Credit: Bita Geramizadeh, Mahsa Marzban, and Andrew Churg. Role of Immunohistochemistry in the Diagnosis of Solitary Fibrous Tumor, a Review. Iran J Pathol. 2016 Summer; 11(3): 195–203).

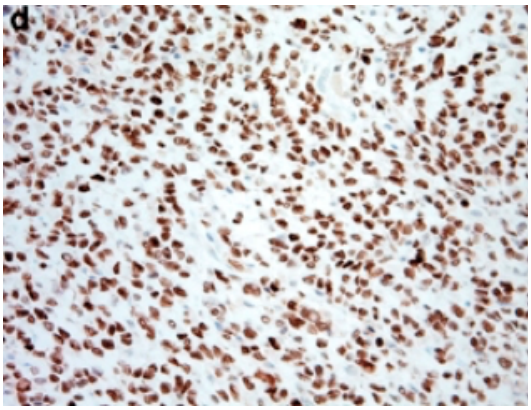

Figure 17. STAT6 immunophenotypical profile of a malignant solitary fibrous tumor (Credit: Dagrada GP, Spagnuolo RD, Mauro V, Tamborini E, Cesana L, Gronchi A, et al. Solitary fibrous tumors: loss of chimeric protein expression and genomic instability mark dedifferentiation. Mod Pathol 2015; 28(8): 1074–1083).

Conventional treatment with anthracyclines has shown limited efficacy in SFTs (Stacchiotti et al, 2013). Other drugs such as bevacizumab, sorafenib, pazopanib and IGF1R inhibitors have also proved to be efficacious in

treating advanced SFTs, but the complementary nature of the receptor tyrosine kinases (RTKs) activated in SFTs and the RTKs inhibited by sunitinib suggests that sunitinib should be more effective. Moreover, stromal components such as the PDGFRB-expressing pericytes and the VEGFR2-expressing endothelial cells may be further targets. Finally, the tumor immune contexture of SFTs changes in response to sunitinib and the host immune response contributes to the drug's efficacy. However, the antitumoral efficacy of sunitinib is transient, and it can be hypothesised that the reduced blood flow and autophagy promoted by prolonged treatment act as adaptive mechanisms that ultimately lead to resistance (Spagnuolo et al, 2016).

2. Aim of the study

Curcumin is demonstrated to be effective and safety. By contrast, lower serum and tissue levels of curcumin irrespective of the route of administration, its rapid metabolism and elimination are major factors curtailing curcumin bioavailability.

The aim of the study is to investigate a new formulation of nanomicelles in order to improve the bioavailability of curcumin and target specific tumoral markers, which correlate with Epithelial-Mesenchymal Transition (EMT) and, by consequence, a poor outcome. To date, clinical trials that evaluate curcumin efficacy are focusing on ovarian, breast and oral cancer. Here, investigations focus on a rare tumor, named solitary fibrous tumor (SFT), in particular on its malignant variant. As reported in literature, conventional treatment with anthracyclines and/or sunitinib has shown transient efficacy in SFTs, making them a good field of research for drug resistance overcoming. Development of treatment resistance and adverse toxicity associated with classical chemotherapeutic agents highlights the need for safer and effective therapeutic approaches, such as a combined treatment with curcumin. Nowadays, novel delivery strategies offer significant promise and are worthy of further exploration in attempts to enhance the bioavailability of curcumin. The advent of nanotechnology in cancer treatment could be useful to lower the concentration of chemotherapeutic agents, already in use in clinical therapy, involving a reduction of side effects in patients. Moreover, curcumin is reported to sensitize cancer cells to standard chemotherapy thus overcoming drug resistance. After setting up the conditions for the construction of curcumin-loaded nanomicelles (i.e. C_{16}-DAPMA, C_{16}-SPM and C_{16}-SPD), their citostatic/citotoxic activity will be evaluated taking advantage of an in vitro SFT model. Furthermore, the

expression status of specific EMT markers will be analyzed by means of biochemical approaches.

Therefore, primary goals of this study are to determine whether nanoparticles loaded with curcumin can arrest the EMT process and to investigate if a combined treatment with chemotherapeutic drugs (i.e. Vorinostat, SAHA) could be effective in SFT cell line.

Moreover, another therapy design could be the combination of low concentration of curcumin/nanomicelles loaded with curcumin with blue laser light. Photodynamic therapy will be applied to SFT cells to investigate the photodynamic properties of curcumin on a cancer cell line.

3. Materials and Methods

3.1 Ethics statement

Investigation has been conducted in accordance with the ethical standards and according to the Declaration of Helsinki and according to national and international guidelines and has been approved by the authors' institutional review board. The Independent Ethics Committee of the Fondazione IRCCS Istituto Nazionale dei Tumori di Milano approved the study. The patients whose biological samples were included in the study gave their signed consent to donate the tissues remaining after the diagnostic procedures had been completed.

3.2 Patients and Primary tumors

The case material for the screening consisted of specimens of all of the available cases of solitary fibrous tumors diagnosed and treated between 2003 and 2013, together with frozen samples of a small group of usual and malignant solitary fibrous tumors surgically treated in the same period. As our institute is a referral centre for patients with rare sarcomas, solitary fibrous tumors with an extrapleural location and malignant features are overrepresented. Unfortunately, among all the collected samples, fresh tissue to get a primary cell culture, taken from the sunitinib-naïve surgical specimen, was available for only one patient.

3.3 Examined Sample, Primary SFT cell culture and Stabilized SFT cell line

Formalin-fixed paraffin-embedded (FFPE) and cryopreserved material was obtained from one patient with advanced and progressive malignant SFT,

who underwent surgery after being treated with sunitinib. The diagnosis was confirmed by means of immunohistochemistry/immunofluorescence (IHC/IF: nuclear STAT6 positivity) and real-time polymerase chain reaction (RT-PCR: NAB2-STAT6 rearrangement). This patient was a 38 years-old (at the onset) female, affected by a pelvic relapse of SFT characterised by multiple peritoneal lesions, and was continuously treated with sunitinib 37.5 mg/day for six months, which led to a RECIST partial response (PR), and followed by surgery. She subsequently remained disease-free for eight months before experiencing an abdominal relapse that was continuously treated with the same sunitinib dose for eight months. The treatment led to RECIST stable disease (SD), and the residual tumor was excised.

3.3.1 IHC and IF analyses

STAT6 IHC

IHC analysis was carried out on 2µm FFPE sections, using a polyclonal rabbit antibody (S20, sc-621, Santa Cruz Biotechnologies, Santa Cruz, CA, USA) against the STAT6 C-terminal at a dilution of 1:400 at room temperature for 30 minutes and, after antigen retrieval (96°C EDTA buffer pH8 for 30 minutes), the samples were stained by using a Dako Autostainer link48 (Dako, Glostrup, Denmark). The slides were counterstained with Mayer's hematoxylin.

STAT6 IF

In parallel, IF analysis was carried out using above-mentioned primary antibody against STAT6 as well as the same antigen retrieval protocol, with an overnight incubation at 4°C. Then, the samples were immunolabelled with an Alexa Fluor 488 (Invitrogen, Carlsbad, CA, USA) diluted 1:1000 in Dulbecco's Phosphate Buffered Saline (DPBS) (Gibco, Paisley, UK). Nuclei were counterstained with Vectashield antifade mounting medium with DAPI

(Vectorlab, Burlingame, CA, USA). The samples were observed through a Leica DM6000B microscope equipped with a 100 W mercury lamp; excitation was obtained using Spectrum Green and DAPI excitation filters. The images were acquired using 20x and 40x oil immersion objectives, and analyzed using Cytovision software. The images show extended depth-of-field frames in stack with focal regions selected on the basis of their maximum intensity. Although histologic characteristics and frequent CD34 expression allow an accurate diagnosis of SFT cases, molecular analyses have discovered that almost all SFTs harbor an the *NAB2-STAT6* fusion gene, which is considered specific to this tumor type. Recent studies have suggested that STAT6 IHC is a reliable surrogate for detection of the fusion gene. Nuclear STAT6 positive intense staining was present in SFT FFPE surgical sample. It was investigated by means of both IHC and IF (Fig.18).

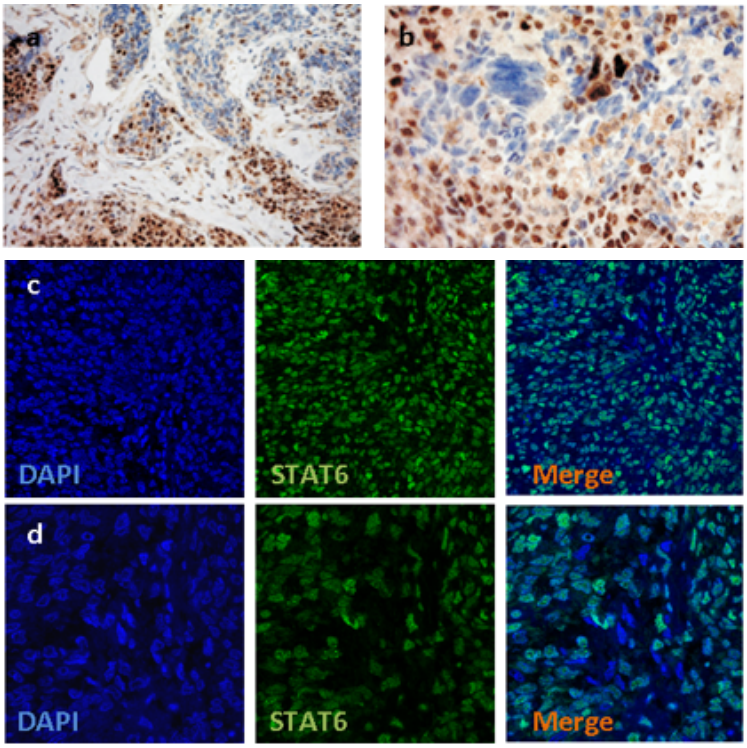

Figure 18. STAT6 nuclear IHC staining (a;b: higher magnification). STAT6 nuclear IF staining 20X (c) and 40X (d): nuclei were counterstained with DAPI (blue), STAT6 with Alexa fluor 488 (green).

Vimentin IHC

Vimentin IHC analysis was carried out on 2μm FFPE sections, using a anti-Vimentin monoclonal mouse antibody (clone Vim3B4, Dako) which reacts strongly with human intermediate filament protein vimentin and labels cells of mesenchymal origin. The samples were stained by using a Dako Autostainer link48, vimentin antibody was diluted at 1:400. Then, the slides were counterstained with Mayer's hematoxylin.

3.3.2 NAB2-STAT6 RT-PCR

Total RNA was extracted from frozen tumoral sample using Epicenter (Madison, WI, USA) followed by DNAse treatment, and its concentration and quality was assessed by using NanoVue (VWR, Radnor, PA, USA). A total of 1 μg of RNA per sample was retrotranscribed and the primers used to detect NAB2/STAT6 fusion products were the following: NAB2ex5F(CCTGTCTGGGGAGAGTCTGGATG)/ STAT6ex20R(GGGGGGATGGAGTGAGAGTGTG). After treatment with ExoSap IT (Affymetrix, Santa Clara, CA, USA), the amplified products were directly sequenced using a Big Dye v1.1 cycle sequencing kit and a 3500Dx genetic analyzer (Thermo Fisher Scientific, Waltham, MA, USA).

The classification of *NAB2/STAT6* fusion types is challenging because of their variety and complexity. Furthermore, the absence of an acknowledged numbering system for *STAT6* exons causes confusion and makes it cumbersome to compare results from different groups. In terms of size, *NAB2/STAT6* fusion variants can be tentatively grouped into two categories: those with distal *STAT6* breakpoints (exons 17–19) whose chimeric proteins have a similar size to that of STAT6 (small), and those with *STAT6* proximal breakpoints (exons 1b–4), which produce outsized

chimeric proteins (large). *NAB2* breakpoints are also heterogeneous and fall in proximal (exons 3–5) or distal exons (exons 6–7). Furthermore uncommon variants with intronic and/or intraexonic breakpoints have been described (Chmielecki et al, 2013; Robinson et al, 2013; Mohajer et al, 2013).

NAB2/STAT6 fusion transcripts were investigated by means of RT-PCR on frozen surgical sample. It revealed the presence of two distinct fusion transcripts (Nakada et al,2015), which after Sanger-sequencing were recognized as a canonical exon 6-17 and a non-canonical fusion involving a NAB2-intronic breakpoint.

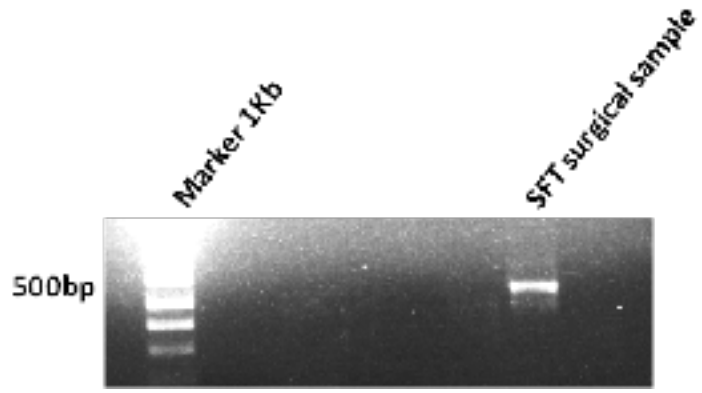

Figure 19. SFT surgical sample fusion variants investigated by means of RT-PCR.

3.3.3 Primary cell culture and Stabilized SFT cell line

Dissociation of Cells from Primary Tissue

A common method to obtain single cells suspension from fresh and sterile primary tissue is enzymatic disaggregation, using collagenase type2 (Worthington Biochemical Corporation, Lakewood, NJ, USA). The cells were exposed to enzymes for a minimal amount of time (about 4 hours) to

preserve maximum viability. The following procedures disaggregate whole tissue to obtain a high yield of viable cells:

- Grind tissue into 3 to 4 mm pieces with a sterile scalpel
- Add 1 ml collagenase diluted in Dulbecco's modiefied eagle medium (DMEM) (Gibco, Paisley, UK) and incubate at 37°C for 4 to 6 hours.
- Filter the cells suspension through a nylon mesh to separate the dispersed cells and tissue fragments from the larger pieces
- Wash suspension several times by centrifugation in DPBS
- Resuspend the pellet in ACK lysis buffer (Lonza, Walkersville, MD, USA) to eliminate red blood cells
- Wash suspension several times by centrifugations in DPBS
- Resuspend the pellet in DMEM with the addition of Penicillin/ Streptomycin (Gibco, Grand Island, NJ, USA), gentamicin (Gibco, Paisley, UK) and 10% Fetal Bovine Serum (FBS) (Carlo Erba, Milan, Italy)
- Count and seed the cells for culture in incubator, 37°C with 5%CO_2

In order to confirm that the cells cultured are from SFT and they are not fibroblasts, the nuclear expression of STAT6 in paraffin-embedded cell block (Bioagar, Bioptica, Milan, Italy) cells (passage p1) was verified by means of IHC/IF and NAB2-STAT6 rearrangement by RT-PCR.

Stabilized SFT cell line

The primary cell line was stabilised by means of the retroviral delivery of SV40 large T-antigen (pWZL-neo Large T-Ag) in accordance with standard procedures (Demontis et al, 2005): a SV40 LgT-SFT bulk cell population was used throughout the study. SV40 T (large T) antigen has been shown to be the simplest and most reliable agent for the immortalization of many different cell types in culture, and the mechanism has been well documented. For the most part, viral genes achieve immortalization by inactivating the tumor suppressor genes (p53, Rb, and others) that can induce a replicative senescent state in cells. Recent studies have also shown that SV40 T-antigen can induce telomerase activity in the infected cells (Spagnuolo et al, 2016).

The nuclear expression of STAT6 in FFPE cytoblock was verified by means of IHC/IF and NAB2-STAT6 rearrangement by RT-PCR. Nuclear STAT6 positive intense staining was present in the SFT cell line making it a good model to investigate SFT. STAT6 IHC/IF were carried out in FFPE cytoblock (Fig.20) and RT-PCR on cell lysate (Fig.21).

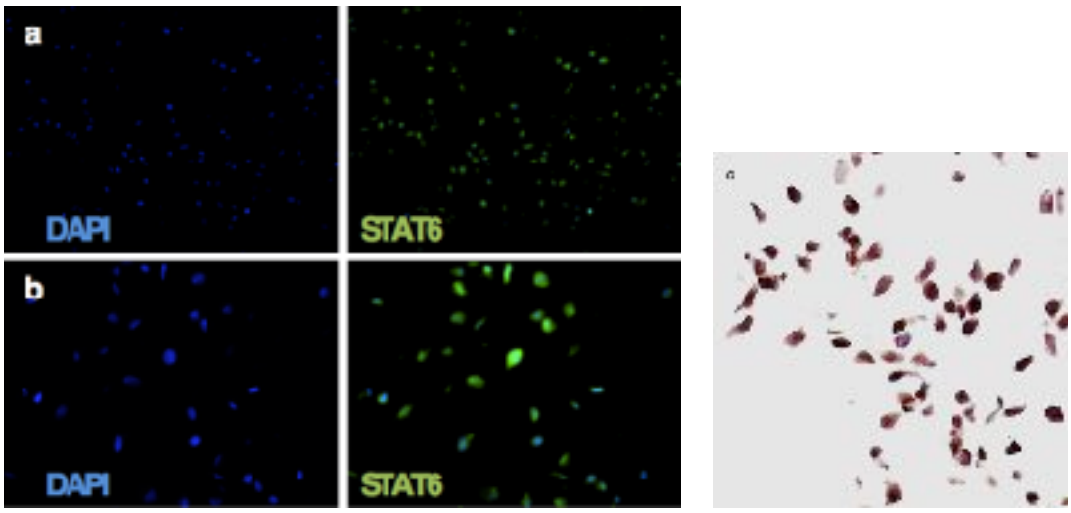

Figure 20. STAT6 IF/IHC staining (cytoblock slides representative fields). STAT6 nuclear IF staining 20X (a) and 40X (b): nuclei were counterstained with DAPI (blue), STAT6 with Alexa fluor 488 (green). STAT6 IHC nuclear staining 20X (c).

NAB2/STAT6 fusion transcripts were investigated by means of RT-PCR on cell lysate taken from 7 indipendent SFT cell clones. All the clones analyzed presented the same PCR pattern with the two products as seen in the surgical sample. This result showed that both fusion variants were produced from the same cell.

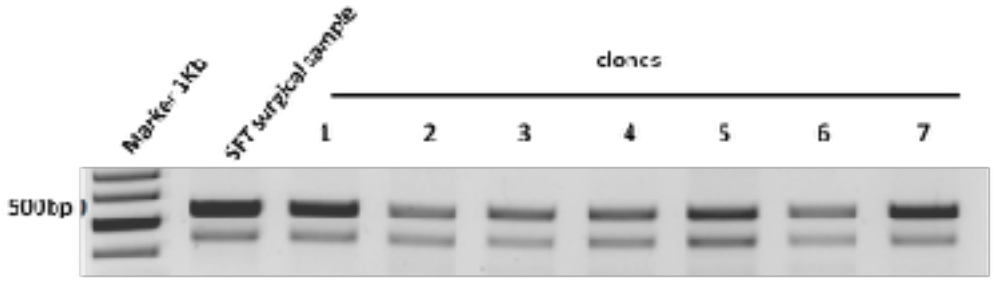

Figure 21. SFT cell line fusion variants investigated by means of RT-PCR.

3.4 Curcumin Encapsulation

Curcumin (0.32mg) (C1386, Sigma-Aldrich, Munich, Germany) was dissolved in 1.0 ml mixed solvent (chloroform:methanol = 3:2, vol/vol). The drug was then mixed with 3 mg of nanomicelles in 3.0 ml of mixed solvent. The solvent was then removed by dry heated nitrogen evaporator (VLM GmbH, Bielefeld, Germany) to form a dry film. The dried film was hydrated with Hepes buffer (10 mM, pH 7.4) at 60 °C for 30 minutes under stirring. Nonencapsulated curcumin was separated by filtration through a 0.45-μm polycarbonate membrane (Millipore Co.) followed by 9 h dialysis (changing water every hour) using a membrane with molecular weight cutoff of 2,000 Da. The product in the dialysis tube was subsequently lyophilized by means of a concentrator plus (Eppendorf, Hamburg, Germany). The amount of curcumin encapsulated in the nanomicelles was measured using a spectrophotometer (Ultrospec 3100pro, Amersham Bioscience, GE

Healthcare, Buckinghamshire, UK) with wavelength at 420 nm. Blank nanomicelles were prepared using the same procedures without curcumin addition. The drug-loading content was calculated using a standard curve made on specific curcumin concentrations dissolved into the same mixed solvent (Table 2).

curcumin standard (2mg/ml)	Absorbance#1	Absorbance#2	Mean of absorbance	Relative absorbance	
1 mg/ml	20,50	27,02	23,76	26,70	
2 mg/ml	45,50	46,12	45,81	22,91	
4 mg/ml	90,10	91,56	90,83	22,71	
6 mg/ml	125,40	126,37	124,89	20,81	
8 mg/ml	187,80	188,90	188,35	23,61	mean value
12 mg/ml	199,80	196,68	197,74	16,48	22,21

Table 2. Curcumin standard values.

3.5 SFT cell line culture treatments

Cell culture is one of the major tools used in cellular and molecular biology that provide an excellent model for studying the normal cells physiology and biochemistry, effects of drugs and toxic compounds on the cells and carcinogenesis. The major advantage is the solidity and reproducibility of results that can be achieved from using a batch of clonal cells.

3.5.1 Curcumin treatments

$3x10^5$ cells were seeded in each plate using DMEM/Penicillin/Streptomycin/ gentamicin/10%FBS and incubated (37°C, 5%CO_2) for 3 days before any treatment, without medium restoring. Then, curcumin was added at different concentration (10μM, 20μM, 50μM in DMSO, dimethyl sulfoxide, (Carlo Erba, Milan, Italy) and plates were incubated for 24 and 48 hours at 37°C, 5%CO_2. Regarding cell viability assay (MTT, (3-(4,5-dimethylthiazol-2-yl)-2,5-diphenyltetrazolium bromide) (M5655,Sigma, Munich, Germany)) analyses, $5x10^3$ cells/well were seeded 3 days before in a 96-well plate. Moreover cells were treated with different concentrations of curcumin ranging from 2.5μM to 50μM for 24 and 48 hours at 37°C, 5%CO_2. Then,

MTT working solution was prepared by adding 25mg of MTT powder to 5ml of sterile DPBS. After curcumin treatments, 20µl MTT working solution were added to each well and the 96-well plate was incubated for 4 hours at 37°C, 5%CO_2. Once eliminated the medium with MTT, 100 µl of DMSO the plate was read at Infinite1000 TECAN (Männedorf, Switzerland) at 550nm wavelength.

3.5.2 Curcumin-loaded nanomicelles treatments

Cell culture condition and MTT assay were the above-mentioned. Cells were treated with 500nM and 1µM of each different nanomicelles (C_{16}-DAPMA, C_{16}-SPM and C_{16}-SPD) for 24 and 48 hours at 37°C, 5%CO_2.

3.5.3 Combined treatments

Cell culture condition and MTT assay were above-mentioned. Suberoylanilide Hydroxamic Acid (SAHA, Vorinostat; MK0683, Selleckchem, Houston, TX, USA) has been added to the usual curcumin and nanomicelles treatments. Following the MTT experiments in order to determine the optimal SAHA concentration, the SFT cells were dispensed with a concentration of 5µM of SAHA for 24 and 48 hours at 37°C, 5%CO_2.

3.6 Curcumin uptake and phalloidin IF

3x10^5 cells were seeded in each plate using DMEM/Penicillin/Streptomycin/gentamicin/10%FBS and incubated (37°C, 5%CO_2) for 3 days before any treatment, without medium restoring. Autoclaved coverslips has been added to each plate in order to allow cells to grow on them. Moreover, SFT cells were treated as described before with curcumin, nanomicelles and SAHA. The last day of treatment, coverslips were removed and then fixed with methanol (curcumin uptake assay) or paraformaldehyde (phalloidin

staining). The distribution of curcumin inside SFT cells was observed on fluorescent images obtained from a fluorescence microscopy with excitation wavelength of 488nm. Furthermore, curcumin endocytosis was monitored for 2 hours after nanomicelles treatment by means of juLI stage (Nanoentek, Seoul, Korea) taking advantage of curcumin autofluorescence (excitation wavelength of 488nm).

Moreover, taking advantage of wheat germ agglutinin (WGA), which is a carbohydrate-binding protein that selectively recognizes sialic acid and N-acetylglucosaminyl sugar residues predominantly found on the plasma membrane, changes in the structure of SFT cells after SAHA treatment were observed as well as curcumin site of accumulation. Phalloidin (1:200 in DPBS, 2 hours incubation, Alexa Fluor, 488) was used to observed actin fiber changes after SAHA treatments. DAPI (blue signal) counter stained nuclei. Representative fields were captured with Leica.

3.7 Invasion assay

Transwell membrane (Corning, Incorporated, Tokyo, Japan) coated with Matrigel (BD Biosciences Discovery Labware, Durham, NC, USA) was used for invasion assay. After collecting and centrifuging, SFT cells were resuspended at $1,25x10^5$ cells/ml. Then, 2ml of cells suspension ($2,5x10^5$cells) were seeded to upper wells of precoated Transwell chambers. Cells were then incubated with 10μM, 20μM and 50μM curcumin resuspended in DMEM. Moreover, cells were treated with 500nM and 1μM of different nanomicelles (in combination or not with SAHA) resuspended in DMEM. DMEM alone was used as control. In parallel, 500μl of DMEM+10%FBS was placed in the lower chambers as a chemoattractant.

After 24 hours of incubation, cells in the upper chamber were removed, fixed in methanol and stained with crystal violet. Finally, cells attached through the matrigel were counted in five random (centre and at the borders) microscope field (200x).

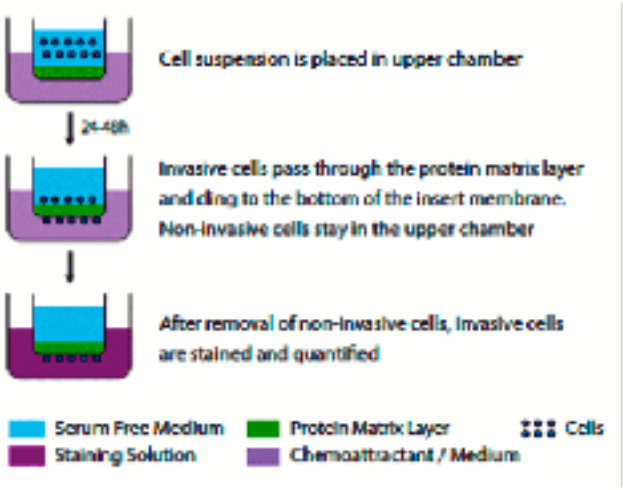

Figure 22. Schematic protocol for invasion assay.

3.8 Biochemical analysis

At the end of each treatment, SFT adherent cells were scraped off the plates using a plastic cell scraper, resuspended in 500µl of PLCLB lysis buffer (150 mM NaCl, 5% (vol/vol) glycerol,1% (vol/vol) Triton X-100, 1.5M $MgCl_2$, and 50mM Hepes; pH7.5) supplemented with protease inhibitors and maintain on constant agitation for 2 hours at 4°C. Then, cells were centrifuged in a microcentrifuge at 4°C for 30 minutes. The aspirated supernatants were place in fresh tubes kept on ice and the pellets were discarded. The whole protein lysates were preserved at -80°C. Equal amounts of protein were loaded into the wells of the SDS-PAGE gel (Bolt 4-12%, Invitrogen, Carlsbad, CA, USA), along with molecular weight marker (Precision plus protein

standards Dual Color, Biorad, Hercules, CA, USA). The gel ran for about 90 minutes at 150mV in running buffer. Proteins were then transferred on a PVDF membrane after 90 minutes running at 200mA in transfer buffer. The membrane was blocked for 30 minutes at room temperature (RT) using Bovine Serum Albumine (BSA)(Roche, Mannheim, Germany). The membrane was incubated with appropriate dilution of primary antibody (Table 3) in BSA with overnight incubation at 4°C. The membrane was washed three times with TBS with Tween20 (Biorad, Hercules, CA, USA) and incubated with the conjugated secondary antibody in BSA at RT for 1 hour. Images were acquire using darkroom development techniques for chemiluminescence (ECL western blotting reagents, GE Healthcare, Buckinghamshire, UK). To control for variability, actin was involved in normalization and densitometric analyses were carried out. Each filter was stripped using Restore Western Blot (ThermoScientific, Waltham, MA, USA) in order to re-incubate it with another primary antibody.

Antibody	Catalog #	Company	Dilution
EZH2	#5246	CellSignal	1:1000 BSA 5%
YY1	ab109237	Abcam	1:1000 BSA 5%
c-Myc	ab32072	Abcam	1:1000 BSA 5%
SLUG	#9585	CellSignal	1:1000 BSA 5%
Integrinβ3	ab75872	Abcam	1:1000 BSA 5%
HDAC2	ab32117	Abcam	1:1000 BSA 5%
MMP2	ab37150	Abcam	1:1000 BSA 5%
Actin	A2228	Sigma	1:3000 BSA 2%

Table 3. Antibodies used for biochemical analyses.

3.9 Photodynamic therapy (PDT)

SFT cells were incubated for 4 hours with curcumin and nanomicelles loaded with curcumin at concentrations of previous experiment reported above. In PDT experiments, SFT cells were exposed to 445nm blue laser

light (power density 150mW/cm^2, estimated average fluency of 9J/cm^2) (Klaser, Eltech K-Laser, Treviso, Italy). The distance between the laser and the 96wells-plate was intended to enable an identical distribution of light on each well (other 96wells-plates were no irradiated as control). After laser treatments cells were incubated at 37°C 5%CO_2 for 1 hour. Then, 10μM 2',7'-dichlorofluorescin diacetate (H_2DCFDA, #D399, Thermo Fischer Scientific, Waltham, MA, USA) was added to each well and then incubated for 30 minutes 37°C 5%CO_2 to evaluate ROS production. The dye solution was then replaced with DPBS and plates were read by means of spectrophotometer at 520nm. Moreover, MTT analyses were carried out on the same plates after DPBS washing. In order to investigated the ROS production, ratio ROS/n°viable cells was calculated. MTT analyses were carried out also after 24 hours.

4. Results

Various evidence has shown that curcumin, a natural compound, can inhibit tumor growth, metastasis formation and Epithelial-Mesenchymal Transition (EMT). Starting from this notion, a solitary fibrous tumor (SFT) cell line was treated with different concentrations of free-curcumin, in order to investigate its effects on cell viability, cell invasiveness and EMT markers expression.

Moreover, due to its low toxicity, curcumin could be administered in combination with other drugs, such as histonedeacetylase inhibitors (HDACi, i.e. Vorinostat, SAHA), which can inhibit migration and tumor growth. Therefore, another goal of this study will be the investigation of free-curcumin effect on EMT process, in combination with SAHA.

4.1 Free-curcumin

Curcumin uptake

Experimental design involved the confirmation of curcumin uptake by the SFT cells. The distribution of free-curcumin inside SFT cells was observed on fluorescent images obtained from a fluorescence microscopy with excitation wavelength of 488nm. As expected, weak green fluorescence intensity was observed for the sample treated with 10μM curcumin. The intensity of the signal was directly proportional to the amount of loaded curcumin (Fig.23).

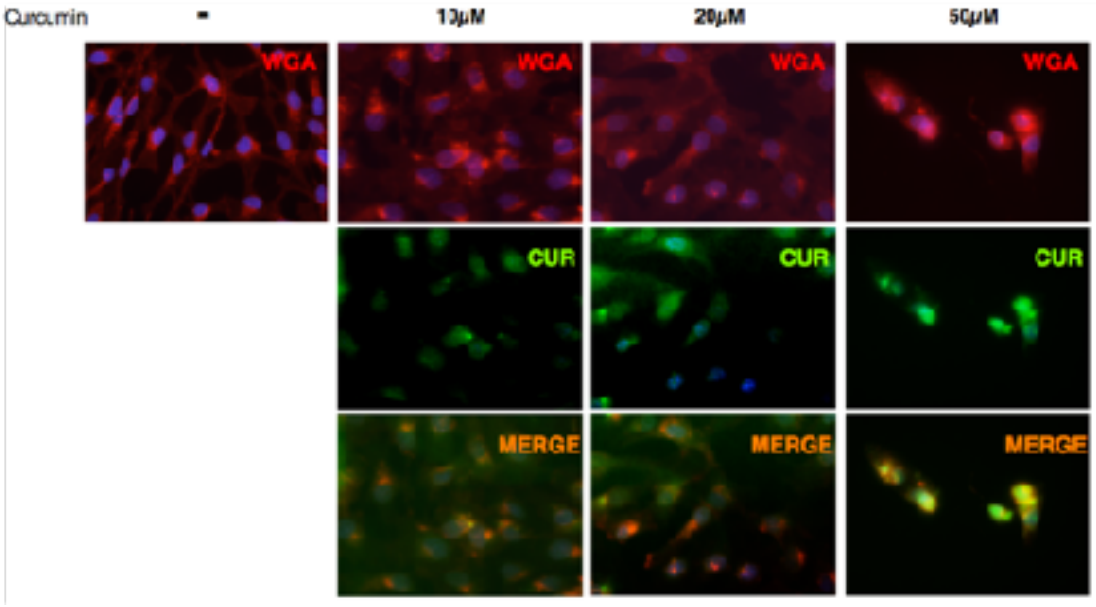

Figure 23. Free-curcumin uptake after 24 hours on SFT cells which were stained with red (WGA Alexa fluor 546) for plasma membranes and blue (DAPI) for nuclear counter stain. Curcumin autofluorescence was capture at 488nm (green) wavelength. Representative fields (magnification 40X).

Since curcumin resulted quantitatively accumulated in the cells, the next step was to verify the free-curcumin cytotoxic effect, in order to set up the working concentrations for further experiments.

Free-curcumin treatments reduce cell viability

The cytotoxic effect of free-curcumin treatments was determined by means of MTT assays, in which a wide range (2,5μM-50μM) of free-curcumin concentrations was investigated (Fig.24).

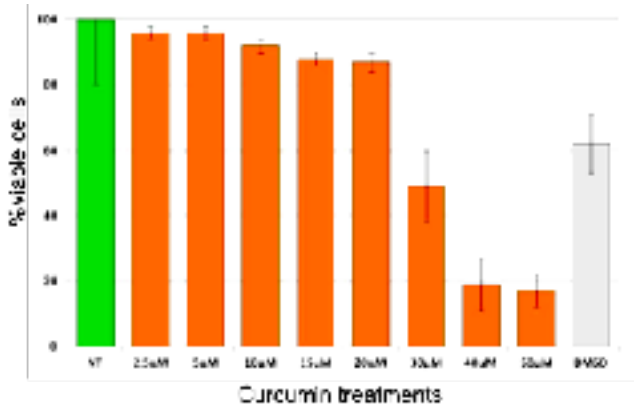

Figure 24. Viability of SFT cells treated with curcumin (2,5μM-50μM) after 24 hours was investigated by means of MTT assays. NT: not treated. DMSO was administered at the maximum concentration, as in 50μM curcumin treatment, in order to underline the cytotoxic effect of the DMSO used to dilute curcumin.

10μM, 20μM and 50μM of curcumin were established as working concentrations for further *in vitro* experiments: 10μM treatment induce no variation in cells viability, 20μM could induced a minimal decrease while 50μM effect strongly lower the number of viable cells. Indeed, increasing concentrations of curcumin were able to induce a cytostatic/cytotoxic effect on SFT cell line as reported in Fig.25. In the first 24 hours of treatment with the highest concentration of curcumin (50μM), the number of viable cells was strongly reduced and the remaining cells showed yellow-coloured aspect, because of the huge amount of curcumin internalized (Fig.25).

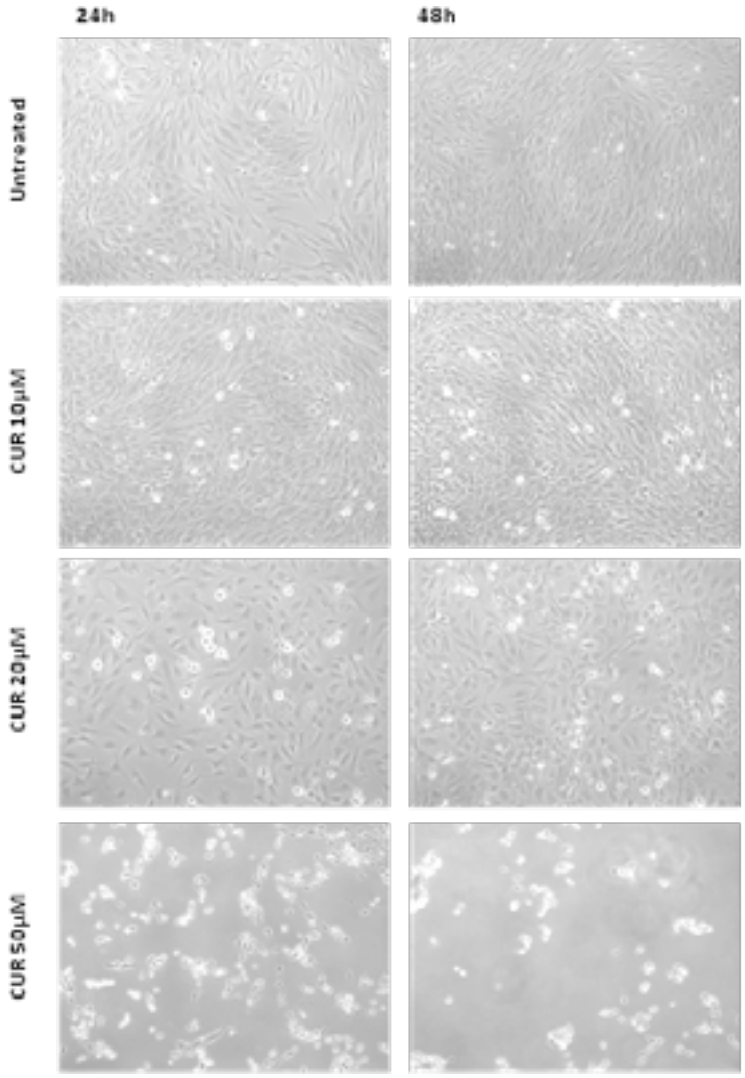

Figure 25. Effect of curcumin treatments (10-50μM) after 24 and 48 hours on SFT cells proliferation and cell death. Representative fields (magnification 20X).

Another important feature of cancer cells is their invasive potential. Indeed, invasion is the crucial step in the progression of cancer metastasis. Starting from the above working concentrations of free-curcumin, invasion assay were set up.

Curcumin reduces SFT invasiveness

The capacity of SFT cells to invade through Matrigel, an artificial extracellular matrix (ECM), was measured following 10μM/20μM/50μM free-curcumin treatments. Then, 10μM curcumin exposure resulted in a 50% reduction in cell invasion, while 50μM curcumin treatment reached a 99% reduction. Histogram analysis reported that fewer cells passed through the filters coated with an artificial ECM, suggesting that the invasive potential of SFT cells was impaired (Fig.26).

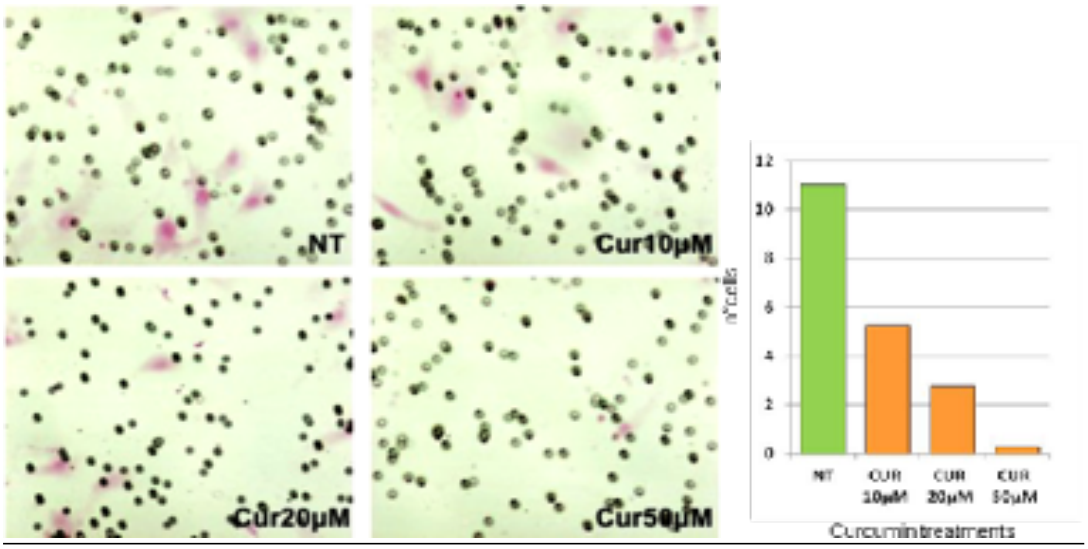

Figure 26. Cell invasive assay. SFT cells treated with 10-50μM curcumin. Representative fields of invasive cells on the membrane (magnification 200X, left panel) and the average number of migratory cells per field (right panel). NT: not treated sample.

As confirmed by these experiments, free-curcumin is able to inhibit the cancer cells invasive potential. This effect on invasiveness may be due to the curcumin action on specific pathways involved in metastasis initiation, may be related to EMT. To this aim, EMT markers expression status has been investigated in SFT cell line treated with free-curcumin.

Curcumin decreases EMT markers expression

EZH2, YY1, c-Myc, SLUG and integrin β3 expression was investigated by means of WB analyses. EZH2 expression resulted null after 50μM curcumin treatment. It is worth mentioning the quite restored of EZH2 and YY1 expression after 48 hours of treatment with 10μM and 20μM curcumin, possibly due to the fact that no fresh DMEM with curcumin has been added after the first 24 hours. c-Myc was characterized by a very low expression level after all treatments, with both 10μM and 20μM curcumin. By contrast, the higher concentration of 50μM curcumin wasn't able to abrogate its expression, which was weak but still present. SLUG was less expressed after only 24 hours with 10μM curcumin treatment. Its expression level was directly proportional to the concentration of curcumin treatment administered. Integrin β3 protein expression was not affected by any curcumin treatments, except the more concentrated (50μM) (Fig.27). In order to make WB data more explicit, densitometric analyses were performed on the entire WB filters (Fig.28).

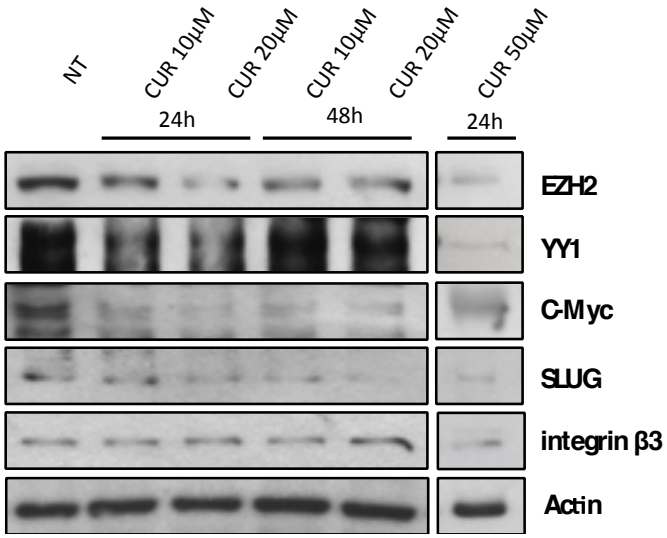

Figure 27. Curcumin treatments. SFT cell line protein extracts were analyzed by direct WB for the expression of EZH2, YY1, c-Myc, SLUG and integrinβ3. WB anti-actin antibody was used for loading control. NT: not treated sample.

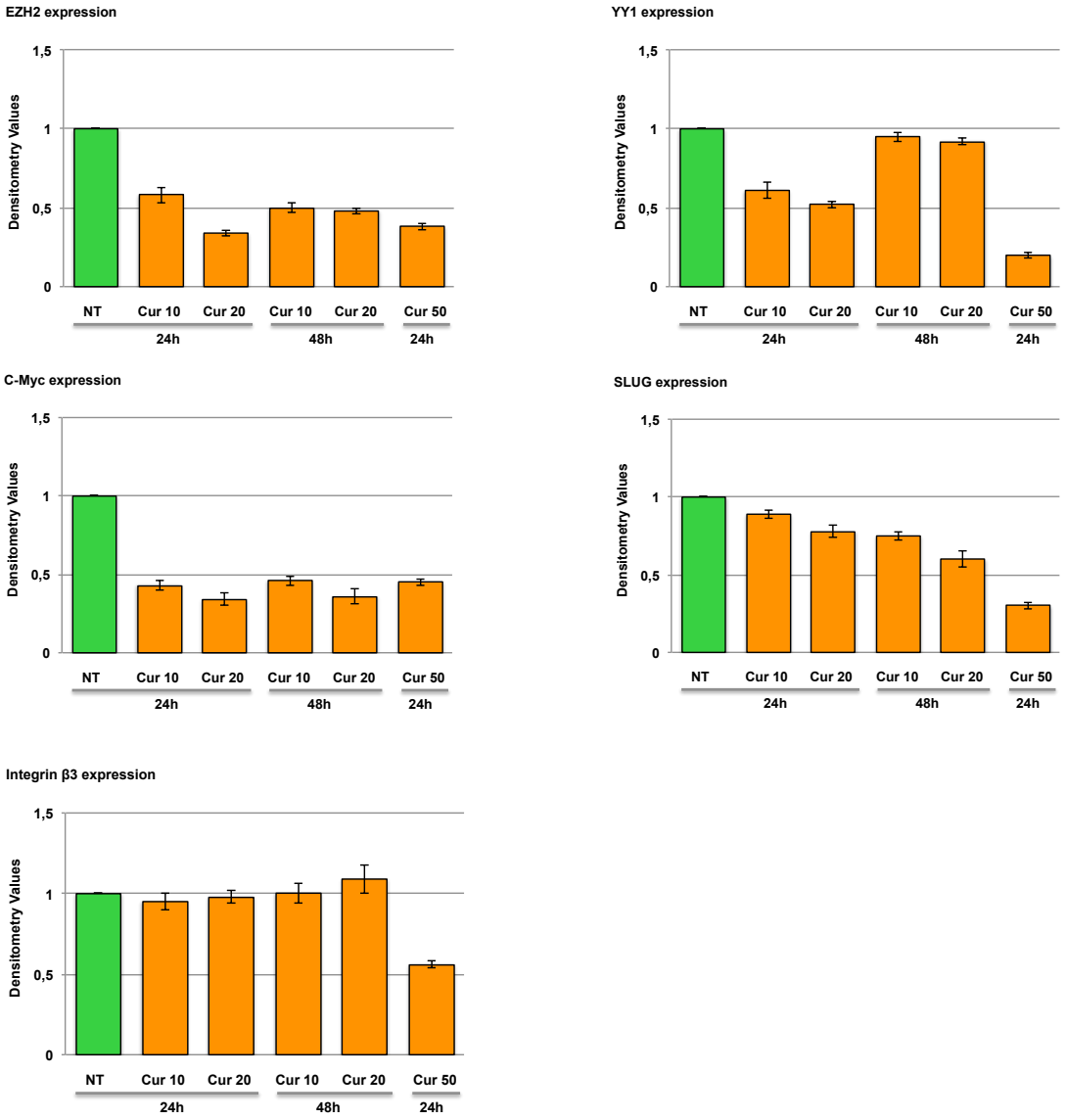

Figure 28. Densitometric analyses of WB experiments. Levels of each protein are expressed as normalized values in comparison with the not treated (NT) sample.

The expression of the mesenchymal marker vimentin, often associated with the loss of the epithelial marker E-cadherin, was investigated by means of IHC on cytoblocks obtained from SFT cell line. Previous studies have shown that vimentin is upregulated in several types of cancer with poor prognoses, which highly correlated with the upregulation of the EMT-related transcription factor, SLUG, and the downregulation of the adherent protein,

E-cadherin. As shown in Fig 29, curcumin 50μM treatment has led to a slight reduction in vimentin expression.

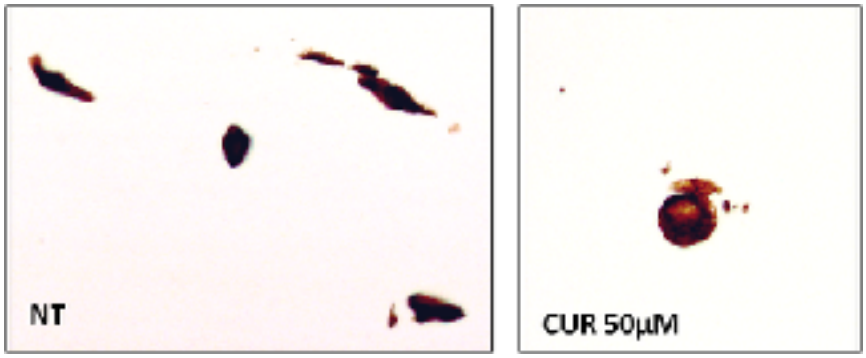

Figure 29. Vimentin IHC on SFT cytoblocks. NT: not treated sample.

In order to understand if a combined treatment using SAHA could be effective on SFT cells, MTT assay and biochemical analyses were performed. Lin and colleagues (2012) reported the efficacy of combined treatment with free-curcumin and SAHA in inhibiting migration, tumor growth and metastasis formation in xenografts. To determine whether SAHA can enhance the growth inhibition of SFT cells by curcumin, cells were treated with different concentrations of SAHA or free-curcumin alone or in combination.

Effect of combined treatment with free-curcumin and SAHA on cell viability

After 24 hours of combined treatment no significant reduction in cell viability was observed by MTT assay. Furthermore, 48 hours of SAHA 5μM administered with curcumin 10/20/50μM mainly exerted a significant reduction of viable cells although combined treatment induces an increase

in cell viability at any increased concentration of curcumin administered (Fig.30).

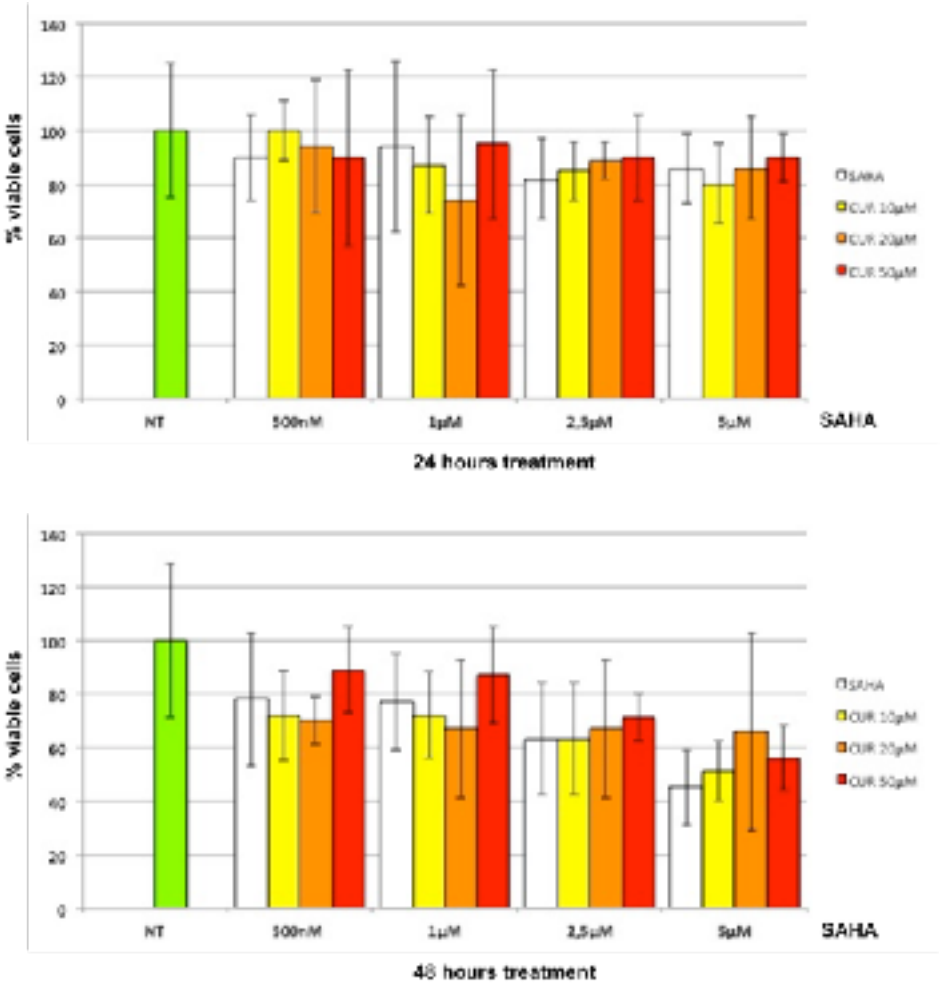

Figure 30. Viability of SFT cells treated with SAHA, curcumin and combined treatments for 24 hours (upper panel) and 48 hours (lower panel), investigated by means of MTT assays. NT: not treated sample.

Since the combination of SAHA and free-curcumin did not lead to a significant cytotoxicity improvement, it was thought that the combined treatment could impair the curcumin uptake.

Curcumin uptake during combined treatment with SAHA

The distribution of curcumin inside SFT cells was observed by fluorescence microscopy with excitation wavelength of 488nm. The intensity of the signal increased directly proportional to the concentration of curcumin administered. Moreover, taking advantage of wheat germ agglutinin (WGA), which selectively recognizes the plasma membrane, changes in the structure of SFT cells after SAHA treatment were observed as well as curcumin site of accumulation. SFT cells showed epithelial features and, nevertheless, they appear less spindle compared to the untreated sample (Fig.31).

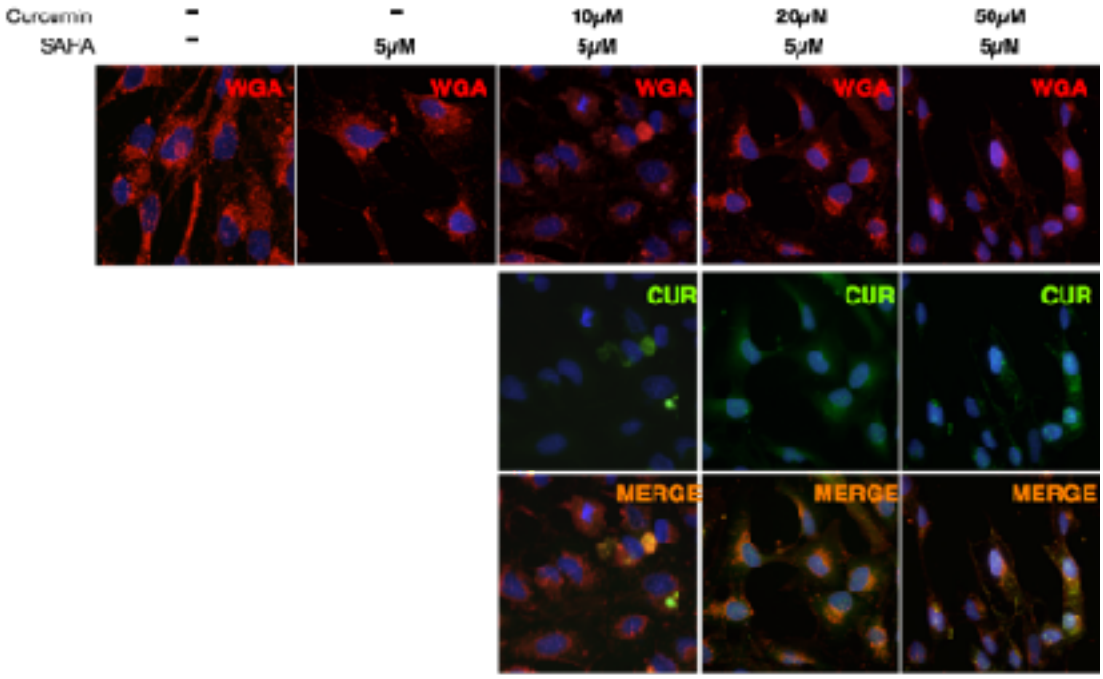

Figure 31. Effect of SAHA, curcumin and combined treatments (curcumin and SAHA) after 24 hours on SFT cells which were stained with red (WGA Alexa fluor 546) for plasma membranes and blue (DAPI) for nuclear counter stain. Curcumin autofluorescence was capture at 488nm (green) wavelength. Representative fields (magnification 40X).

HDAC inhibitors, like SAHA, can modulate a variety of cellular functions including growth, differentiation, and survival due, in part, to their ability to enhance acetylation of a wide range of proteins, including transcription factors, molecular chaperones, and structural components. Phalloidin immunofluorescence (IF) is a useful tool for investigating the distribution of F-actin fibers and then to investigate changes in cellular structure. IF carried out on SFT cells underlines a partial reversal of the mesenchymal phenotype, as evidenced by a shift from spindle shaped cells with visible actin stress fibers to predominantly cuboidal shape, following 24 hours os treatment (Fig.32).

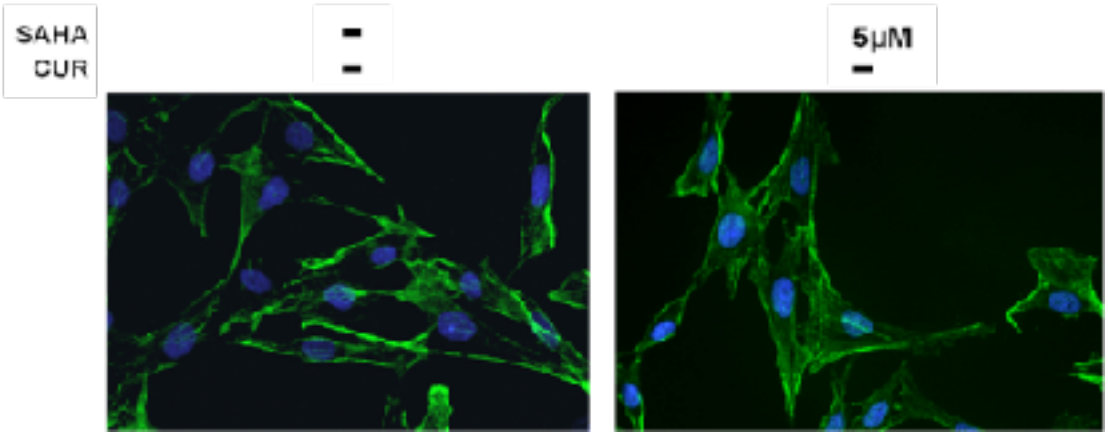

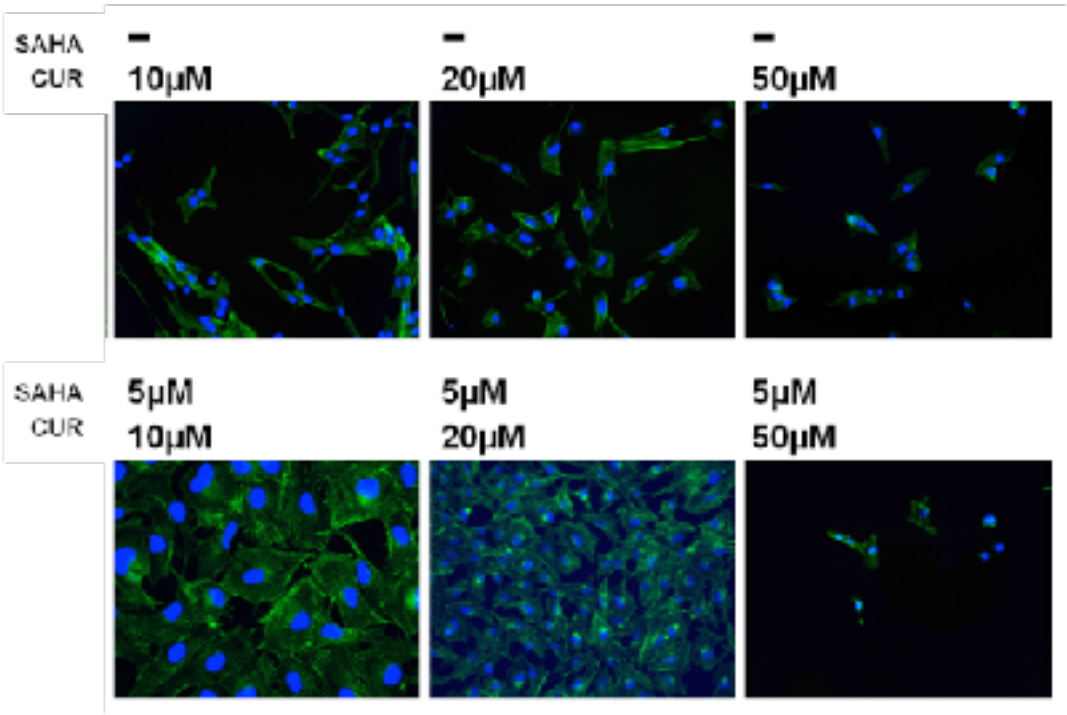

Figure 32. Effect of SAHA, curcumin and combined treatments (curcumin and SAHA) after 24 hours on SFT cells which were stained with green (phalloidin Alexa fluor 488) for actin filaments and blue (DAPI) for nuclear counter stain. Representative fields (magnification 100X and 40X).

Starting from these results obtained after the combined treatment, which showed an early inhibition of EMT process without any significant increase in cell death, the invasive potential of SFT cells was investigated.

Invasiveness potential of SFT cells after combined treatments with curcumin and SAHA

Curcumin combined with SAHA showed no increasing therapeutic efficacy when compared with the corresponding free-curcumin treatment alone in SFT cells (Fig.33).

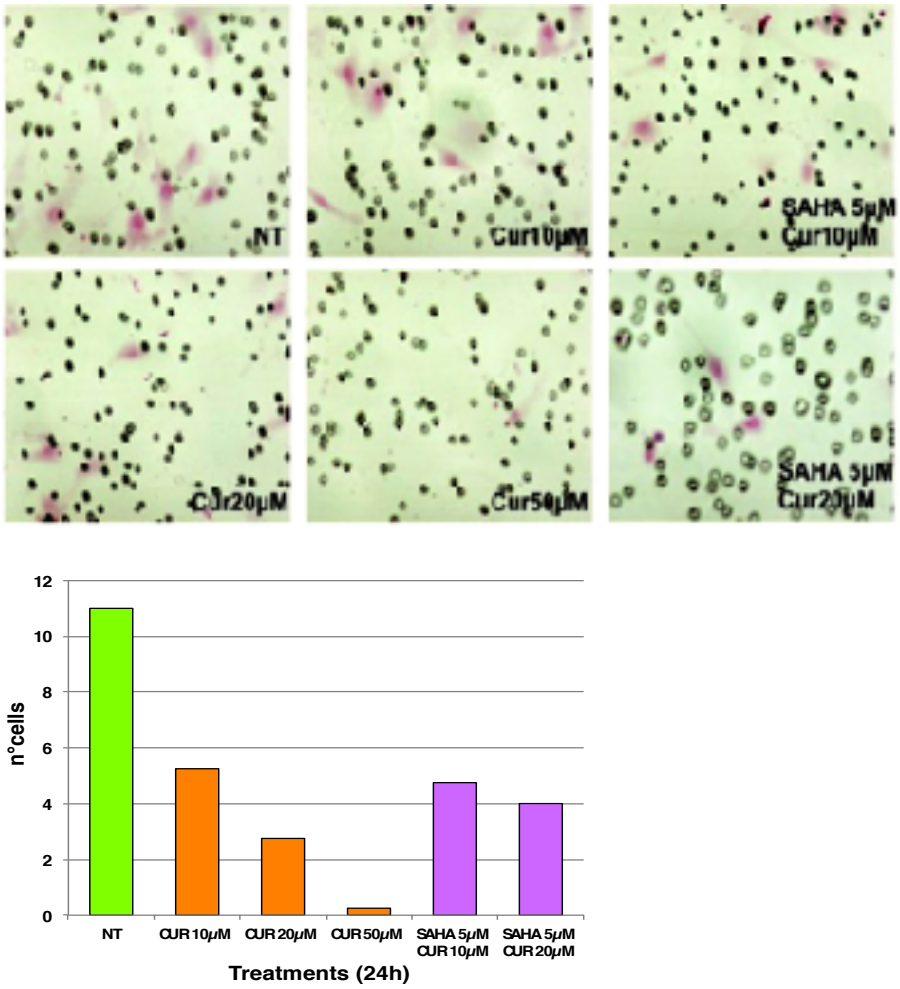

Figure 33. Cell invasive assay. Representative fields of invasive cells on the membrane (magnification 200X, upper panel) and the average number of migratory cells per field (lower panel).

In vitro free-curcumin-SAHA combined treatments

SAHA and/or curcumin suppressed cell growth by decreasing proliferation and increasing cell death. An increased number of death cells was obtained after 48 hours of treatment with SAHA alone or in combination (Fig.34).

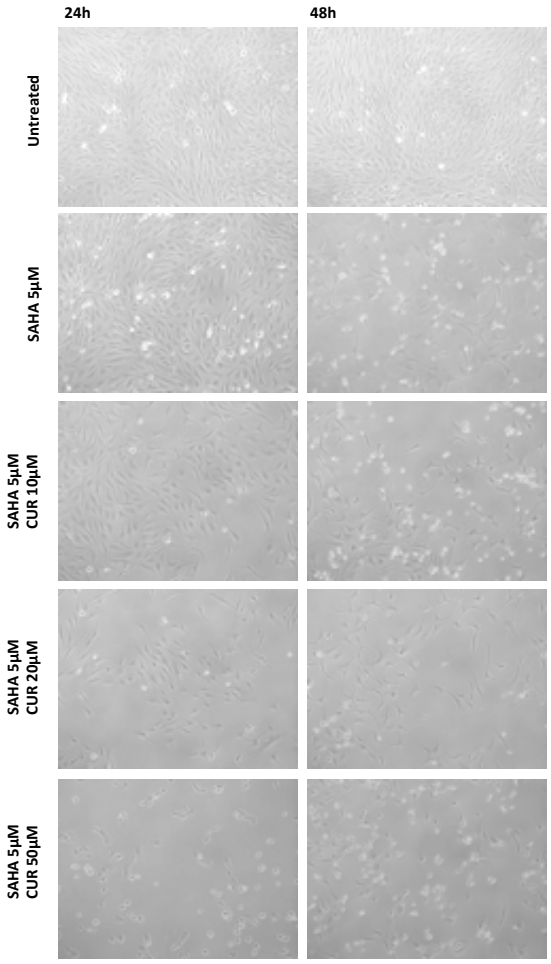

Figure 34. Effect of curcumin and SAHA alone or in combined treatments after 24 and 48 hours on cell proliferation and cell death. Representative fields (magnification 20X).

Since SAHA main target is represented by HDAC2, biochemical analyses were performed in order to investigate HDAC2 expression status. Moreover as reported in literature, SAHA could inhibit the expression of metalloproteinase-2 (MMP2), which play a pivotal role in extracellular matrix (ECM) degradation, promoting invasiveness and metastasis formation.

Free-curcumin treatment: expression status of HDAC2 and MMP2

Curcumin alone was not able to significantly reduce HDAC2 or MMP2 expression, but administering its higher concentration of 50µM.

Furthermore, MMP2 was characterized by a low expression after 20μM curcumin treatments (Fig.35). Moreover, densitometric analyses were performed on the entire WB filters (Fig.36).

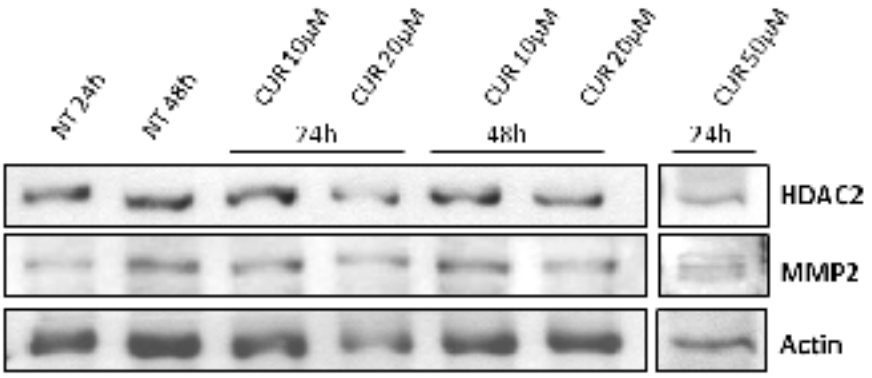

Figure 35. Effect of curcumin treatments after 24 and 48 hours on HDAC2 and MMP2 expression investigated by means of WB analysis. Treated cells were compared with the untreated (NT) cells as control.

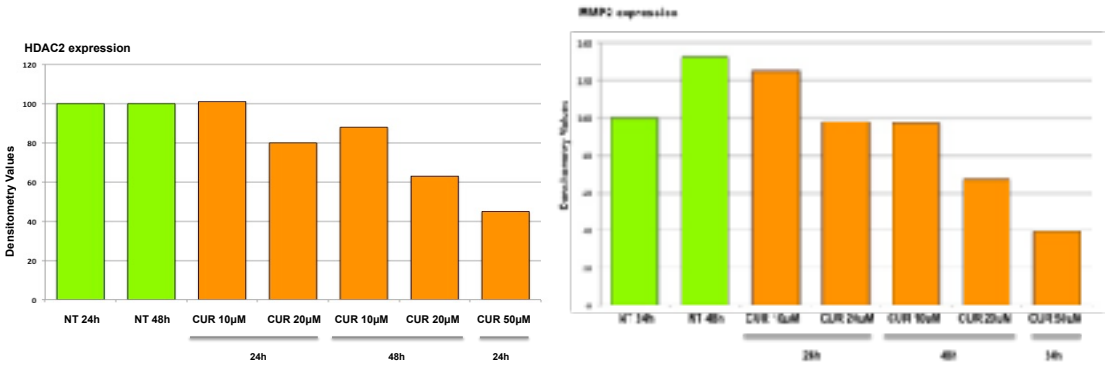

Figure 36. Densitometric analyses of curcumin WB experiments. Levels of each protein are expressed as normalized values in comparison with the not treated (NT).

Curcumin-SAHA combined treatment: expression status of HDAC2 and MMP2

To determine whether SAHA can enhance curcumin effect on HDAC2 and MMP2 expression, 5μM SAHA was administered in combination with 10-20

and 50μM for 24 and 48 hours. Unfortunately, the combined treatment increased both HDAC2 and MMP2 levels. SAHA alone, on the other hand, decrease MMP2 expression (Fig.37). Moreover, densitometric analyses were performed on the entire WB filters (Fig.38).

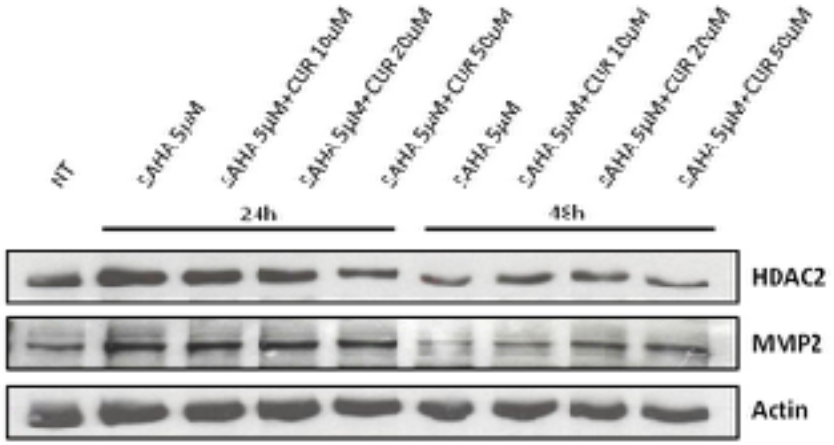

Figure 37. Effect of curcumin and SAHA treatments after 24 and 48 hours on HDAC2 and MMP2 expression investigated by means of WB analysis. Treated cells were compared with the untreated (NT) cells as control.

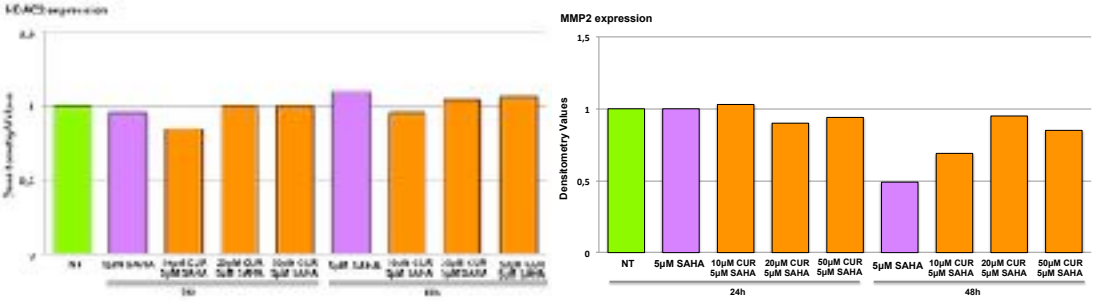

Figure 38. Densitometric analyses of curcumin and SAHA WB experiments. Levels of each protein are expressed as normalized values in comparison with the not treated (NT).

These results shed light on the efficacy of free-curcumin treatment that can induce epigenetic modifications, such as EMT marker expression status, leading to the inhibition of tumor growth and metastases formation. During

EMT process, the tumor cell loses its epithelial characteristics, such as polarization, intercellular junctions, cytoskeletal structure, to acquire mesenchymal properties that confer invasiveness, migration and ultimately the formation of metastasis and drug resistance. The reduced expression of EMT specific markers was found after 50μM free-curcumin treatment administered for 24hours. Unfortunately, such concentration, *in vivo*, could result in heavy side effects. The application of nanotechnologies (nanomicelles) could result in a reduction of the expression of these specific EMT markers, administering curcumin doses significantly lower than free-curcumin alone. For this purpose, C_{16}-DAPMA, C_{16}-SPD and C_{16}-SPM nanomicelles have been used to self-assemble in micelles encapsulating the curcumin within their inner core. Nanomicelles were then administered to SFT cell line initially omitting the curcumin encapsulation inside and subsequently an initial MTT analysis was performed to evaluate the intrinsic cytotoxic potential of these nanomicelles.

4.2 Nanomicelles

Nanomicelles show low intrinsic toxicity

Starting with the notion that bulky amount of curcumin can't be administered to patients, because of their heavy side effects, nanomicelles appeared to be a solution. Indeed, nanomicelles were encapsulated with a low concentration of curcumin and then, their effectiveness on SFT cell line and, in particular, on the EMT markers expression was evaluated. Firstly, nanomicelles intrinsic toxicity was investigated on SFT cell line in order to avoid misreading in data interpretation. It is well known that nanostructures could be cytotoxic themselves. C_{16}-DAPMA, C_{16}-SPD and C_{16}-SPM were

diluted at the concentration of 500nM and 1μM, without any curcumin encapsulations (blank-nanomicelles). C_{16}-SPM resulted the less toxic nanomicelles, even if also the other nanostructures didn't affect significantly cell viability (Fig.39).

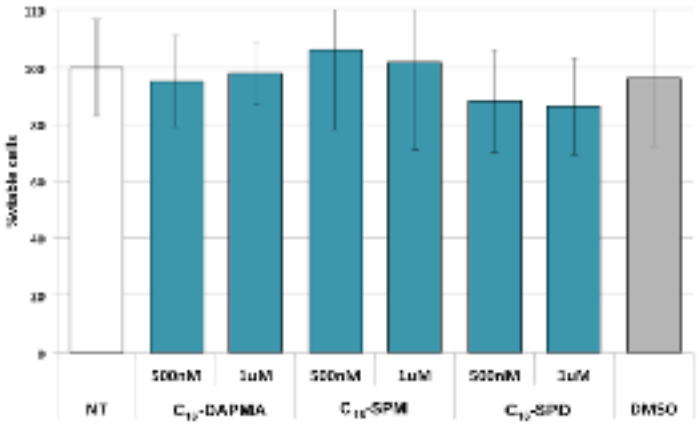

Figure 39. Viability of SFT cells treated with blank-nanomicelles (500nM-1μM) for 24 hours investigated by means of MTT assays. NT: not treated sample. DMSO was administered at the maximum concentration, as in 1μM blank-nanomicelles treatment, in order to underline the cytotoxic effect of the DMSO used to dilute the nanomicelles.

Given the bio-safety of the blank-nanomicelles, following experiments were carried out after curcumin encapsulation, using all the three kind of nanomicelles. Firstly, nanomicelles encapsulated with curcumin were tested in order to determine if, despite using a very low amount of curcumin, a significant antitumor effect would be achieved.

Nanomicelles encapsulated with curcumin decrease SFT cells viability

MTT assays were carried out with nanomicelles encapsulated with curcumin at 10μM, 5μM, 2,5μM and 1μM. In parallel, the same amount of free-

curcumin alone was administered to the SFT cell line for 24 hours. C_{16}-DAPMA and C_{16}-SPD resulted to be more effective on SFT cells viability rather than the same concentration of curcumin alone treatments. C_{16}-SPM reduced in a less significant way SFT cell viability than the other nanomicelles (Fig.40).

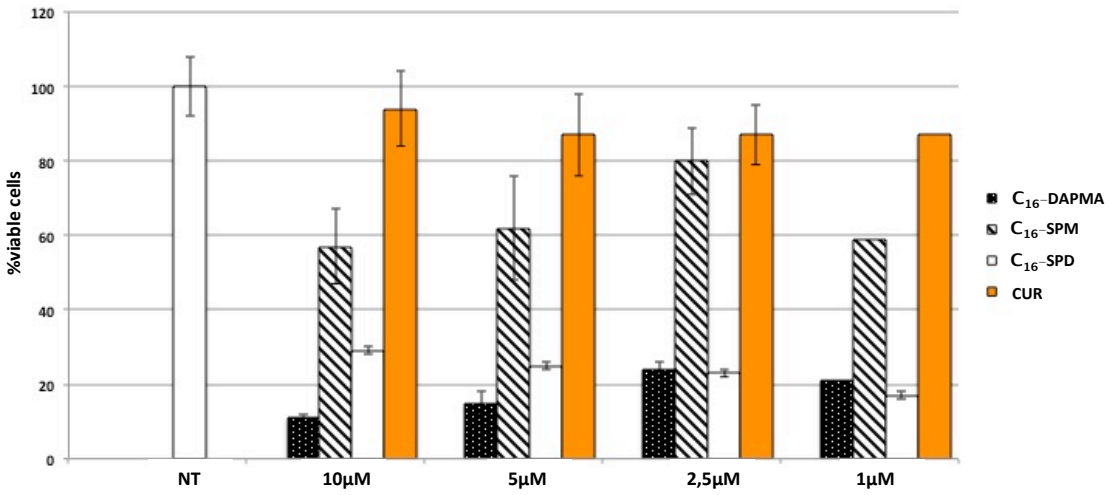

Figure 40. Viability of SFT cells treated with nanomicelles (C_{16}-DAPMA, C_{16}-SPD and C_{16}-SPM) and curcumin alone as reference was investigated by means of MTT assays. SFT cells were treated for 24 hours with curcumin alone or encapsulated into nanomicelles. NT: not treated sample.

Moreover, C_{16}-DAPMA, C_{16}-SPD and C_{16}-SPM encapsulated with curcumin were diluted at 500nM and 1µM, as done before for MTT assays with blank-nanomicelles for 24 hours. Results reported in Fig.41 confirmed their effect on SFT cells.

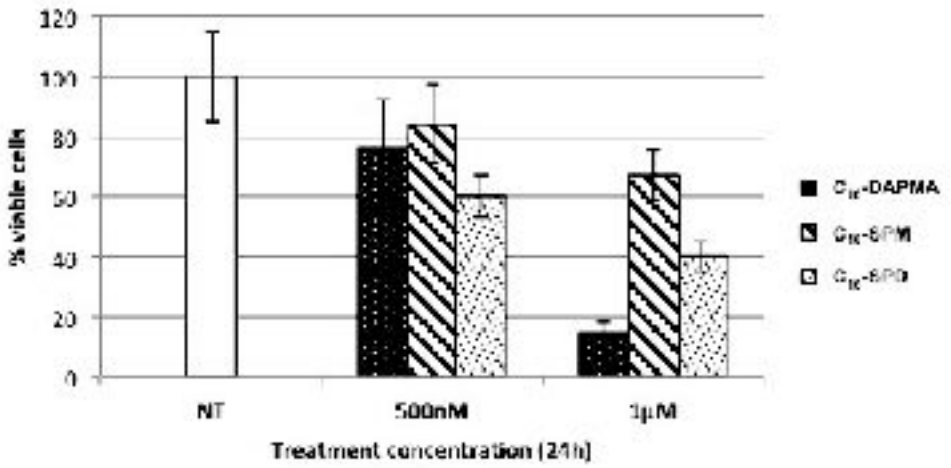

Figure 41. Viability of SFT cells treated with nanomicelles (C_{16}-DAPMA, C_{16}-SPD and C_{16}-SPM) investigated by means of MTT assays. SFT cells were treated (500nM-1µM) for 24 hours with nanomicelles encapsulated with curcumin. NT: not treated sample.

Moreover, experimental design involved the confirmation of curcumin uptake by the SFT cells after nanomicelles treatments. The purpose of this further uptake experiments was to confirm that, despite only 500nM and 1µM of curcumin was encapsulated, a corresponding amount was internalized by SFT cells.

Curcumin uptake during combined treatment with C_{16}-DAPMA, C_{16}-SPD and C_{16}-SPM

The distribution of curcumin inside SFT cells was observed by fluorescence microscopy with excitation wavelength of 488nm. The amount of curcumin detected inside cells was comparable to treatment with free-curcumin 50µM, although here the concentrations administered were considerably reduced (500nM and 1µM) (Fig.42).

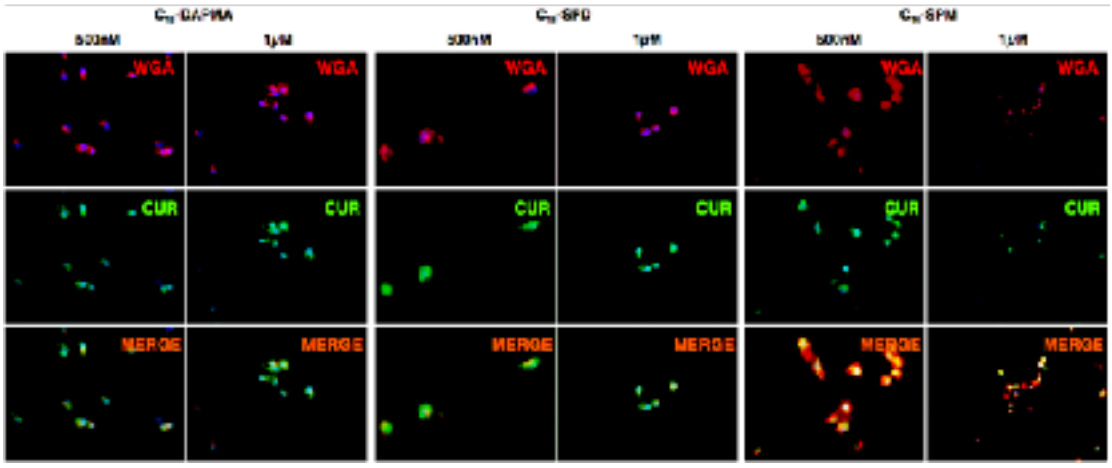

Figure 42. Effect of nanomicelles after 24 hours on SFT cells which were stained with red (WGA Alexa fluor 546) for plasma membranes and blue (DAPI) for nuclear counter stain. Curcumin autofluorescence was capture at 488nm (green) wavelength. Representative fields (magnification 40X).

Taking advantage of these preliminary results after nanomicelles encapsulated with curcumin treatment, which have allowed to obtain a considerable curcumin uptake, the experimental design have progressed with the analysis of each single nanomicelle. As for free-curcumin, nanomicelles encapsulated with curcumin were investigated in order to asses their invasive-inhibiting potential, their cytotoxic/cytostatic activity *in vitro* and their effect on EMT marker expression after 24 and 48 hours of treatment.

4.2.1 C_{16}-DAPMA

C_{16}-DAPMA encapsulated with curcumin abrogate cell invasiveness

To validate the effect of C_{16}-DAPMA encapsulated with curcumin, invasion assay was performed on SFT cells after 24 hours of nanomicelles exposure (500nM and 1μM). C_{16}-DAPMA significantly inhibited cell invasiveness, while untreated sample migrated promptly through the matrigel. (Fig.43).

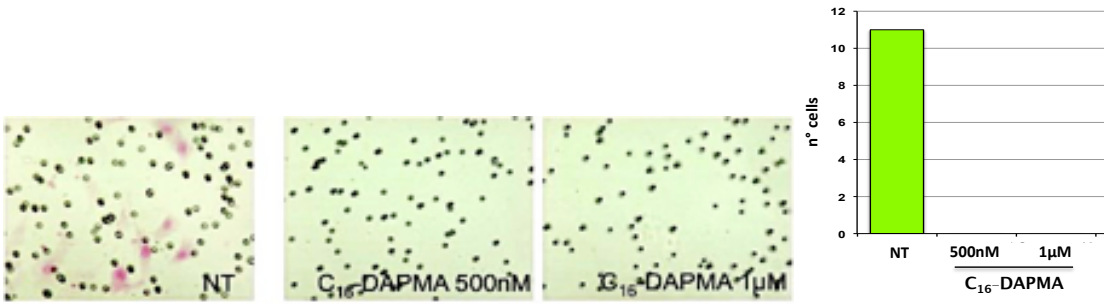

Figure 43. Cell invasive assay. Representative fields of invasive cells on the membrane (magnification 200X, left panel) and the average number of migratory cells per field (right panel). NT: not treated sample.

C_{16}-DAPMA encapsulated with curcumin reduced SFT cells viability

In vitro experiments carried out with 500nM and 1μM C_{16}-DAPMA treatments for 24 and 48 hours have evidenced their cytostatic/cytotoxic action on SFT cell line. Treatment with C_{16}-DAPMA resulted in higher cell death compared to blank-nanoparticles treatment and the untreated cells (Fig.44).

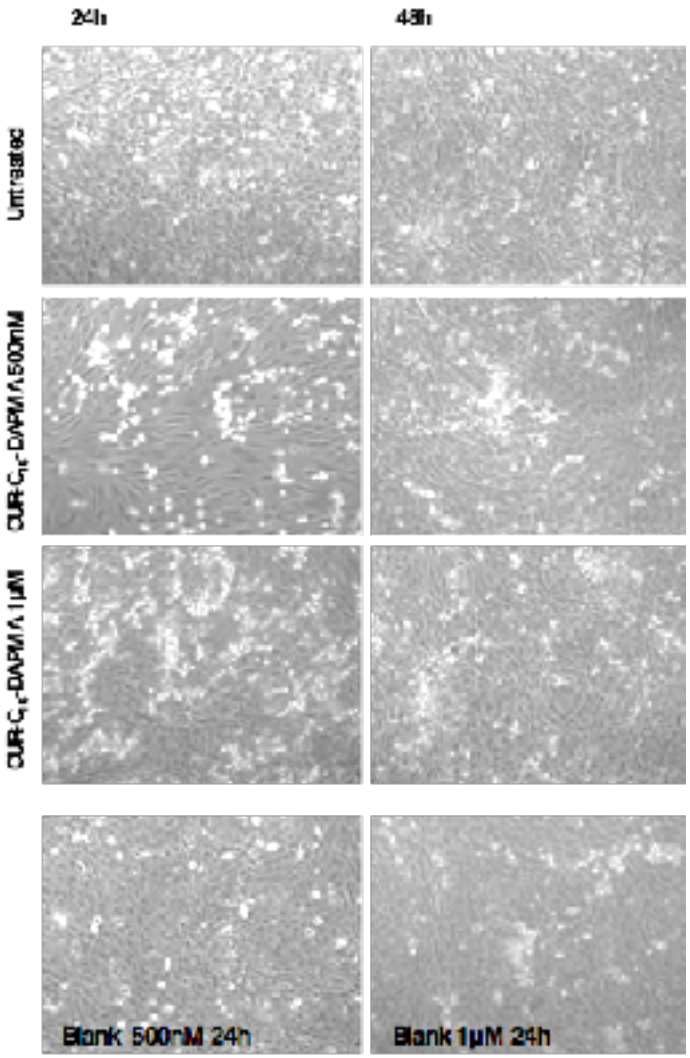

Figure 44. Effect of C_{16}-DAPMA treatments (500nM-1µM) after 24 and 48 hours on cell proliferation and cell death. Representative fields (magnification 20X). Blank-nanomicelles were used as control for nanomicelles intrinsic cytotoxic/cytostatic effect for 24 hours.

C_{16}-DAPMA encapsulated with curcumin slightly reduce EMT markers expression

WB analyses revealed that SFT cells expressed lower amount of EMT markers after 48 hours of treatment, but the integrin β3, which turned out to be only slightly reduced. EZH2 and YY1 resulted lower expressed after 24 hours of treatment with C_{16}-DAPMA and this decreased expression was

maintained till the end of the treatment. Nanomicelles treatment slightly decreased the expression of c-Myc after 48 hours while SLUG expression decreased after 24 hours of treatment and it was quite abrogated after 48 hours. Blank-nanomicelles didn't affect EMT markers expression (Fig.45). Moreover, densitometric analyses were performed on the entire WB filters (Fig.46).

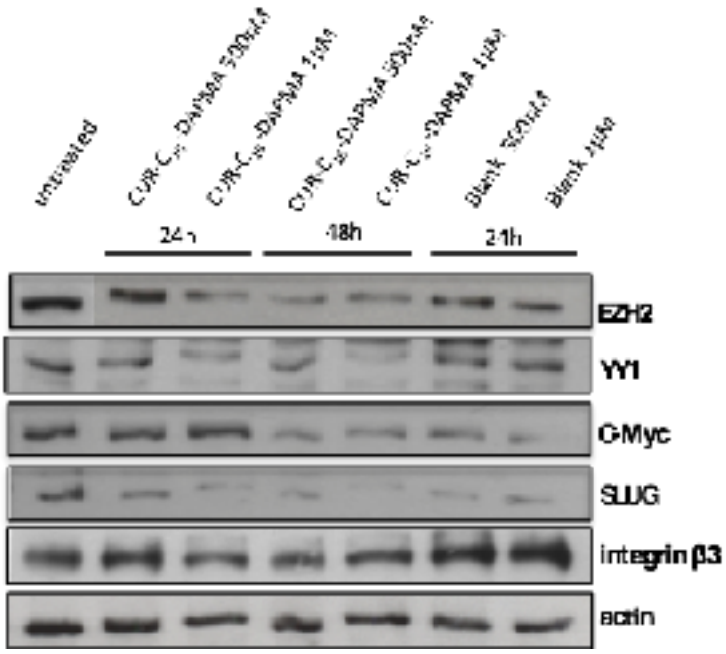

Figure 45. Effect of C_{16}-DAPMA treatments after 24 and 48 hours on EMT markers expression investigated by means of WB analysis. Treated cells were compared with the blank-nanomicelles treatment and the untreated cells as control.

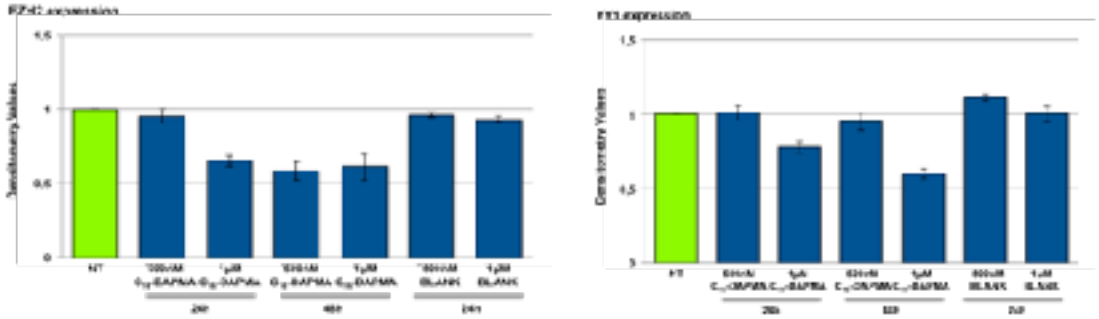

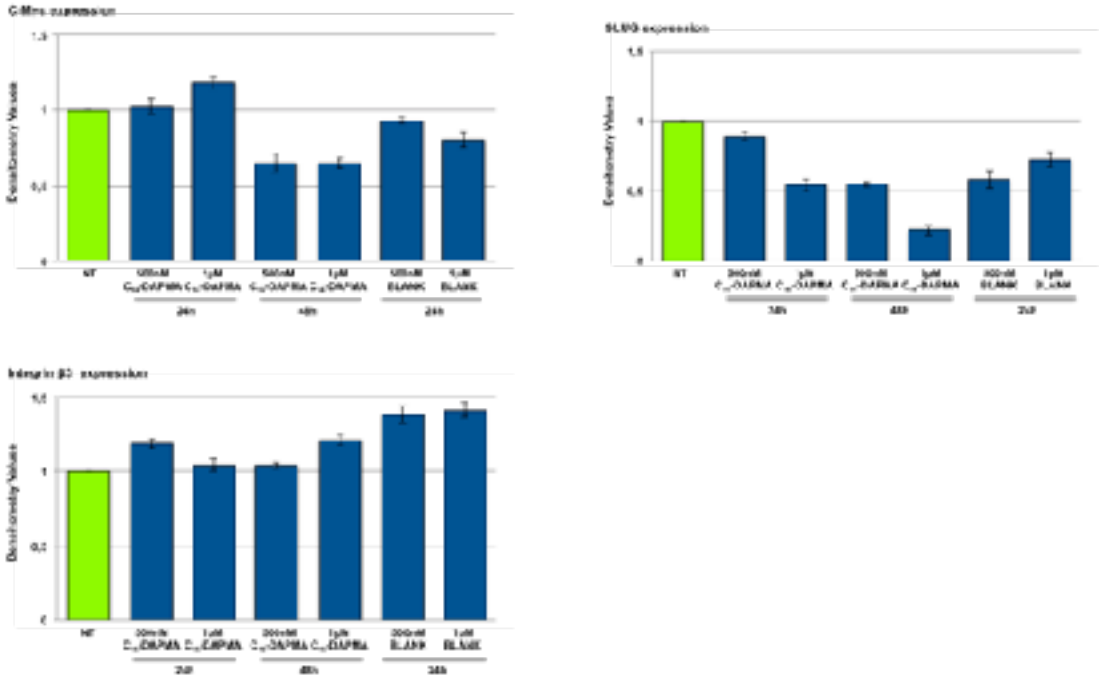

Figure 46. Densitometric analyses of C_{16}-DAPMA WB experiments. Levels of each protein are expressed as normalized values in comparison with both the not treated (NT) and the blank-nanomicelles samples.

Moreover, vimentin expression was evaluated by means of IHC. Unfortunately, C_{16}-DAPMA 1μM nanomicelles treatment did not affect its expression status (Fig.47), despite a slight change in cell structure, which appears to be more round shaped.

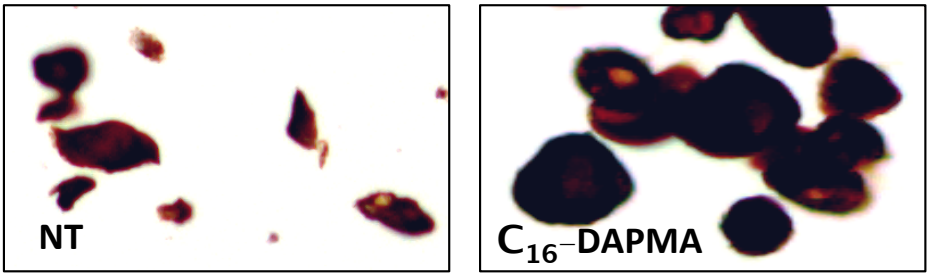

Figure 47. Vimentin IHC on SFT cytoblocks. NT: not treated sample.

As previously investigated for free-curcumin, C_{16}-DAPMA were administrated to SFT cells in combination with SAHA, in order to analyzed their effect on cell viability, since the previous combined treatment with free-curcumin resulted inefficient in increasing cell death. Here, by means of MTT assay, cell viability after combined treatment will be evaluated.

Cell viability after combined treatments (C_{16}-DAPMA and SAHA)

To determine the sensitivity of SFT cell line to the cytotoxic/cytostatic effects of the combined treatment, the cells were seeded into the microplates and incubated with 500nM/1μM concentrations of C_{16}-DAPMA and 5μM SAHA for 24 hours. As shown in Fig.48, the combined treatments with C_{16}-DAPMA worked, surprisingly, as growth stimulator.

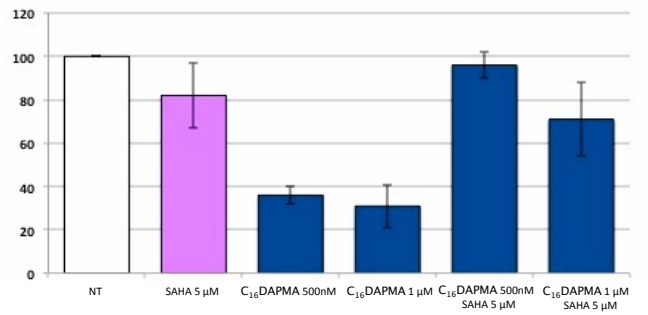

Figure 48. Viability of SFT cells treated for 24 hours with C_{16}-DAPMA and SAHA, investigated by means of MTT assays. NT: not treated sample.

As done before for the combined treatment with free-curcumin and SAHA, phalloidin IF evidenced the distribution of F-actin fibers and the changes in cellular structure after C_{16}-DAPMA/SAHA treatment. Combined treatments involved a strong decrease of viable cells. Nevertheless, SFT cells exhibited partial reversal of the mesenchymal phenotype, as evidenced by a shift from spindle shaped cells with visible actin stress fibers to predominantly epitheliod-like shape, following 24 hours treatment. The phalloidin signal

intensity tended to decrease after treatments, while SFT cells assumed more epithelial-like features before dying (Fig.49).

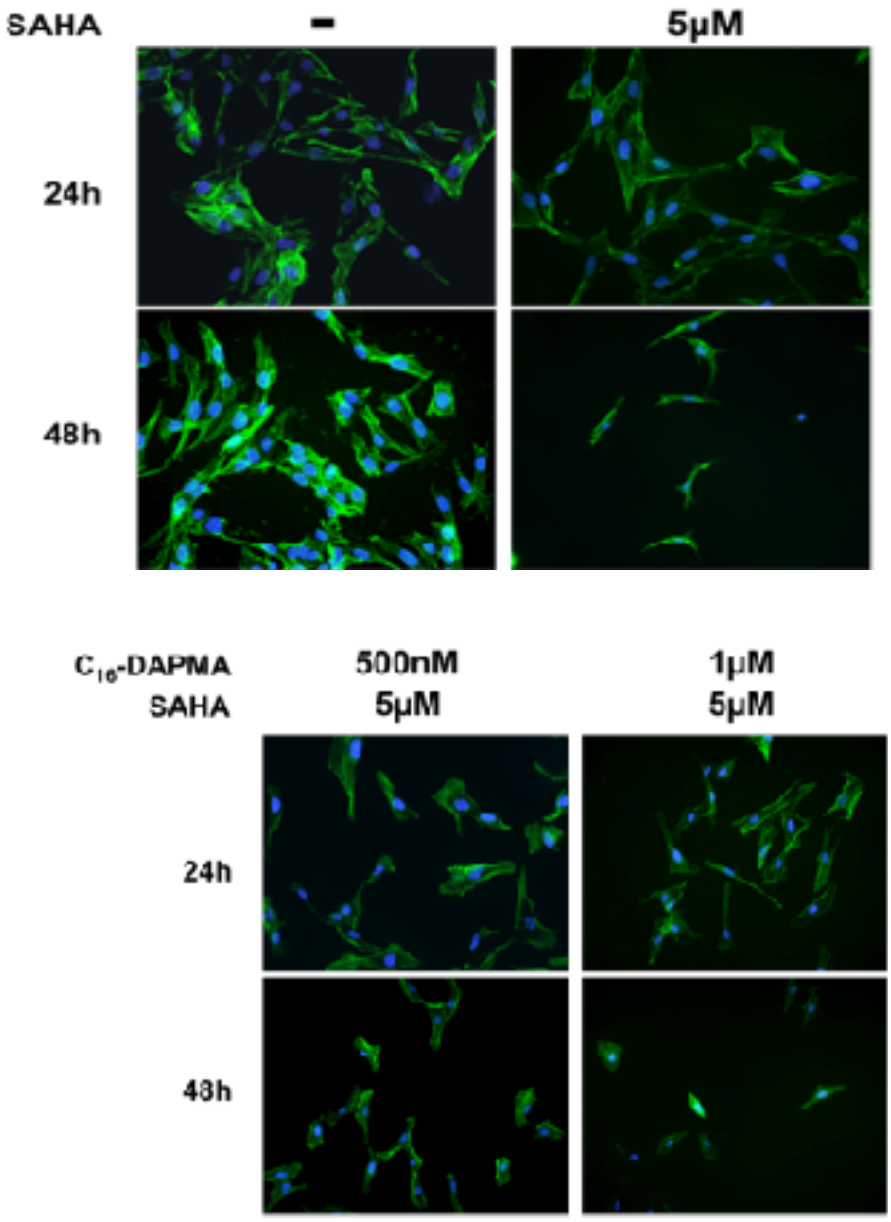

Figure 49. Effect of SAHA, C_{16}-DAPMA and combined treatments (C_{16}-DAPMA and SAHA) after 24 and 48 hours on SFT cells which were stained with green (phalloidin Alexa fluor 488) for actin filaments and blue (DAPI) for nuclear counter stain. Representative fields (magnification 100X).

To validate the effect of C_{16}-DAPMA encapsulated with curcumin in combination with SAHA on cell behaviour, an invasion assay was performed on SFT cells after 24 hours of nanomicelles exposure (500nM and 1μM). The number of cells still characterized by invasive potential was found to be very high (Fig.50), unexpectedly, since treatment with C_{16}-DAPMA alone had abolished this invasiveness (see Fig.43).

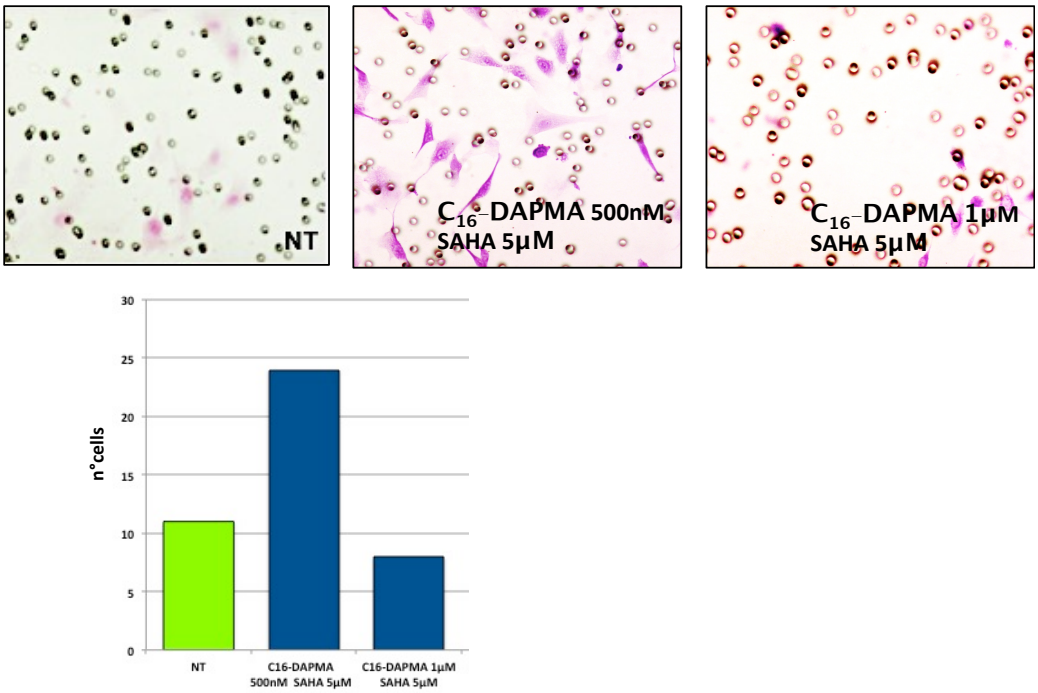

Figure 50. Cell invasive assay. Representative fields of invasive cells on the membrane (magnification 200X, upper panel) and the average number of migratory cells per field (lower panel). NT: not treated sample.

In vitro C_{16}-DAPMA and SAHA treatments

C_{16}-DAPMA and SAHA (in combination or alone) increased the number of dying cells after 24 hours of treatment. Interestingly, SAHA alone induce significant cell death. Blank-nanomicelles and no administration of SAHA didn't affect SFT cells (Fig.51).

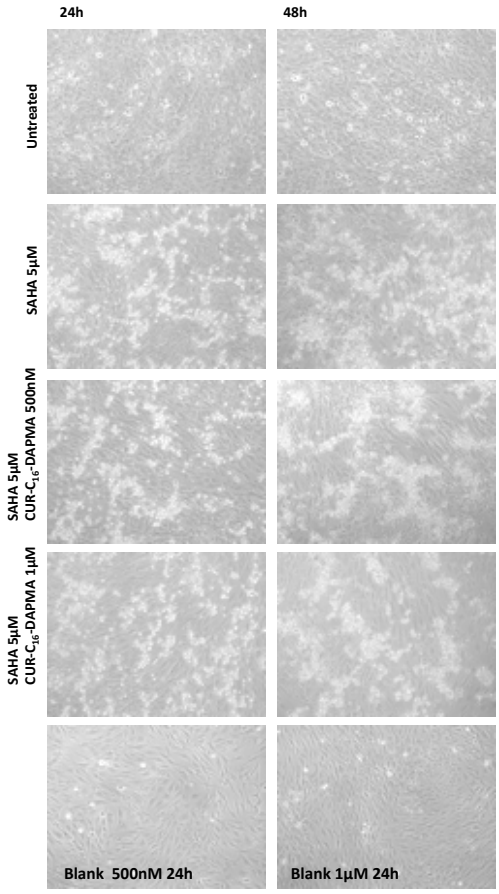

Figure 51. Effect of C_{16}-DAPMA and SAHA alone or in combined treatments after 24 and 48 hours on cell proliferation and cell death. Representative fields (magnification 20X).

Expression status of HDAC2 and MMP2 after C_{16}-DAPMA-SAHA treatment

Combined treatment with SAHA 5μM and C_{16}-DAPMA 1μM after 24 hours reduced HDAC2 expression, while MMP2 expression resulted decreased after all the combined treatments. This represents the consequence of C_{16}-DAPMA (combined with SAHA) 48 hours treatments that induced the abrogation of cell viability and in turn, HDAC2 and MMP2 expression (Fig. 52). Moreover, densitometric analyses were performed on the entire WB filters (Fig.53).

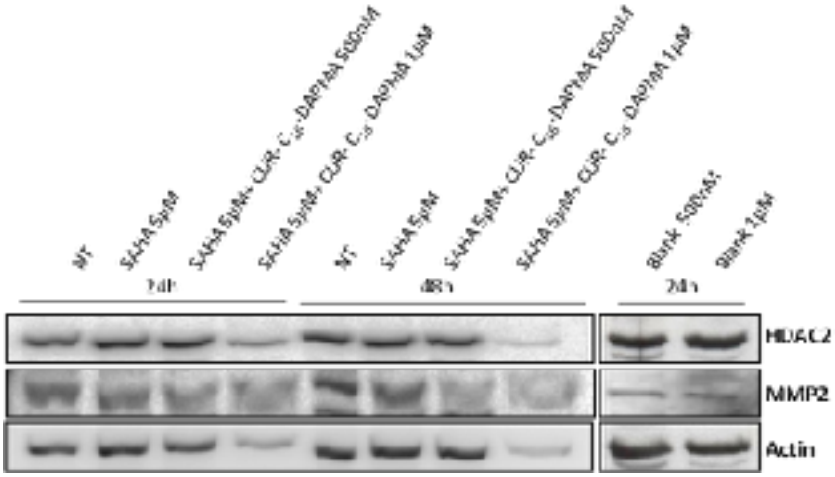

Figure 52. Effect of combined treatments (C_{16}-DAPMA and SAHA) after 24 and 48 hours on HDAC2 and MMP2 expression investigated by means of WB analysis. Treated cells were compared with the blank-nanomicelles treatment and the untreated cells as control.

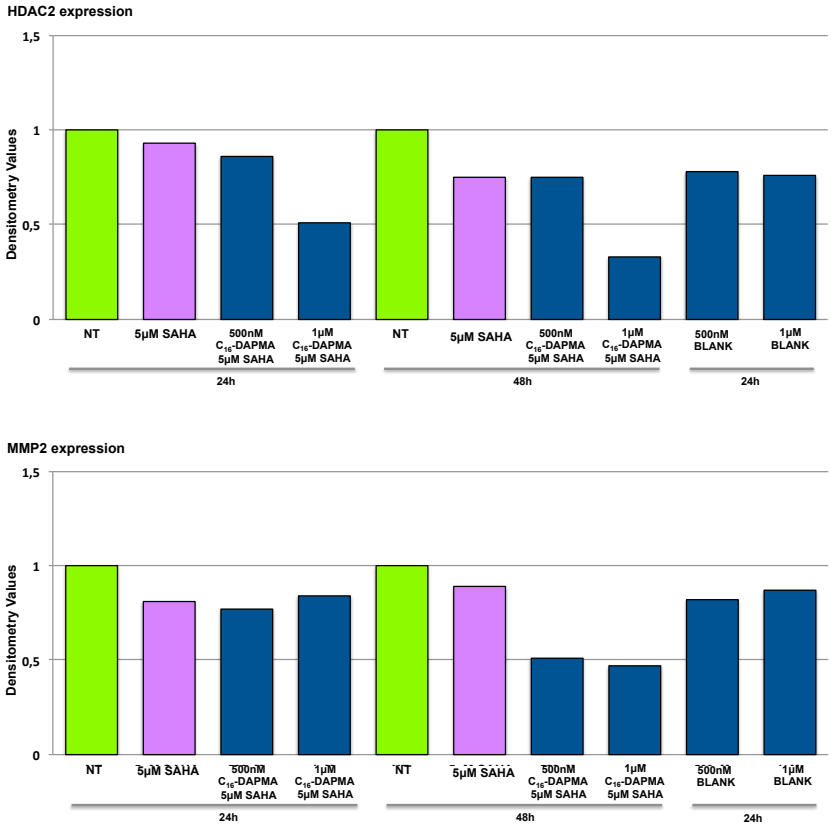

Figure 53. Densitometric analyses of C_{16}-DAPMA/SAHA WB experiments. Levels of each protein are expressed as normalized values in comparison with both the not treated (NT) and the Blank-nanomicelles samples.

4.2.2 C_{16}-SPD

C_{16}-SPD encapsulated with curcumin abrogate cell invasiveness

To validate the effect of C_{16}-SPD encapsulated with curcumin, invasion assay was performed on SFT cells after 24 hours of nanomicelles exposure (500nM and 1μM). C_{16}-SPD significantly inhibited cell invasiveness, while untreated sample migrated promptly through the matrigel (Fig.54).

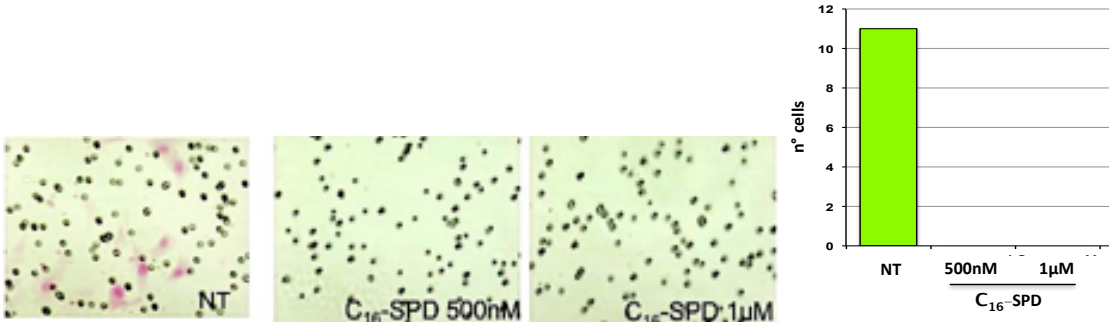

Figure 54. Cell invasive assay. Representative fields of invasive cells on the membrane (magnification 200X, left panel) and the average number of migratory cells per field (right panel). NT: not treated sample.

C_{16}-SPD encapsulated with curcumin strongly reduced SFT cells viability

C_{16}-SPD encapsulated with curcumin (500nM and 1μM) treatments for 24 and 48 hours increased cell death, as reported in Fig.55. After only 24 hours of treatment a strong cytotoxic effect was present. By the second day, few viable cells were detected. Blank-nanomicelles didn't affect SFT cells.

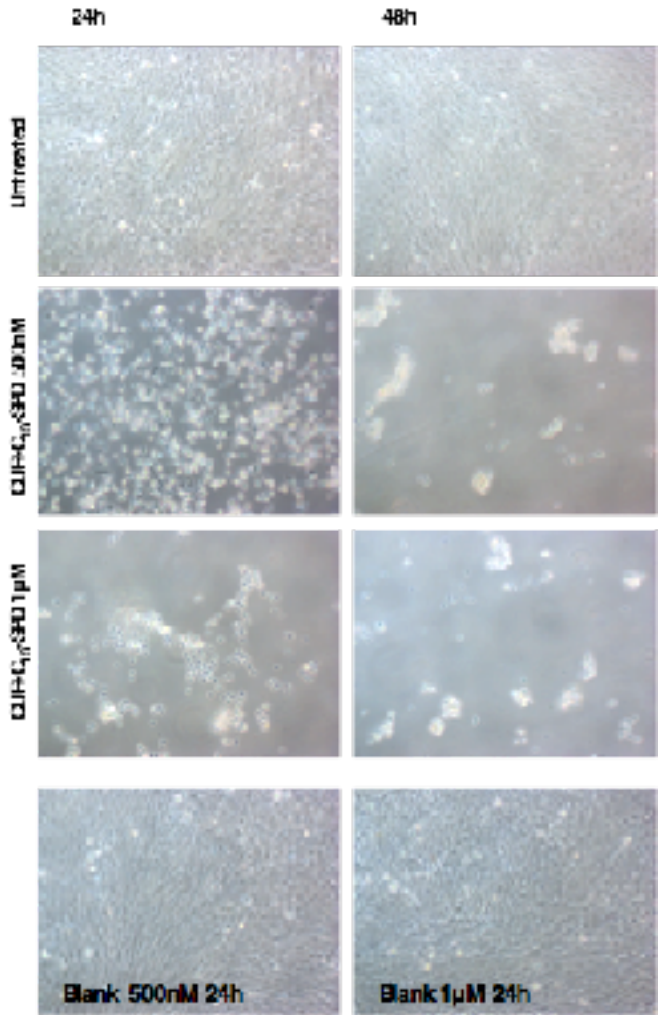

Figure 55. Effect of C_{16}-SPD treatments after 24 and 48 hours on cell proliferation and cell death. Representative fields (magnification 20X). Blank-nanomicelles were used as control for nanomicelles intrinsic cytotoxic/cytostatic effect for 24 hours.

C_{16}-SPD encapsulated with curcumin strongly reduce EMT markers expression.

The effect of C_{16}-SPD encapsulated with curcumin on expression of all the EMT markers was analysed by means of WB. After 24 hours of treatment EZH2, YY1, c-Myc, SLUG and integrin β3 expression was markedly decreased. The low amount of actin was due to the few remaining viable cells. SFT cells treated with blank-nanomicelles continued to express the

same amount of EMT markers as well as the untreated cells (Fig.56). Furthermore, densitometric analyses were performed on the entire WB filters (Fig.57).

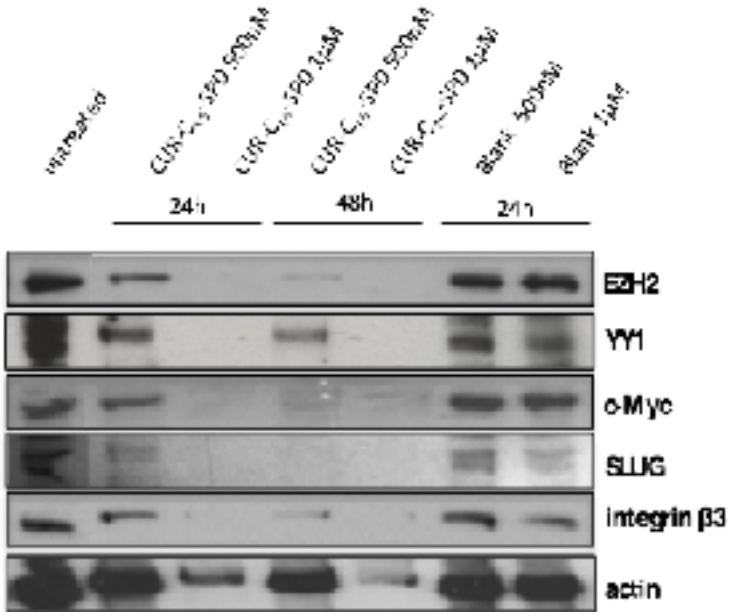

Figure 56. Effect of C_{16}-SPD treatments after 24 and 48 hours on EMT markers expression investigated by means of WB analysis. Treated cells were compared with the blank-nanomicelles treatment and the untreated cells as control.

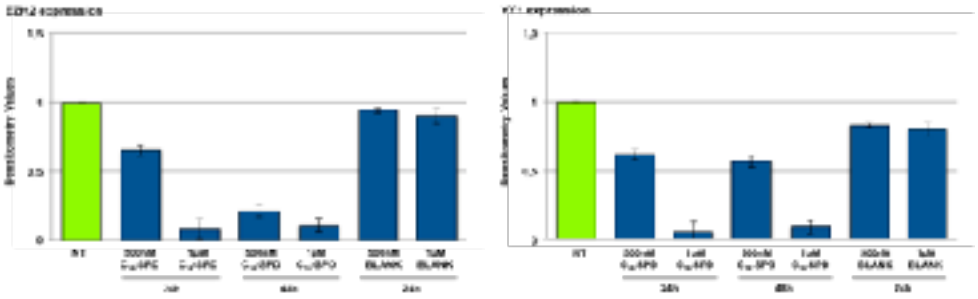

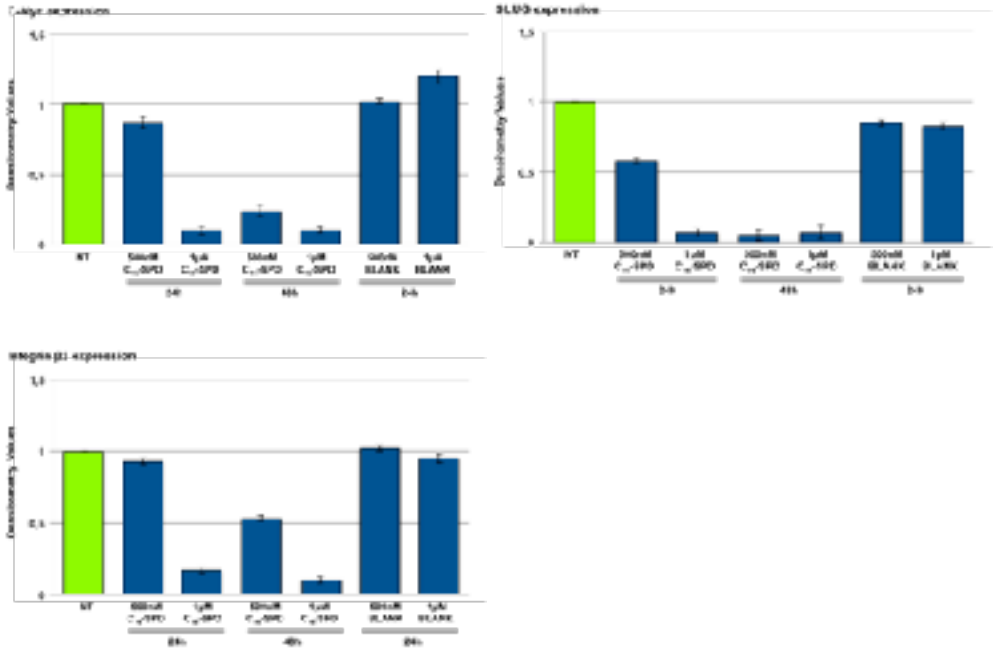

Figure 57. Densitometric analyses of C_{16}-SPD WB experiments. Levels of each protein are expressed as normalized values in comparison with both the not treated (NT) and the blank-nanomicelles samples.

Furthermore, vimentin expression was evaluated by means of IHC. C_{16}-SPD 1μM nanomicelles treatment can induce a minimal decreased in vimentin expression, associated with a more round-shaped feature (Fig.58).

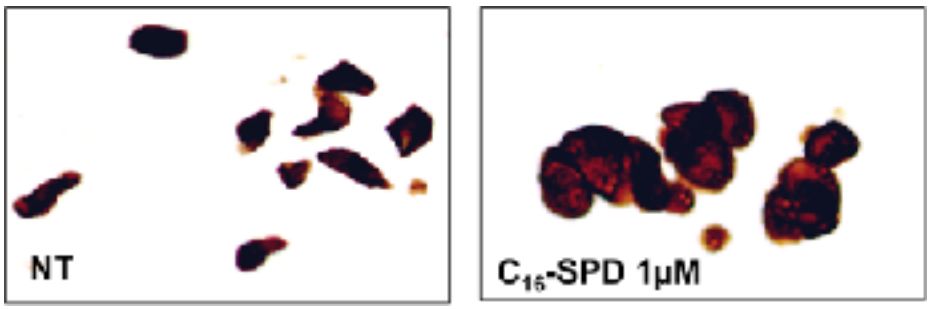

Figure 58. Vimentin IHC on SFT cytoblocks. NT: not treated sample.

Cell viability after combined treatments (C_{16}-SPD and SAHA)

To determine the sensitivity of SFT cell line to the cytotoxic/cytostatic effects of the combined treatment with C_{16}-SPD and SAHA, the cells were seeded into the microplates and incubated with 500nM/1μM concentrations of C_{16}-SPD and 5μM SAHA for 24 hours. As shown in Fig.59, the combined treatments with C_{16}-SPD results in cell death as well as the nanomicelles treatment alone.

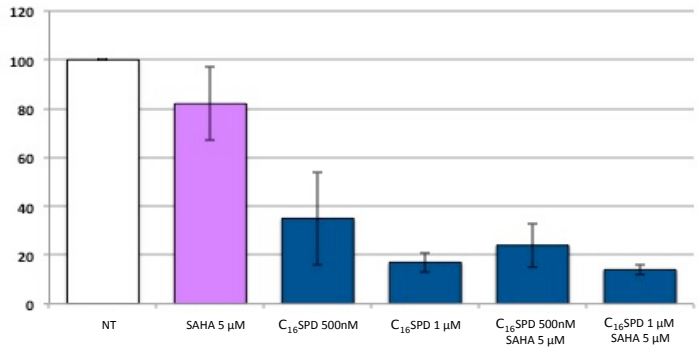

Figure 59. Viability of SFT cells treated for 24 hours with C_{16}-SPD and SAHA, investigated by means of MTT assays. NT: not treated sample

Combined treatments with C_{16}-SPD involved a strong decrease of viable cells. In this scenario, phalloidin signal intensity was restricted to specific cellular districts, before cell death (no more viable cells were observed after 48 hours C_{16}-SPD-SAHA treatments) (Fig.60).

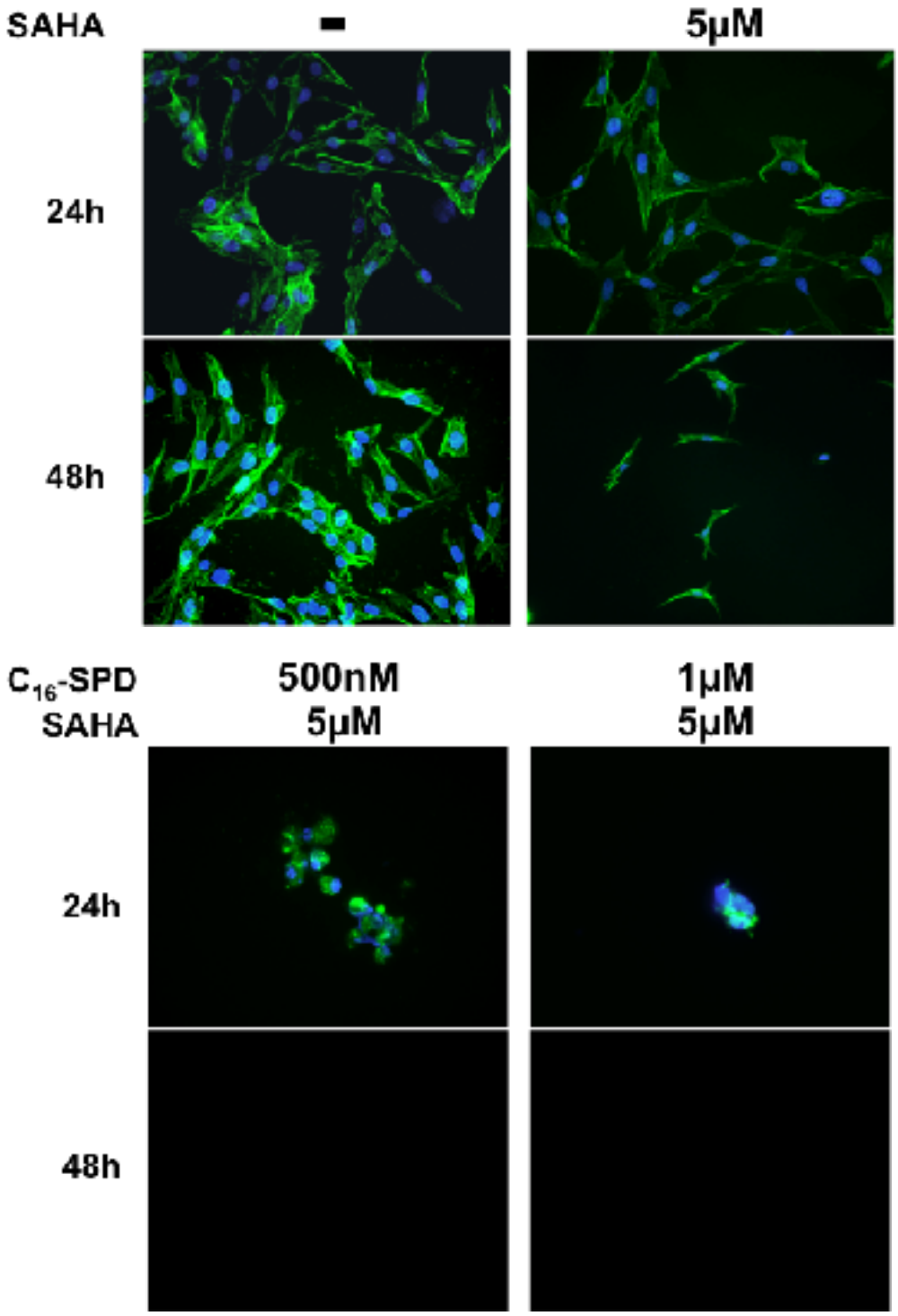

Figure 60. Effect of SAHA, C_{16}-SPD and combined treatments (nanomicelles and SAHA) after 24 and 48 hours on SFT cells which were stained with green (phalloidin Alexa fluor 488) for actin filaments and blue (DAPI) for nuclear counter stain. Representative fields (magnification 100X).

To validate the effect of C_{16}-SPD encapsulated with curcumin and SAHA combined treatment, invasion assay was performed on SFT cells after 24 hours of nanomicelles exposure (500nM and 1μM). The administration of the combined treatment lead to the abrogation of invasiveness as reported before after the treatment with nanomicelles alone.

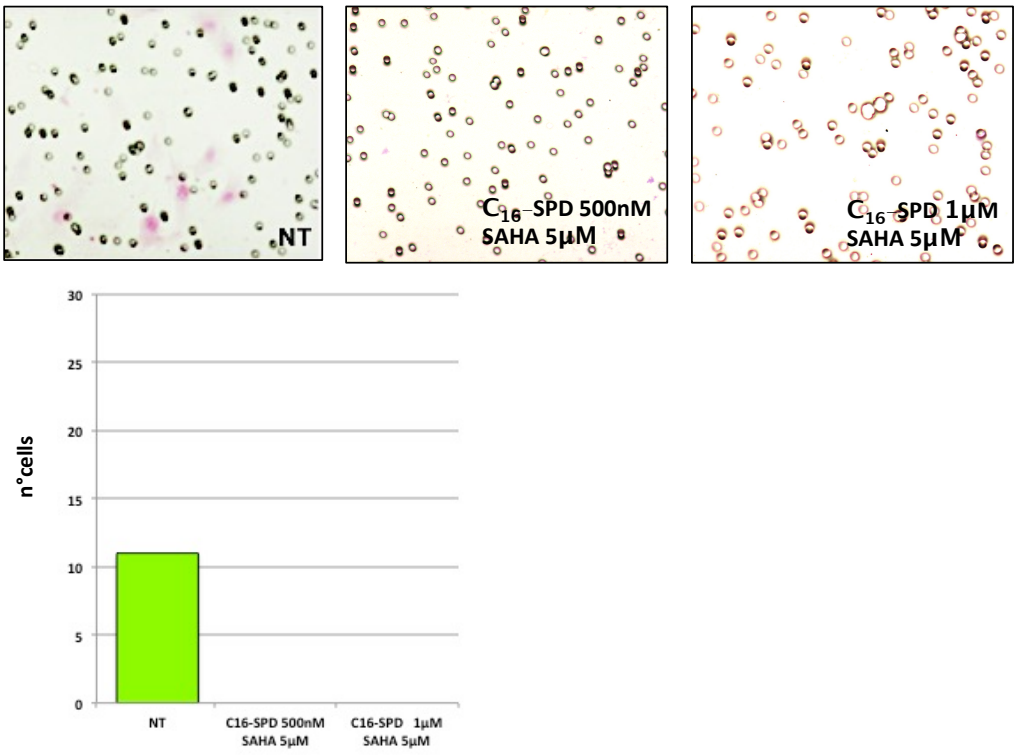

Figure 61. Cell invasive assay. Representative fields of invasive cells on the membrane (magnification 200X, upper panel) and the average number of migratory cells per field (lower panel). NT: not treated sample.

In vitro C_{16}-SPD and SAHA treatments

C_{16}-SPD and SAHA suppressed cell growth by decreasing proliferation and increasing cell death. Low cell viability was observed after C_{16}-SPD 1μM-SAHA treatments. Blank-nanomicelles and no administration of SAHA didn't affect SFT cells (Fig.62).

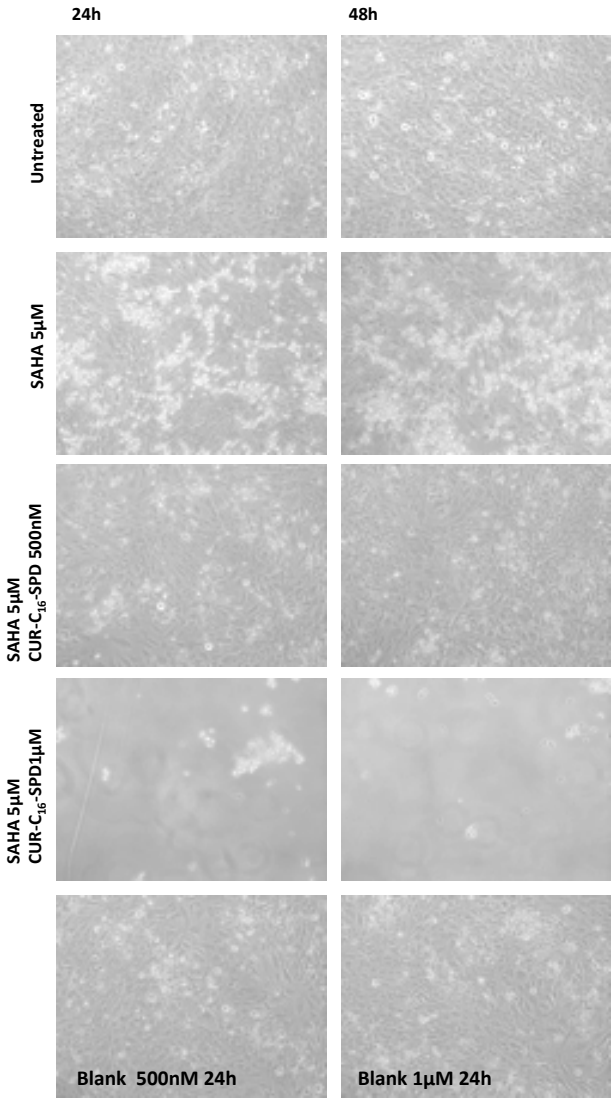

Figure 62. Effect of C_{16}-SPD and SAHA alone or in combined treatments after 24 and 48 hours on cell proliferation and cell death. Representative fields (magnification 20X).

The combined treatment with SAHA 5μM and C_{16}-SPD 1μM after 24 hours did not affect HDAC2 status. By contrast, HDAC2 expression increased after SAHA 5μM alone or in combination with 500nM C_{16}-SPD after 24 hours. MMP2 expression resulted decreased after all the combined treatments. In particular, a significant protein expression decrease was observed after 48 hours (Fig.63). Moreover, densitometric analyses were performed on the entire WB filters (Fig.64).

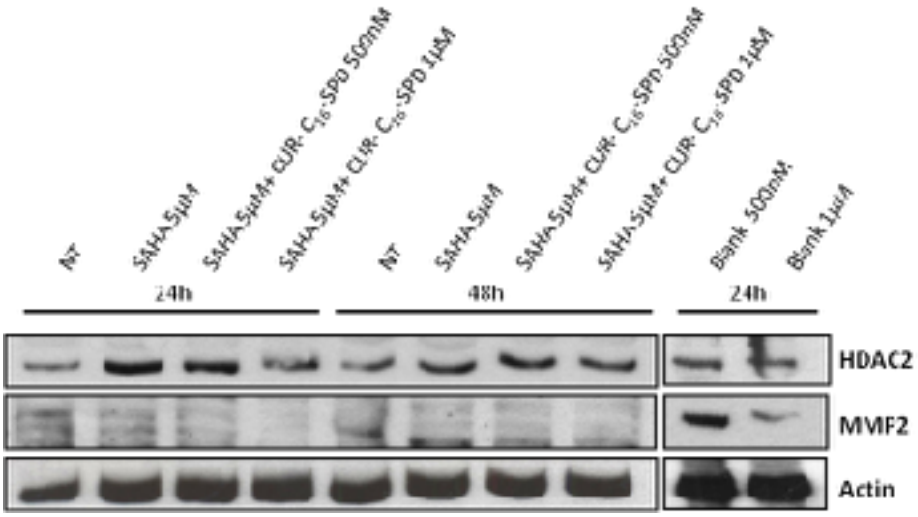

Figure 63. Effect of combined treatments (C_{16}-SPD and SAHA) after 24 and 48 hours on HDAC2 and MMP2 expression investigated by means of WB analysis. Treated cells were compared with the blank-nanomicelles treatment and the untreated cells as control.

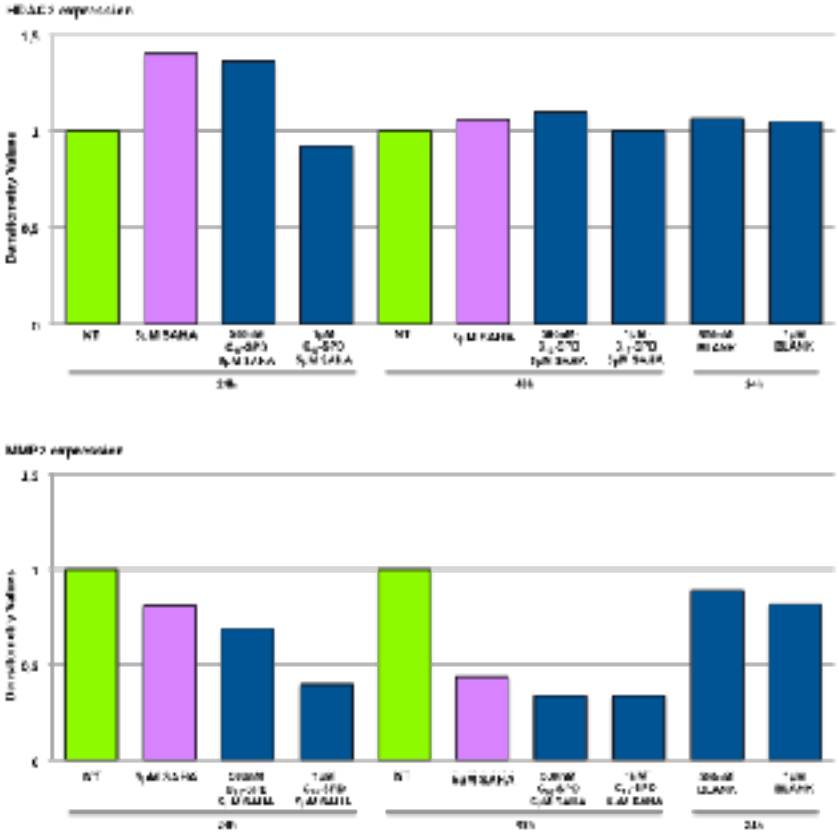

Figure 64. Densitometric analyses of C_{16}-SPD/SAHA WB experiments. Levels of each protein are expressed as normalized values in comparison with both the not treated (NT) and the Blank-nanomicelles samples.

4.2.3 C_{16}-SPM

C_{16}-SPM encapsulated with curcumin abrogate cell invasiveness

To validate the effect of C_{16}-SPM encapsulated with curcumin, invasion assay was performed on SFT cells after 24 hours of nanomicelles exposure (500nM and 1μM). C_{16}-SPM significantly inhibited cell invasiveness, despite after 500nM treatment few cells migrated through the matrigel (Fig.65).

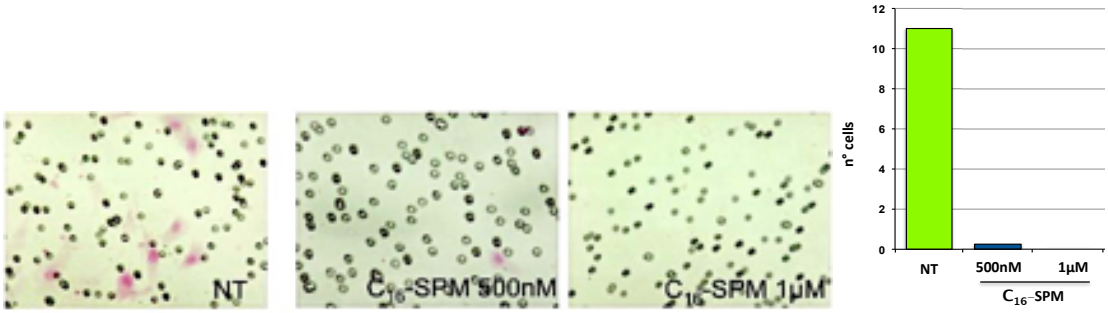

Figure 65. Cell invasive assay. Representative fields of invasive cells on the membrane (magnification 200X, left panel) and the average number of migratory cells per field (right panel). NT: not treated sample.

C_{16}-SPM encapsulated with curcumin strongly reduced SFT cells viability

C_{16}-SPM encapsulated with curcumin (500nM and 1μM) treatments for 24 and 48 hours exerted a cytostatic effect on SFT cells and slightly increased cell death. Blank-nanomicelles didn't affect SFT cells (Fig.66).

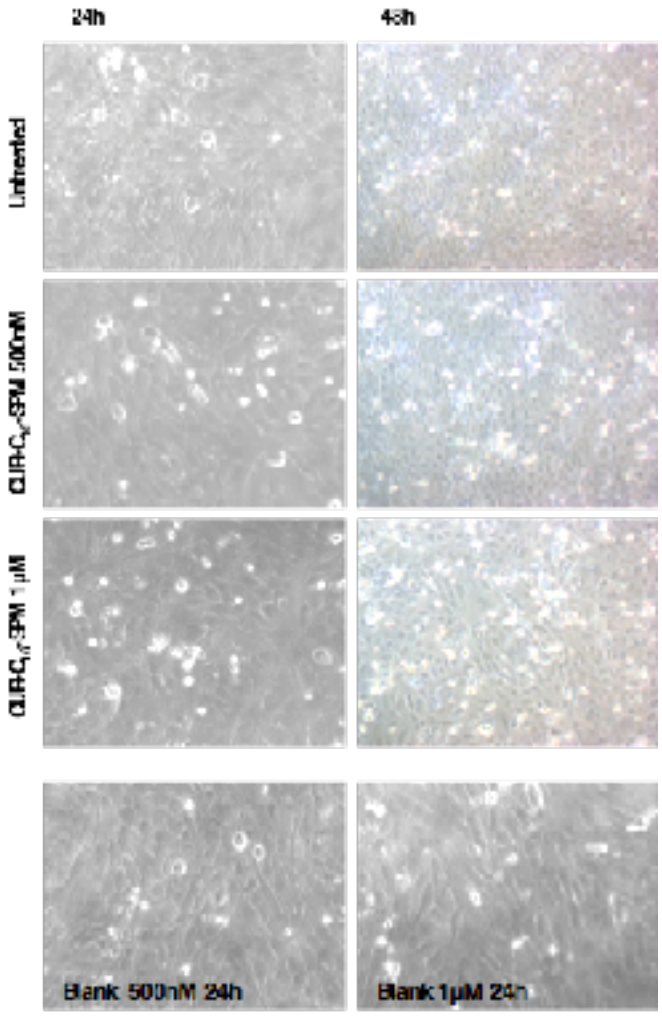

Figure 66. Effect of C_{16}-SPM treatments after 24 and 48 hours on cell proliferation and cell death. Representative fields (magnification 20X). Blank-nanomicelles were used as control for nanomicelles intrinsic cytotoxic/cytostatic effect for 24 hours.

C_{16}-SPM encapsulated with curcumin reduce SLUG and c-Myc expression

EZH2 expression wasn't affected by any nanomicelles treatment. By contrast, 500nM and 1µM C_{16}-SPM treatments resulted in reduced expression of c-Myc and SLUG after 24 and 48 hours. The effect of C_{16}-SPM on YY1 and integrin β3 was showed after 48 hours with the lowest concentration. As expected, SFT cells treated with blank-nanomicelles

continued to express the same amount of EMT markers as well as the untreated cells (Fig.67). Moreover, densitometric analyses were performed on the entire WB filters (Fig.68).

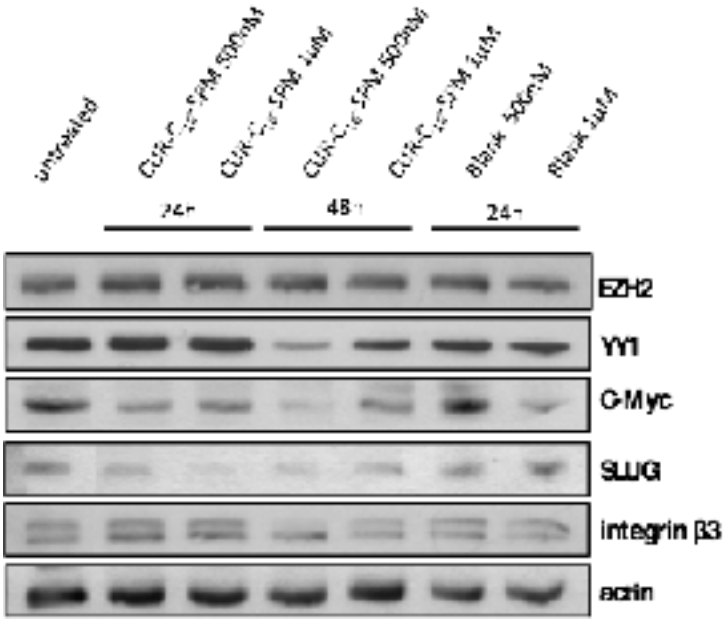

Figure 67. Effect of C_{16}-SPM treatments after 24 and 48 hours on EMT markers expression investigated by means of WB analysis. Treated cells were compared with the blank-nanomicelles treatment and the untreated cells as control.

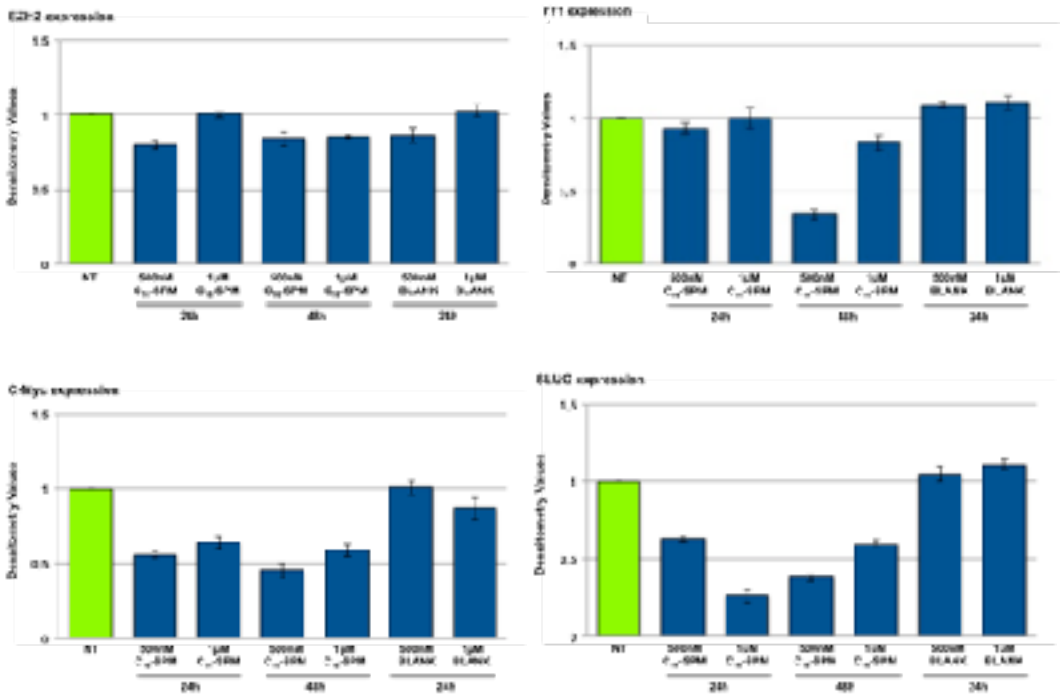

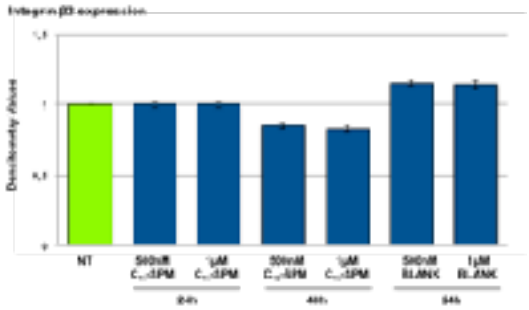

Figure 68. Densitometric analyses of C_{16}-SPM WB experiments. Levels of each protein are expressed as normalized values in comparison with both the not treated (NT) and the blank-nanomicelles samples.

Moreover, vimentin expression was evaluated by means of IHC and, unfortunately, C_{16}-SPM 1μM nanomicelles treatment did not affect its expression status . But, as seen for C_{16}-SPD and C_{16}-DAPMA, treated cells were characterized by a more rounded shape (Fig.69).

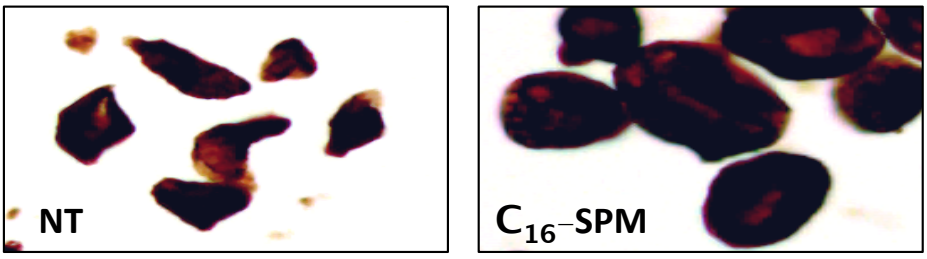

Figure 69. Vimentin IHC on SFT cytoblocks. NT: not treated sample.

Cell viability after combined treatments (C_{16}-SPM and SAHA)

The combined treatments with SAHA and C_{16}-SPM induced, surprisingly, growth increasing, as seen previously after C_{16}-DAPMA treatment (Fig.70).

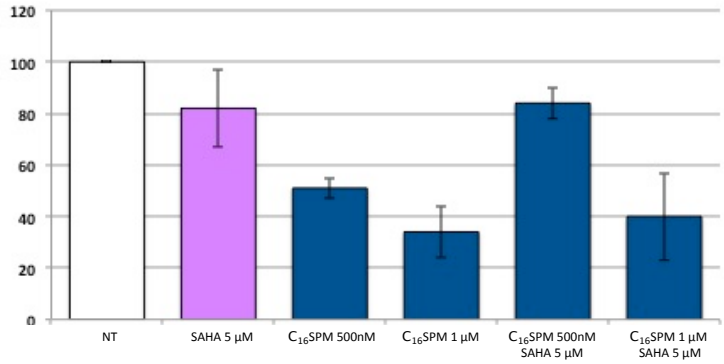

Figure 70. Viability of SFT cells treated for 24 hours with C_{16}-SPM and SAHA, investigated by means of MTT assays. NT: not treated sample.

As done before for the combined treatment with the other nanomicelles and SAHA, phalloidin IF evidenced the distribution of F-actin fibers and the changes in cellular structure. Combined treatments involved a strong decrease of viable cells. The phalloidin signal intensity tended to decrease after treatments, while SFT cells assumed more epithelial-like features before dying (Fig.71).

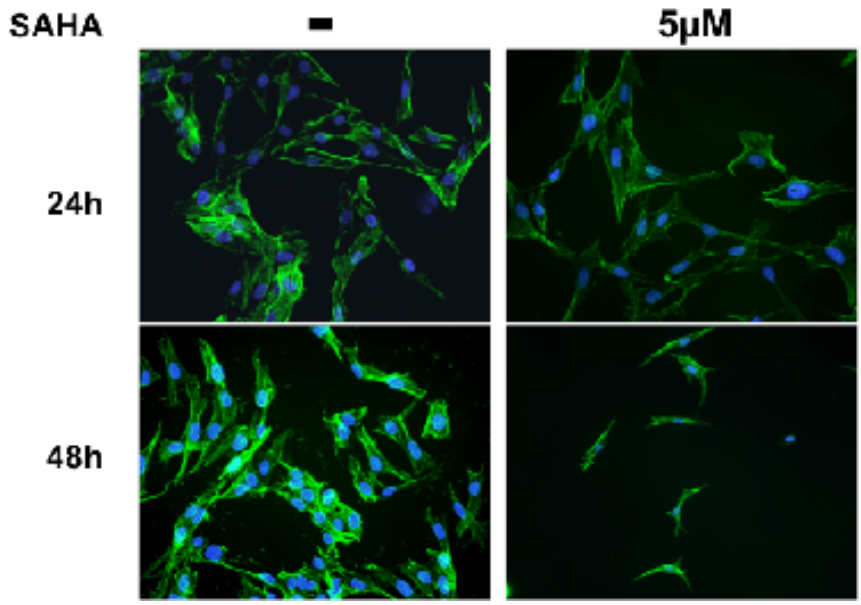

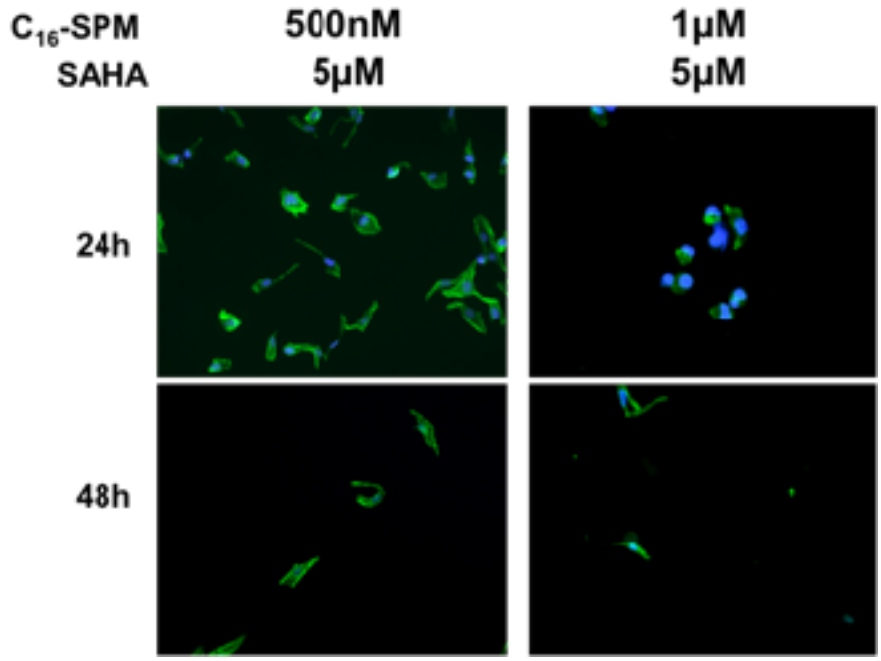

Figure 71. Effect of SAHA, C_{16}-SPM and combined treatments (nanomicelles and SAHA) after 24 and 48 hours on SFT cells which were stained with green (phalloidin Alexa fluor 488) for actin filaments and blue (DAPI) for nuclear counter stain. Representative fields (magnification 100X).

To validate the effect of C_{16}-SPM encapsulated with curcumin and SAHA combined treatment, invasion assay was performed on SFT cells after 24 hours of nanomicelles exposure (500nM and 1µM). The administration of the combined treatment lead to the abrogation of invasiveness (Fig.72) as well as after the C_{16}-SPD treatment.

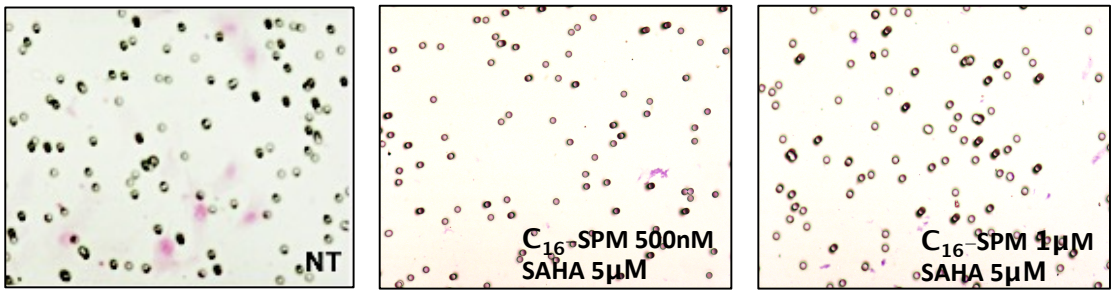

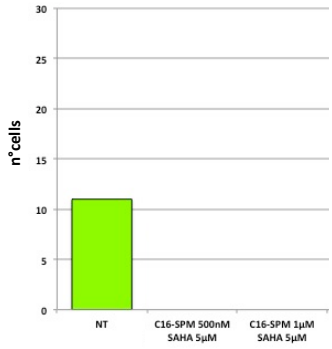

Figure 72. Cell invasive assay. Representative fields of invasive cells on the membrane (magnification 200X, upper panel) and the average number of migratory cells per field (lower panel). NT: not treated sample.

In vitro C_{16}-SPM and SAHA treatments

C_{16}-SPM significantly suppressed cell growth decreasing proliferation and increasing cell death. Blank-nanomicelles and no administration of SAHA didn't affect SFT cells (Fig.73).

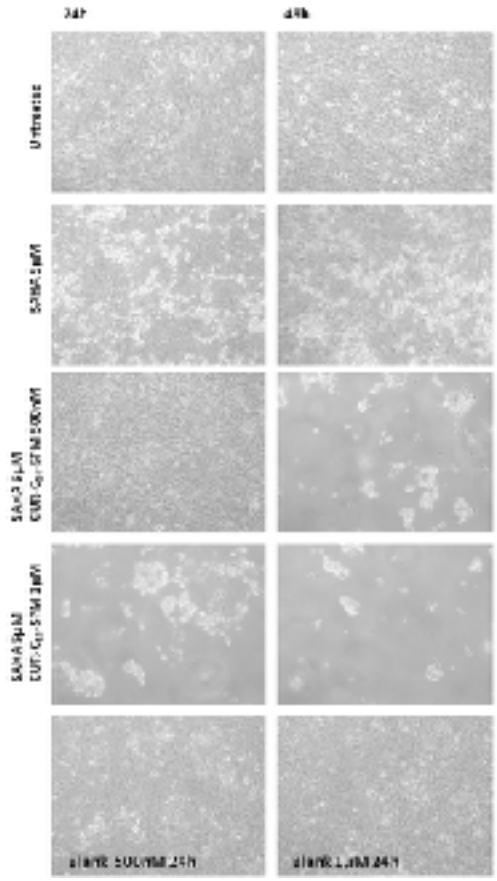

Figure 73. Effect of C_{16}-SPM and SAHA alone or in combined treatments after 24 and 48 hours on cell proliferation and cell death. Representative fields (magnification 20X).

Expression status of HDAC2 and MMP2 after C_{16}-SPM-SAHA treatment

HDAC2 status was not affected by the combined treatment with SAHA 5μM and C_{16}-SPM 1μM after 24 hours. MMP2 expression resulted decreased after all the combined treatments. In particular, a significant protein expression decrease was observed after 48 hours of combined treatments. C_{16}-SPM (combined with SAHA) 48 hours treatments induced the abrogation of cell viability (low actin signal) and in turn, HDAC2 and MMP2 expression (Fig.74). Moreover, densitometric analyses were performed on the entire WB filters (Fig.75).

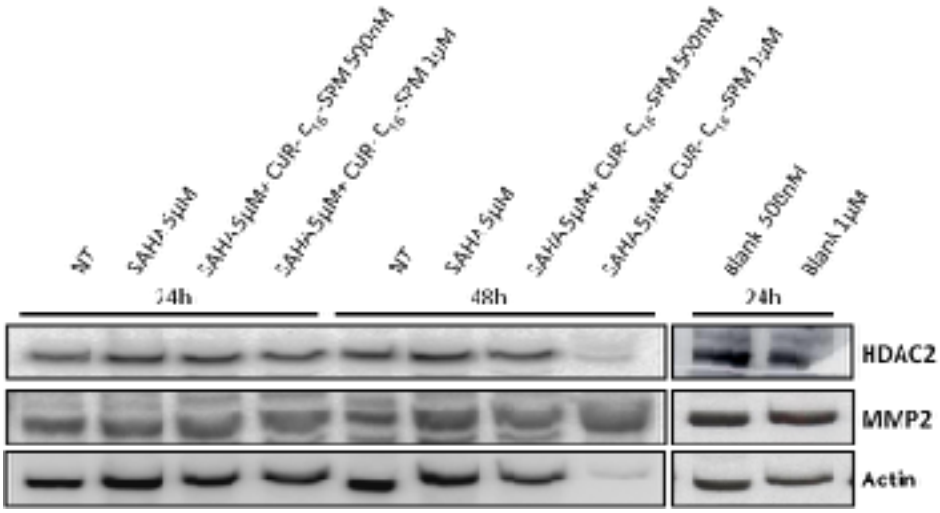

Figure 74. Effect of combined treatments (C_{16}-SPM and SAHA) after 24 and 48 hours on HDAC2 and MMP2 expression investigated by means of WB analysis. Treated cells were compared with the blank-nanomicelles treatment and the untreated cells as control.

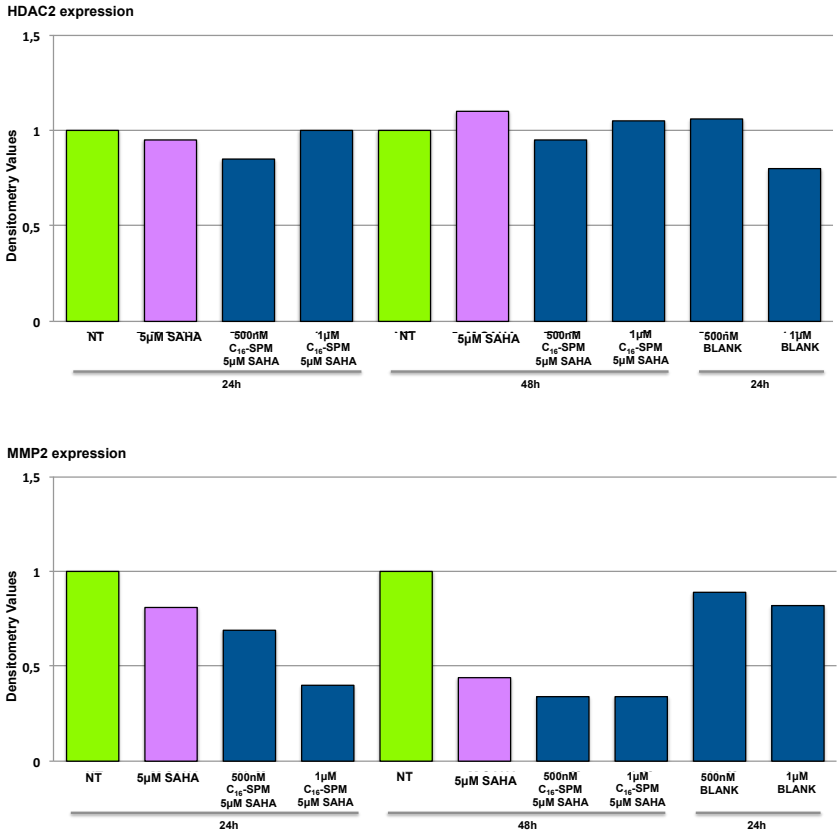

Figure 75. Densitometric analyses of C_{16}-SPM/SAHA WB experiments. Levels of each protein are expressed as normalized values in comparison with both the not treated (NT) and the Blank-nanomicelles samples.

Photodynamic Therapy (PDT) is an innovative minimally invasive technique, is not subject to resistance, is easily manageable, selective, does not involve systemic toxicity such as standard chemotherapy and does not induce resistance phenomena. Recent studies also report that, the cytotoxic effect obtained using low concentrations of curcumin, administered in combination with blue light (laser) on tumor cell lines, was particularly significant using nanomicelle-encapsulated with curcumin. In line with studies already published, preliminary MTT assay was performed on SFT cells after blue laser treatment in combination with nanomicelles loaded with curcumin.

4.3 PDT

Curcumin treatment: MTT and ROS generation at T0

Generation of reactive oxygen species (ROS) is a well known parameter for the evaluation of phototoxic potential of photosensitizing compounds, such as curcumin (Yin et al, 2012). Monitoring the generation of ROS after curcumin (alone or encapsulated in nanomicelles) and blue laser treatment was chosen to investigated whether curcumin exploit a similar mode of action.

No significant induction of ROS was detected after treatment with curcumin alone at T0 without irradiation. On the contrary, administering a high dose of curcumin, ROS production diminished (Fig.76). No change in cell viability was recorded at T0 (Fig.77). By administering the highest concentrations of curcumin (20μM and 50μM), in association with the blue laser irradiation, a significant increase in ROS production was assessed (Fig.76). This had an impact on cell viability which resulted significantly reduced (Fig.77).

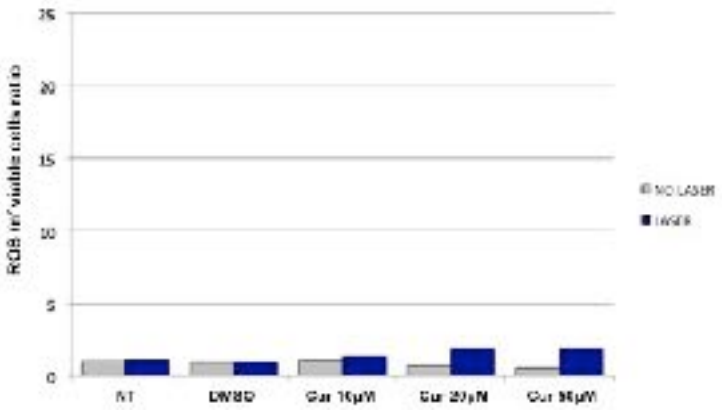

Figure 76. Intracellular ROS accumulation, as indicated by H_2DCFDA-derived fluorescence, in SFT cells treated with curcumin at different concentrations at T0. Grey column: no laser treatment. Blue column: blue laser treatment.

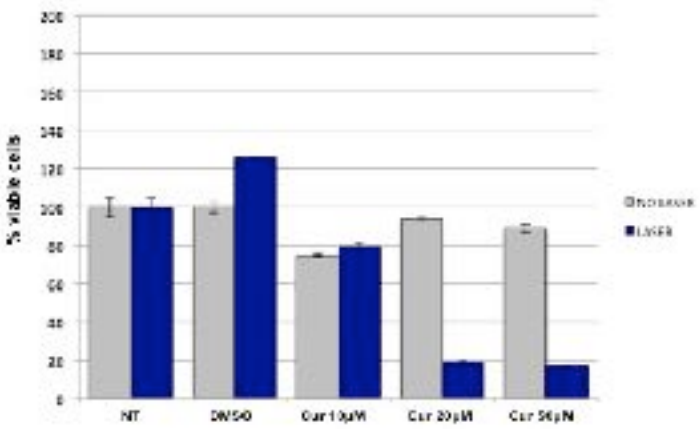

Figure 77. Changes in cell viability, as determined by MTT assay, after curcumin treatments at T0. The absorption values are represented in relation to the NT (not treated sample), which received the arbitrary value of 100. Grey column: no laser treatment. Blue column: blue laser treatment.

SFT cells, after nanomicelles treatment at T0, achieved high ROS level, mainly significant after C_{16}-DAPMA administration (with or without laser) (Fig.78A), which in turn decreased cell viability (Fig.79A). Unexpectedly, treatment with C_{16}-DAPMA 100nM decreed an increase in cell viability at T0, particularly significant after laser treatment (Fig.79A). Combined treatment with C_{16}-SPD and C_{16}-SPM and laser irradiation has resulted in an increase,

albeit not always significant, in ROS generation compared to the corresponding no-laser treatment (1μM and 500nM) (Fig.78B-C). C_{16}-SPD and C_{16}-SPM 1μM treatments decreased cell viability with or without laser (Fig.79B-C), while treatments with 250nM and lower doses showed an increase in cell viability, compared to untreated sample (Fig.79B-C).

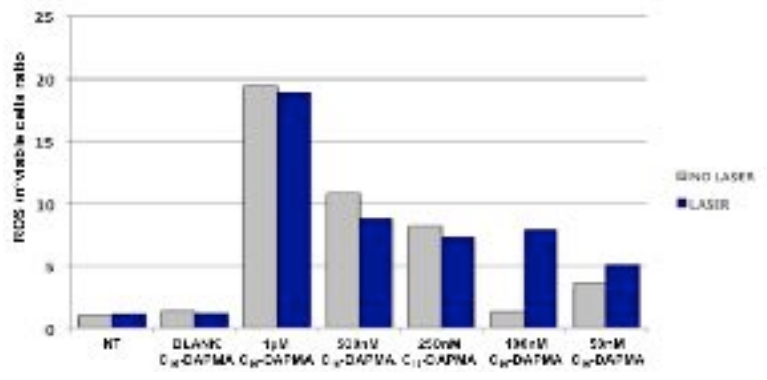

A

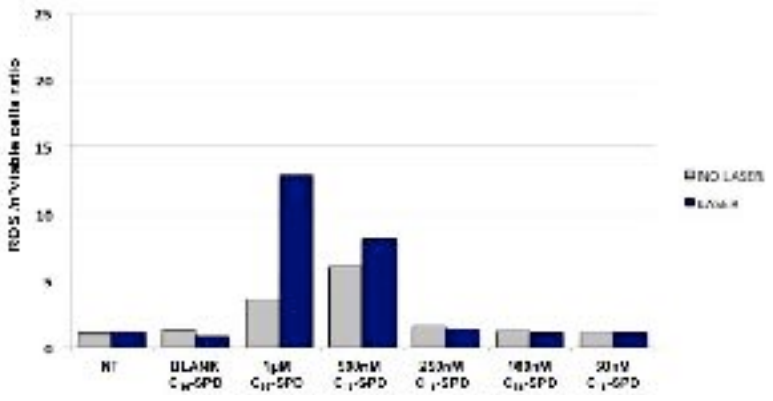

B

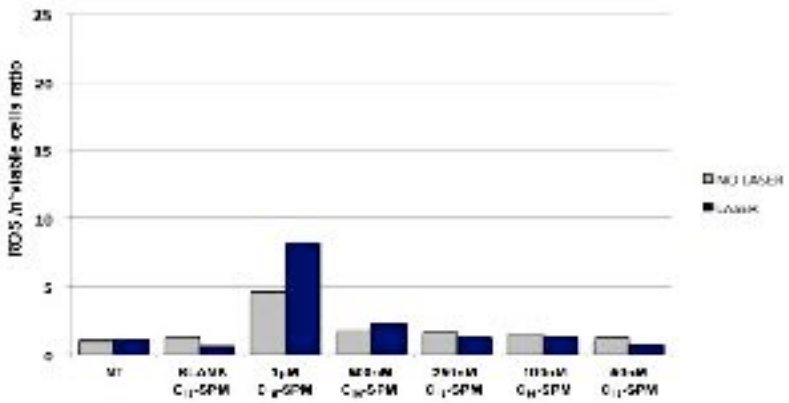

C

Figure 78. Intracellular ROS accumulation, as indicated by H_2DCFDA-derived fluorescence, in SFT cells treated with C_{16}-DAPMA (A), C_{16}-SPD (B) and C_{16}-SPM (C) at different concentrations at T0. Grey column: no laser treatment. Blue column: blue laser treatment.

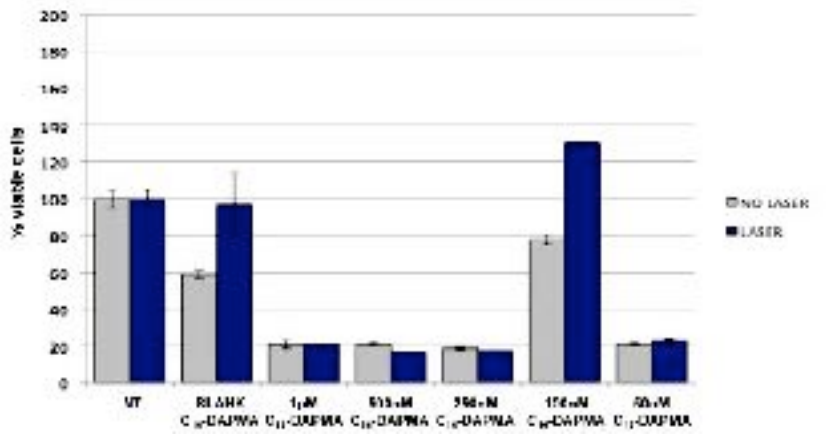

A

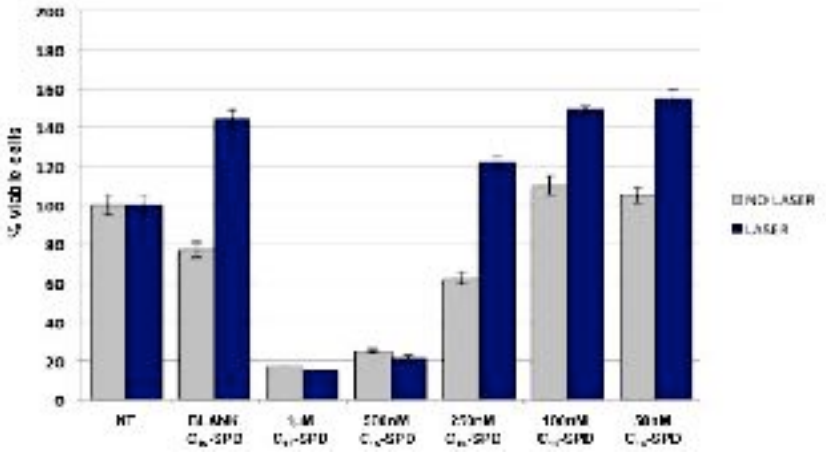

B

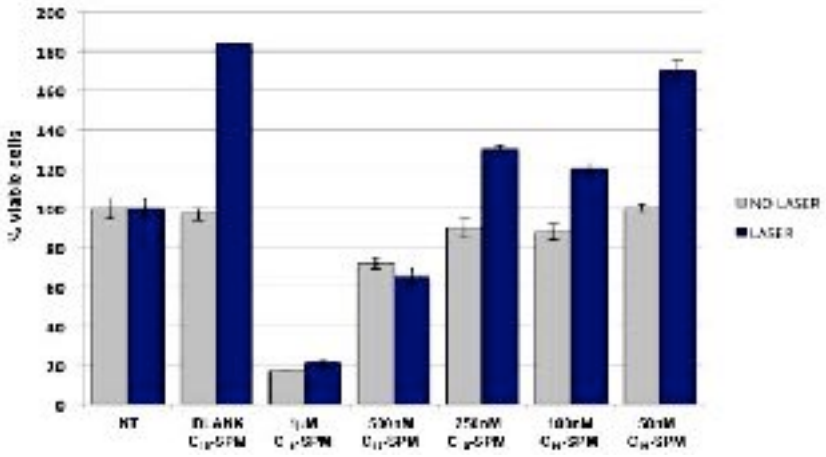

C

Figure 79. Effect on cell viability, as determined by MTT assay, after treatments with C_{16}-DAPMA (A), C_{16}-SPD (B) and C_{16}-SPM (C) at T0. The absorption values are represented in relation to the NT (not treated sample), which received the arbitrary value of 100. Grey column: no laser treatment. Blue column: blue laser treatment.

Curcumin/nanomicelles treatment: MTT at T24

Data on cell viability after curcumin treatment (Fig.80) were superimposed on the data obtained in previous experiments performed to evaluate the curcumin cytotoxicity on SFT cells by means of MTT . The same was true for nanomicelles treatment, with the exception of C_{16}-SPM lower concentrations (never tested before) which did not show any cytotoxicity on SFT cells (Fig.81C). The single exposure to the blue laser has resulted in a reduction in cell viability even in the absence of treatment whether it is curcumin or nanomicelles (Fig.80, Fig.81A-C). Viability abrogation was induced after curcumin 20μM and 50μM treatment with laser irradiation (Fig.80), which was comparable to that obtained after nanomicelles treatment (without laser exposure). Low dose nanomicelles treatment with laser caused a decreased cell viability, such as curcumin 10μM treatment with laser (Fig.81A-C).

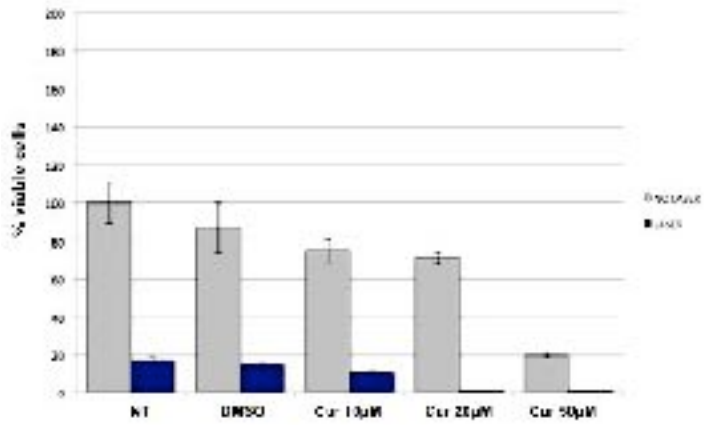

Figure 80. Changes in cell viability, as determined by MTT assay, after curcumin treatments at T24. The absorption values are represented in relation to the NT (not

treated sample), which received the arbitrary value of 100. Grey column: no laser treatment. Blue column: blue laser treatment.

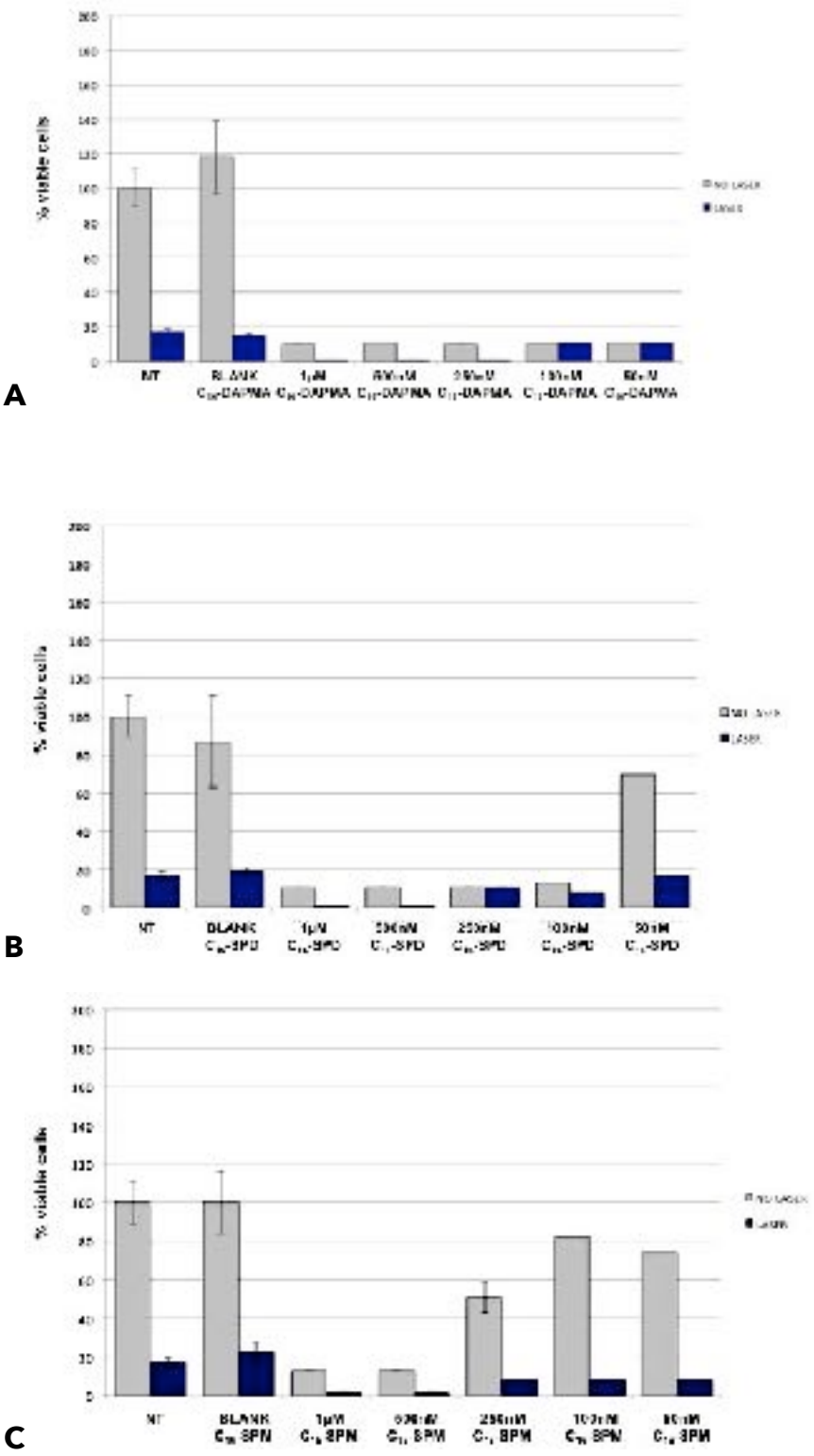

Figure 81. Effect on cell viability, as determined by MTT assay, after treatments with C_{16}-DAPMA (A), C_{16}-SPD (B) and C_{16}-SPM (C) at T24. The absorption values are

represented in relation to the NT (not treated sample), which received the arbitrary value of 100. Grey column: no laser treatment. Blue column: blue laser treatment.

4.4 Global evaluation of C_{16}-DAPMA, C_{16}-SPD and C_{16}-SPM on SFT cell line

Viability assay.

Increasing concentrations of curcumin (10μM, 20μM and 50μM) were able to induce a cytostatic/cytotoxic effect on SFT cell line. By using the highest concentration of curcumin, 50μM, a strong reduction of viable cells was observed, after 24 hours of continuous treatment. By contrast, MTT analysis of curcumin-encapsulated nanomicelles compared to free-curcumin treatment, demonstrated that the cytotoxic potential of C_{16}-DAPMA, C_{16}-SPD and C16-SPM was achieved by using significantly lower curcumin concentrations (500nM, 1μM), at least 100 time less. Overall, C_{16}-DAPMA and C_{16}-SPD resulted to be more effective on SFT cells viability rather than C_{16}-SPM .

As reported in the literature, nanomicelles treatment induces apoptosis. In order to verify if also in SFT cells the cytotoxic effect is exerted throughout apoptosis, immunofluorescence time-lapse experiments were carried out. Apoptotic bodies were easily detected, and identified as small sealed membrane vesicles typically produced in cells undergoing programmed cell death. In this context, nanomicelles loaded with curcumin could enhance cellular uptake of curcumin thus exerting cytotoxicity and apoptotic effect. The hypothesis was confirmed by the experimental results of cellular uptake reported above (Fig.42). Firstly, cells lost adherence and

assumed a rounded shape. Afterwards, apoptotic bodies were observed (Fig.82 and Fig.83).

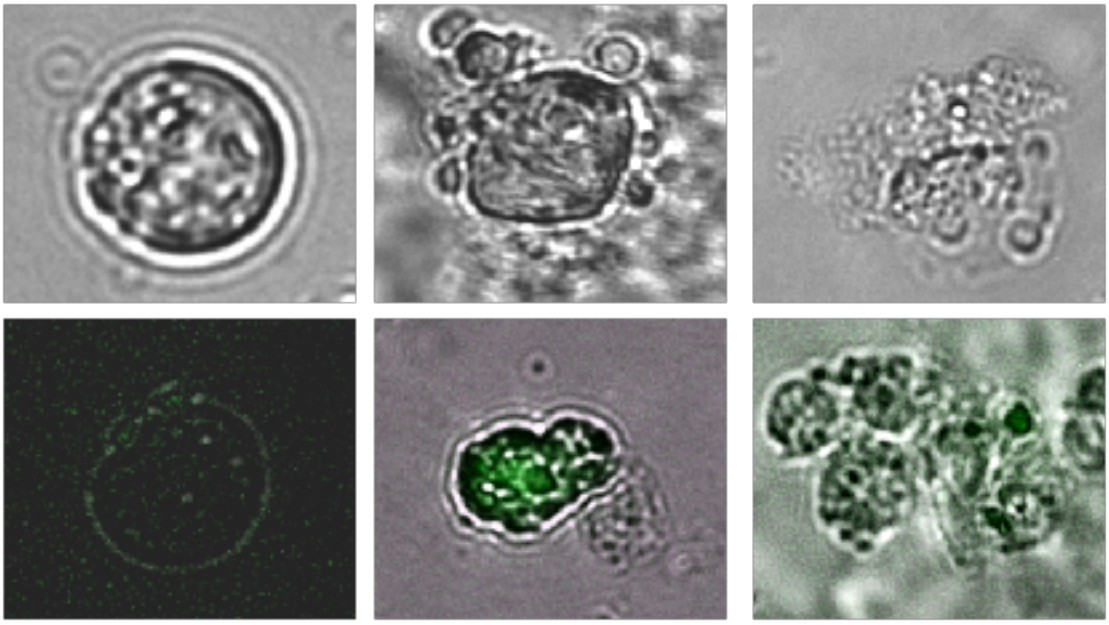

Figure 82. Representative images of nanomicelles loaded with curcumin (1μM) during endocytosis which lead to apoptosis. Green signal: curcumin autofluorescent signal.

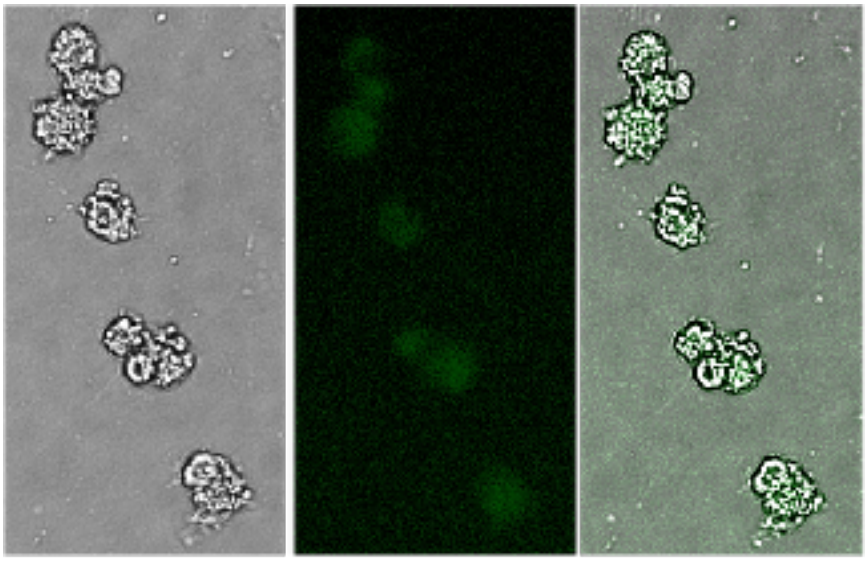

Figure 83. Representative images of nanomicelles loaded with curcumin (1μM) undergoing apoptosis. Green signal: curcumin autofluorescent signal.

Invasive potential.

C_{16}-DAPMA, C_{16}-SPD and C_{16}-SPM treatments are able to inhibit cell invasiveness. Cells treated with C_{16}-SPM (500nM) migrated more, even if not significantly, when compared to cells treated with C_{16}-DAPMA and C_{16}-SPD. Overall, all the nanomicelles used in these experiments induce invasiveness inhibition and interestingly, this inhibitions was achieved with lower concentration than those obtained with free-curcumin.

Moreover, C_{16}-SPD and C_{16}-SPM, administered in combination with SAHA, significantly inhibited cell invasiveness, compared to the untreated sample. On the contrary, after combined treatment with C_{16}-DAPMA and SAHA, the number of cells still characterized by invasive potential was very high. This was as unexpected result, since treatment with C_{16}-DAPMA alone had abolished this invasiveness.

EMT markers expression.

WB analyses revealed that SFT cells treated with C_{16}-DAPMA and C_{16}-SPM expressed lower amount of EZH2 compared with C_{16}-SPD. YY1 expression resulted slight reduced after 1μM C_{16}-DAPMA and C_{16}-SPD treatments. C_{16}-SPD was the only nanomicelle formulation which was able to strongly inhibit c-Myc expression. On the other hand, SLUG expression was abolished after treatments with all the three different nanomicelles. Integrin β3 expression status was not affected by any treatment, but C_{16}-SPD.

Overall, C_{16}-SPD appears to be the most effective nanomicelle treatment in EMT markers expression inhibition. Moreover, C_{16}-SPD treatments induces a minimal, but present, reduction of vimentin expression.

SAHA combined treatments.

Free-curcumin alone was able to reduce HDAC2 and MMP2 expression, only when used at a high concentration, 50μM. Unfortunately, the combined treatment increased both HDAC2 and MMP2 levels, while SAHA alone strongly decrease MMP2 expression.

Combined treatment with 5μM SAHA and 1μM C_{16}-DAPMA reduced HDAC2 expression. By contrast, HDAC2 status was not affected by either treatment with C_{16}-SPD and C_{16}-SPM. Furthermore, HDAC2 expression increased after SAHA 5μM alone or in combination with 500nM C_{16}-SPD. MMP2 expression resulted decreased after all the nanomicelle combined treatments. In particular, a significant protein expression decrease was observed mainly after C_{16}-SPD and C_{16}-SPM administration.

5. Discussion

Solitary fibrous tumors (SFTs) are ubiquitous but rare soft tissue sarcomas bearing the *NAB2/STAT6* fusion gene that are characterised by a spectrum of "usual", "malignant" and "dedifferentiated" histological variants (Fletcher et al, 2013; Mosquera et al, 2009; Collini et al, 2012). The majority of SFTs behave in a relatively indolent fashion and are usually treated by surgical resection. The reported median 10-year overall survival (OS) rates for patients with SFTs range from 54% to 89% after complete surgical resection of localized disease (Magdeleinat et al, 2002; Harrison-Phipps et al, 2009). However, for the approximately 20%–30% of patients with SFTs in which local recurrences and/or distant metastases eventually develop, options for effective treatment are limited. SFTs are generally regarded as relatively chemoresistant tumors, but nowadays, the efficacy of systemic chemotherapy for SFTs has been established. Conventional chemotherapy (such as anthracyclines and/or ifosfamide) is effective in controlling or stabilizing locally advanced and metastatic SFTs (Stacchiotti et al, 2013). More recently, the role of second-generation small-molecules, potent and selective multi-targeted receptor tyrosine kinase inhibitors (TKIs) (i.e. Sunitinib) active against vascular endothelial growth factor receptors (VEGFR) 1, 2, and 3, platelet-derived growth factor receptors (PFGFR) were established. Sunitinib was reported to be active in SFTs: a less aggressive morphology corresponded to an increased response rate (Stacchiotti et al., 2012). Moreover, Stacchiotti and colleagues provided morphological and functional explanations for the clinical differences in sunitinib activity observed in SFT patients, and indicate that the drug's effectiveness or detrimental action is dictated by the presence of clear-responsive areas (a marker of disease response) or necrotic-progressive foci (a marker of

disease progression). They also showed that effective autophagy can induce sunitinib response activating an adaptive immune configuration, whereas defective autophagy induces resistance counteracting the immune response triggered by the treatment and this coincided with the advanced form of malignant SFTs. Currently available drugs for the treatment of SFT are associated with numerous side effects, resistance and, until now, have not improved significantly patient survival.

In this light, non-toxic and more selective agents are needed for SFTs and also for all other cancer histotypes for which therapeutic option are represented by surgery alone.

Curcumin has been found to possess anti-cancer activities via its effect on several biological pathways involved in mutagenesis, oncogene expression, cell cycle regulation, apoptosis, tumorigenesis, tumor growth, angiogenesis and metastasis. Moreover, one of the emerging hallmarks of cancer is the avoidance of immune system. Several strategies are adopted by tumors to escape immune surveillance and successfully develop in the body. Recent studies show that curcumin can target this process and restore the immune activity against cancer. Several processes mediate by curcumin are restoration of CD4+/CD8+ T cell populations, reduction of Treg cell population and suppression of T cell apoptosis (Sayantan et al, 2015).

A significant interest in developing adjuvant chemotherapies is leading to improve currently available treatment protocols, which may allow decreased side effects and toxicity without compromising therapeutic efficacy.

The sensitivity of SFT cells to curcumin was evaluated *in vitro* using MTT viability assays. The results obtained are consistent with those reported in literature demonstrating a dose-dependent reduction in cell viability

following curcumin treatments. To further elucidate the possible mechanisms of action of curcumin, the autofluorescence property of curcumin was used to determine its intracellular localization as analyzed by fluorescence microscopy. Consistent with the notion that curcumin exerts effects on multiple intracellular signaling pathways (Gupta et al, 2011), our results demonstrate that curcumin displays a pan-cellular localization.

During Epithelial-Mesenchymal Transition (EMT) of cancer cells *in situ*, epithelial cells lose polarity and contact inhibition, undergoing to a cytoskeleton remodeling. Changes in specific protein expression that promote cell-to-cell contact, such as E-cadherin, may be lost and cells may acquire mesenchymal characteristics such as changes in vimentin (Lamuille et al, 2014), EZH2, YY1, SLUG, c-Myc and integrin β3 expression levels, when compared to untreated cells. All these events result in an enhanced ability in cell migration and invasion. To determine the effects of curcumin on EMT protein expression, Western blot (WB) were performed on curcumin-treated SFT cells. Our data demonstrate that free-curcumin at a concentration of 50μM reduces the above mentioned EMT markers.
Unfortunately, such concentration, *in vivo*, could result in heavy side effects. Administration of high doses of curcumin can give gastrointestinal side effects, encourages the gallbladder to produce more bile, which may improve digestion. Because of the extra bile production, people who have gallstones or other conditions that block bile passages shouldn't take curcumin at high doses. In a study (Tang et al, 2008) it was found that participants who took curcumin showed higher urinary oxalate levels, that can bind with calcium to form kidney stones. Moreover, curcumin can also increase the effectiveness of different kind of drugs, including blood

thinners and diabetes medications: taking curcumin with blood thinners can increase the risk of bleeding.

More in general, and not only for curcumin, a major limitation inherent to most conventional anticancer chemotherapeutic agents is their lack of tumor selectivity. Nanostructures, such as nanomicelles, can selectively extravasate in tumor tissues due to its abnormal vascular nature: the tumor curcumin concentration will be several folds higher than that of the plasma, due to lack of efficient lymphatic drainage in solid tumor, an ideal application for EPR-based selective anticancer nanotherapy. The application of nanomicelles loaded with curcumin (C_{16}-DAPMA, C_{16}-SPD and C_{16}-SPM) resulted in a significant decrease of cell viability and in a reduction of the expression of the EMT markers, administering curcumin doses significantly lower than curcumin alone treatment. Our results show that each nanomicelle interacts within the cell with pathways involved in EMT in different ways. C_{16}-DAPMA, C_{16}-SPD were the most effective nanomicelles in reducing the expression of the proteins involved in EMT, except for integrin β3 expression after C_{16}-DAPMA, which resulted expressed as well as the untreated sample. C_{16}-SPD treatment induced the inhibition of the expression of all the EMT markers after 24 hours of treatment, while C_{16}-DAPMA treatment required at least 48 hours to obtain a reduction of YY1 and c-Myc expression. Conversely, C_{16}-SPM treatment resulted in the decrease of YY1, c-Myc and SLUG without any change in EZH2 and integrin β3 expression even after 48 hours. Indeed, the different nanomicelles mode of action observed and affecting EMT markers expression may be due to the interactions of such nanostructures with the lysosomes during their endocytosis (Wei et al, 2015), probably due to their distinctive chemical-physical features. Consequently, this induces different curcumin release inside the cell, exerting distinct interactions between target proteins and

curcumin. The observations that nanomicelles loaded with curcumin dramatically decreased levels of EMT markers is encouraging and this represent another area of investigation that should to be pursued. Furthermore, the fact that cells even after nanomicelles treatment still express vimentin, indicates that curcumin alone can induce a shift towards epithelial features but not entirely. It was not expected that curcumin alone would induce a blockade of EMT, since it is well known that this compound have to be associated with a chemotherapeutic agent to setup a successful therapy.

Metastasis is a complex multistep process, closely related to EMT, which requires detachment from the primary tumor site, migration through the extracellular matrix (ECM) and the colonization of surrounding tissues. The invasion assay demonstrates that all the nanomicelles loaded with curcumin significantly inhibited SFT cells invasion than curcumin alone. Moreover, one of the key factors associated with the invasion and metastasis of cancer cells is matrix metalloproteinase2 (MMP2), which are endopeptidases capable of digesting the ECM, which gives structural support to cells and plays a pivotal role in cell adhesion, proliferation, and migration. Histonedeacetylase inhibitors (HDACi), such as Vorinostat (aka SAHA: Suberoylanilide hydroxamic acid), which targets HDAC2 and MMP2, are promising therapeutic agents that are in clinical cancer trials (Shankar, 2009). In the present study, the treatment of SFT cells with SAHA was corroborated by the notion that NAB2/STAT6 fusion protein, in SFTs, interacts with HDAC2 activity (Robinson et al, 2013). The NAB2/STAT6 fusion protein maintain the EGR1 (early growth response-1)-interacting domain of NAB2, which is implicated in many disease-associated processes such as

EMT (Bhattacharyya et al, 2011). NAB2, in turn, regulates the expression of EGR1 target genes by binding to NuRD complex, which consist of an enzymatic subunit of HDAC1 and HDAC2 (Lai and Wade, 2011). SAHA alone or in combination with curcumin did not affect significantly SFT cell viability, but, on the other hand, SAHA induced down-regulation of the expression of MMP2 compared with the combined treatment with curcumin, as investigated by WB analyses. As already pointed out in the investigation of EMT markers expression, even in this scenario, the use of nanomicelles has allowed to achieve better results in terms of MMP2 expression reduction. In particular, C_{16}-SPD and C_{16}-SPM are able to reduce the expression of MMP2 within 24 hours of treatment, abrogating the invasion rate of SFT cells. Moreover, C_{16}-DAPMA seems to have more effect on HDAC2 expression (after 24 hours) rather than MMP2 (after 48 hours). The low expression of MMP2, indirectly correlates with the high number of tumor cells showing an invasive behavior. C_{16}-DAPMA nanomicelles were probably most involved in HDAC2 inhibition, working synergistically with SAHA, while C_{16}-SPD and C_{16}-SPM decreased MMP2 expression, which may lead to inhibited invasive behavior, reducing metastasis formation *in vivo*.

The most interesting and unexpected effect of SAHA treatment was the change in the structure of the tumor cell. In fact, after SAHA alone or in combination treatment, SFT cells show a more epithelial-like shape, investigated by means of phalloidin immunofluorescence (IF). As reported in literature, SAHA treatment can induce morphological changes in a osteosarcoma cell line and a reduced invasiveness (Mu et al, 2015). Unfortunately, the predominant activity of nanomincelles did not allow to

appreciate the cytoskeleton variations observed in the previous experiments with SAHA and curcumin.

SAHA has been approved to treat cutaneous T cell lymphomas which have failed conventional treatments because of the favorable response rate. By contrast, trials in patients with solid tumors have produced conflicting results (Luu et al, 2008): this compound could exert both pro- and anti-apoptotic pathways. However, based on evidence that SAHA stabilizes disease and exerts partial responses in patients, SAHA remains in clinical trials and is a component of multi-drug therapies (Marks et al, 2007). Our data show that SAHA can inhibit markers of metastasis (MMP2) and SFT cell invasiveness after C_{16}-SPD and C_{16}-SPM nanomicelles combined treatments, while SAHA and C_{16}-DAPMA combination tend to increase the aggressive behavior of cancer cells. C_{16}-DAPMA effect on SFT cells is abrogated by SAHA combination: these results should be investigated more completely in future study, in order to shed light on which pathway are mainly involved using different kind of nanomicelles. In addition, it would be interesting to test the effect of SAHA on other sarcoma cell lines to find a rationale, still unknown, to explain how SAHA can induce both pro- and anti-apoptotic pathways indistinctly.

As an innovative and promising approach in oncological field, the use of photodynamic therapy (PDT) is growing in cancer therapeutics. Combination regimens consisting of PDT and a secondary treatment can be designed to increase the effectiveness of PDT, which requires simultaneously a photosensitizer that can be accumulated in the target cells. The systemic toxicity might be reduced using a lower dose of photosensitizer during combination with PDT. Taking advantage of the numerous publications that report the efficacy of curcumin as

chemopreventive agent, standard cancer therapies could be combined with this compound and PDT, exerting enhanced antitumor activity through synergistic action (Sarkar and Li, 2007). Koon and colleagues (2006) reported that cytotoxicity of curcumin was enhanced by the irradiation of blue light in nasopharyngeal cancer cell lines. The possible molecular mechanisms of phototoxicity of curcumin might be that curcumin photogenerates singlet oxygen and reduced forms of molecular oxygen (Bruzell et al, 2005). In this study it was analyzed whether curcumin can also be administrated to SFT cell line, mainly focusing on cell viability. Of great interest was that SFT cells were more sensitive to the combined curcumin and PDT treatment, which exerted a specific reduction of the proliferative potential. Treating SFT cells using curcumin doses of up to 50μM in combination with blue laser irradiation revealed a concentration dependent viability reduction, immediately after irradiation. The corresponding samples treated with curcumin alone showed no variation in cell viability. The mitochondria are a major source of ROS in cells. As reported, ROS play an important role in controlling proliferation and apoptosis (Thannickal and Fanburg, 2000). The intracellular oxidative stress caused by curcumin alone was further enhanced by the combined therapy (curcumin and PDT). These results suggest that the combined treatment with curcumin and PDT could enhance cytotoxic and apoptotic effects of curcumin on SFT cells via a mitochondria-dependent apoptosis pathway. Experiments carried out using PDT and nanomicelles loaded with curcumin combined treatment resulted in almost total cell viability abrogation 24 hours after laser irradiation. However, the most intriguing aspect, was to detect at T0 that laser irradiation had somehow stimulated SFT cells proliferation. Indeed, at T0, the lowest nanomicelles doses showed a significant increase in cell viability compared to the corresponding group treated only with nanomicelles

without laser irradiation. Probably, the very low concentrations of curcumin encapsulated by nanomicelles, not yet fully internalized by the cells, did not allow curcumin to act as a photosensitizer. Therefore, in this scenario, low nanomicelles concentration and low level laser irradiation (150mW) induced an increase in cell viability and not the opposite as expected. This contradictory result was previously reported by Huertas and colleagues in 2013, which had investigated the effect of low laser irradiation on bone cell proliferation. 24 hours after irradiation, curcumin released within the cells was able to exert its anti-proliferative function, increased by the laser itself. Nevertheless, in this context there is still a discrepancy. Indeed, the blank-nanomicelles treatment also resulted in an increase in cell viability after laser irradiation compared to the untreated control group. This may be due to the presence, in the culture medium, of the nano-structure which somehow did not allow the laser to exert its cytotoxic power. This result obtained at T0, which is conflicting with that obtained at T24, requires further investigation to determine the mechanism underlying the physical interaction between nanostructures and low laser irradiation.

The usefulness of curcumin in cancer therapy is verified by several studies on various cancer cell lines. Despite having some limitations such as water-insolubility and low adsorbsion rate, developing novel strategies based on non-toxic nanocarriers is the successful area of this field. The present study shows the importance of and usefulness in using nanomicelles loaded with curcumin which are found to influence all the investigated EMT markers and invasiveness of SFT cells. The efficacy of nanomicelles to partial inhibit EMT

and aggressive behavior is clearly established by evidence of decreasing EMT markers expression at concentrations well below those shown to be effective with curcumin alone. Furthermore, it is reported here that the combined treatment of nanomicelles with SAHA is capable of inducing a morphologically epitheliod-like shift, supporting the inhibition of EMT. Finally, the approach to combined nanomicelles and blue laser treatment has led to very promising results.

Since the proposed nanomicelles formulation shows great potential *in vitro*, further studies will be focusing on establishing the pharmacokinetic profile and the cytotoxic effect of nanomicelles *in vivo*, in animal models. Additionally, the specificity of nanomicelles will be study in depth to better understand how to minimize their any toxic and side effects in normal tissues. Moreover, nanomicelles combined with laser could depict an alternative option to standard chemotherapy treatments for tumor masses that can be reached by laser irradiation, resulting in an improvement for patients, with a faster recovery and less side effects.

6. References

Allison RR, Moghissi K. Oncologic photodynamic therapy: clinical strategies that modulate mechanisms of action. Photodiagn.Photodyn.Ther.2013,10, 331-341.

Anand P, Kunnumakkara AB, Newman RA, Aggarwal BB. Bioavailability of curcumin: problems and promises. Mol Pharm. 2007 Nov-Dec;4(6):807-18.

Bhattacharyya S, Wu M, Fang F, Tourtellotte W, Feghali-Bostwick C, Varga J. Early growth response transcription factors: key mediators of fibrosis and novel targets for anti-fibrotic therapy. Matrix Biol. 2011 May;30(4):235-42.

Berezovska OP, Glinskii AB, Yang Z, Li XM, Hoffman RM, Glinsky GV. Essential role for activation of the Polycomb group (PcG) protein chromatin silencing pathway in metastatic prostate cancer. CellCycle. 2006 Aug;5(16):1886-901.

Bernd A. Visible light and/or UVA offer a strong amplification of the anti-tumor effect of curcumin. Phytochem Rev. 2014;13:183-189. Epub 2013 May 7.

Bisht S, Feldmann G, Soni S, Ravi R, Karikar C, Maitra A, Maitra A. Polymeric nanoparticle-encapsulated curcumin ("nanocurcumin"): a novel strategy for human cancer therapy. J Nanobiotechnology. 2007 Apr 17;5:3.

Sayantan B, Abir Kumar P, Shravanti M, and Gaurisankar S. Curcumin and tumor immune-editing: resurrecting the immune system Cell Div. 2015; 10: 6.Published online 2015 Oct 12.

Bruzell EM, Morisbak E and Tonnesen HH: Studies on curcumin and curcuminoids. XXIX. Photoinduced cytotoxicity of curcumin in selected aqueous preparations. Photochem Photobiol Sci 4: 523-530, 2005.

Buhrmann C, Kraehe P, Lueders C, Shayan P, Goel A, Shakibaei M. Curcumin suppresses crosstalk between colon cancer stem cells and stromal fibroblasts in the tumor microenvironment: potential role of EMT. PLoS One. 2014 Sep 19;9(9):e107514.

Chmielecki J, Crago AM, Rosenberg M et al. Whole-exome sequencing identifies a recurrent NAB2-STAT6 fusion in solitary fibrous tumors. Nat Genet. 2013;45:131–132.

Collini P, Negri T, Barisella M, Palassini E, Tarantino E, Pastorino U, Gronchi A, Stacchiotti S, Pilotti S. High- grade sarcomatous overgrowth in solitary brous tumors: a clinicopathologic study of 10 cases. Am J Surg Pathol. 2012; 36:1202–15.

Condeelis J, Segall JE. Intravital imaging of cell movement in tumours. Nat Rev Cancer. 2003 Dec;3(12):921-30.

Dahl TA, Bilski P, Reszka KJ, Chignell CF. Photocytotoxicity of curcumin. Photochem Photobiol. 1994 Mar;59(3):290-4.

Davis CD, Ross SA. Dietary components impact histone modifications and cancer risk. Nutr Rev. 2007 Feb;65(2):88-94.

Dean M, Fojo T, Bates S. Tumour stem cells and drug resistance. Nat Rev Cancer. 2005 Apr;5(4):275-84.

Demontis S, Rigo C, Piccinin S, Mizzau M, Sonego M, Fabris M, Brancolini, Maestro R. Twist is substrate for caspase cleavage and proteasome-mediated degradation. Cell Death and Differentiation (2006) 13, 335–345.

Duan W, Chang Y, Li R, Xu Q, Lei J, Yin C, Li T, Wu Y, Ma Q, Li X. Curcumin inhibits hypoxia inducible factor−1α−induced epithelial−mesenchymal transition in HepG2 hepatocellular carcinoma cells. Mol Med Rep. 2014 Nov;10(5):2505-10.

Esquela-Kerscher A, Slack FJ. Oncomirs - microRNAs with a role in cancer. Nat Rev Cancer. 2006 Apr;6(4):259-69.

Fletcher CDM, Bridge JA, Lee JC. Extrapleural solitary brous tumor. In WHO Classi cation of Tumors of Soft Tissue and Bone, (4th edn), IARC Press: Lyon, 2013; 80–82.

Friedl P, Wolf K. Plasticity of cell migration: a multiscale tuning model. J Cell Biol. 2010 Jan 11;188(1):11-9.

Gupta PB, Chaffer CL, Weinberg RA. Cancer stem cells: mirage or reality? Nat Med. 2009 Sep;15(9):1010-2.

Gupta SC, Prasad S, Kim JH, et al. Multitargeting by curcumin as revealed by molecular interaction studies. Nat Prod Rep. 2011;28(12):1937–1955.

Hanahan D, Weinberg RA. The hallmarks of cancer. Cell. 2000 Jan 7;100(1):57-70.

Hanahan D, Weinberg RA. Hallmarks of cancer: the next generation. Cell. 2011 Mar 4;144(5):646-74.

Hood JD, Cheresh DA. Role of integrins in cell invasion and migration. Nat Rev Cancer. 2002 Feb;2(2):91-100.

Harrison-Phipps KM, Nichols FC, Schleck CD, Deschamps C, Cassivi SD, Schipper PH, Allen MS, Wigle DA, Pairolero PC: Solitary fibrous tumors of the pleura: results of surgical treatment and long-term prognosis. J Thorac Cardiovasc Surg 2009, 138(1):19–25.

Hua WF, Fu YS, Liao YJ, Xia WJ, Chen YC, Zeng YX, Kung HF, Xie D. Curcumin induces down-regulation of EZH2 expression through the MAPK pathway in MDA-MB-435 human breast cancer cells. Eur J Pharmacol. 2010 Jul 10;637(1-3):16-21.

Huang T, Chen Z, Fang L. Curcumin inhibits LPS-induced EMT through downregulation of NF-κB-Snail signaling in breast cancer cells. Oncol Rep. 2013 Jan;29(1):117-24.

Huertas RM, De Luna-Bertos E, Ramos-Torrecillas J, Leyva FM, Ruiz C, García-Martínez O. Effect and Clinical Implications of the Low-Energy Diode Laser on Bone Cell Proliferation. Biol Res Nurs. 2013;16(2):191–6.

Jo VY, Fletcher CD. WHO classification of soft tissue tumours: an update based on the 2013 (4th) edition. Pathology. 2014 Feb;46(2):95-104.

Kalluri R, Weinberg RA. The basics of epithelial-mesenchymal transition. J Clin Invest. 2009 Jun;119(6):1420-8.

Kanai M, Otsuka Y, Otsuka K, Sato M, Nishimura T, Mori Y, Kawaguchi M, Hatano E, Kodama Y, Matsumoto S, Murakami Y, Imaizumi A, Chiba T, Nishihira J, Shibata H. A phase I study investigating the safety and pharmacokinetics of highly bioavailable curcumin (Theracurmin) in cancer patients. Cancer Chemother Pharmacol. 2013 Jun;71(6):1521-30.

Kang Y, Chen CR, Massagué J. A self-enabling TGFbeta response coupled to stress signaling: Smad engages stress response factor ATF3 for Id1 repression in epithelial cells. Mol Cell. 2003 Apr;11(4):915-26.

Khan S, Khan SN, Meena R, Dar AM, Pal R, Khan AU. Photoinactivation of multidrug resistant bacteria by monomeric methylene blue conjugated gold nanoparticles. J Photochem Photobiol B. 2017 Sep;174:150-161.

Kessel D1, Oleinick NL. Initiation of autophagy by photodynamic therapy. Methods Enzymol. 2009;453:1-16.

Kim KH, Roberts CWM. Targeting EZH2 in cancer. Nature Medicine 22, 128–134 , 2016.

Koon H, Leung AW, Yue KK and Mak NK: Photodynamic Effect of curcumin on NPC/CNE2 cells. J Environ Pathol Toxicol Oncol 25: 205-216, 2006.

Korpal M, Lee ES, Hu G, Kang Y. The miR-200 family inhibits epithelial-mesenchymal transition and cancer cell migration by direct targeting of E-cadherin transcriptional repressors ZEB1 and ZEB2. J Biol Chem. 2008 May 30;283(22):14910-4.

Kuttan R, Sudheeran PC, Josph CD. Turmeric and curcumin as topical agents in cancer therapy. Tumori. 1987 Feb 28;73(1):29-31.

Lai AY, Wade PA. Cancer biology and NuRD: a multifaceted chromatin remodelling complex. Nat Rev Cancer. 2011 Jul 7;11(8):588-96.

Samy Lamouille,1 Jian Xu,2 and Rik Derynck1Nat Rev Mol Cell Biol. 2014 Mar; 15(3): 178–196. Molecular mechanisms of epithelial–mesenchymal transition

Le MT, Teh C, Shyh-Chang N, Xie H, Zhou B, Korzh V, Lodish HF, Lim B. MicroRNA-125b is a novel negative regulator of p53. Genes Dev. 2009 Apr 1;23(7): 862-76.

Lee AY, Fan CC, Chen YA, Cheng CW, Sung YJ, Hsu CP, Kao TY. Curcumin Inhibits Invasiveness and Epithelial-Mesenchymal Transition in Oral Squamous Cell Carcinoma Through Reducing Matrix Metalloproteinase 2, 9 and Modulating p53-E-Cadherin Pathway. Integr Cancer Ther. 2015 Sep;14(5):484-90.

Li Y, Kong D, Wang Z, Sarkar FH. Regulation of microRNAs by natural agents: an emerging field in chemoprevention and chemotherapy research. Pharm Res. 2010 Jun;27(6):1027-41. doi: 10.1007/s11095-010-0105-y.

Luu TH, Morgan RJ, Leong L, et al. A phase II trial of vorinostat (suberoylanilide hydroxamic acid) in metastatic breast cancer: a California Cancer Consortium study. Clin Cancer Res. 2008;14:7138–42.

Magdeleinat P, Alifano M, Petino A, Le Rochais JP, Dulmet E, Galateau F, Icard P, Regnard JF: Solitary fibrous tumors of the pleura: clinical characteristics, surgical treatment, and outcome. Eur J Cardiothorac Surg 2002, 21(6):1087–1093.

Makishima H, Jankowska AM, Tiu RV, Szpurka H, Sugimoto Y, Hu Z, Sauntharajah Y, Guinta K, Keddache MA, Putnam P, Sekeres MA, Moliterno AR, List AF, McDevitt MA, Maciejewski JP. Novel homo- and hemizygous mutations in EZH2 in myeloid malignancies. Leukemia. 2010 Oct;24(10):1799-804.

Marks PA, Breslow R. Dimethyl sulfoxide to vorinostat: development of this histone deacetylase inhibitor as an anticancer drug. Nat Biotechnol. 2007;25:84–90.

Matsumura Y, Maeda H. A new concept for macromolecular therapeutics in cancer chemotherapy: mechanism of tumoritropic accumulation of proteins and the antitumor agent smancs. Cancer Res. 1986 Dec;46(12 Pt 1):6387-92.

Medina-Franco JL, López-Vallejo F, Kuck D, Lyko F. Natural products as DNA methyltransferase inhibitors: a computer-aided discovery approach. Mol Divers. 2011 May;15(2):293-304. doi: 10.1007/s11030-010-9262-5.

Meja KK, Rajendrasozhan S, Adenuga D, Biswas SK, Sundar IK, Spooner G, Marwick JA, Chakravarty P, Fletcher D, Whittaker P, Megson IL, Kirkham PA, Rahman I. Curcumin restores corticosteroid function in monocytes exposed to oxidants by maintaining HDAC2. Am J Respir Cell Mol Biol. 2008 Sep;39(3):312-23.

Mohajeri A, Tayebwa J, Collin A et al. Comprehensive genetic analysis identifies a pathognomonic NAB2/STAT6 fusion gene, nonrandom secondary genomic imbalances, and a characteristic gene expression profile in solitary fibrous tumor. Genes Chromosomes Cancer 2013;52:873–886.

Mroz P, Hashmi JT, Huang YY, Lange N, Hamblin MR. Stimulation of anti-tumor immunity by photodynamic therapy. Expert Rev Clin Immunol. 2011 Jan;7(1):75-91. doi: 10.1586/eci.10.81.

Mosquera JM, Fletcher CD. Expanding the spectrum of malignant progression in solitary fibrous tumors: a study of 8 cases with a discrete anaplastic component – is this dedifferentiated SFT? Am J Surg Pathol. 2009; 33:1314–21.

Mudduluru G, George-William JN, Muppala S, Asangani IA, Kumarswamy R, Nelson LD, Allgayer H. Curcumin regulates miR-21 expression and inhibits invasion and metastasis in colorectal cancer. Biosci Rep. 2011 Jun;31(3):185-97.

Nakada S, Minato H, Takegami T, Kurose N, Ikeda H, Kobayashi M, Sasagawa Y, Akai T, Kato T, Yamamoto N, Nojima T. NAB2-STAT6 fusion gene analysis in two cases of meningeal solitary fibrous tumor/hemangiopericytoma with late distant metastases. Brain Tumor Pathol. 2015 Oct;32(4):268-74.

Peinado H1, Ballestar E, Esteller M, Cano A. Snail mediates E-cadherin repression by the recruitment of the Sin3A/histone deacetylase 1 (HDAC1)/HDAC2 complex. Mol Cell Biol. 2004 Jan;24(1):306-19.

Prasad S, Tyagi AK, Aggarwal BB. Recent developments in delivery, bioavailability, absorption and metabolism of curcumin: the golden pigment from golden spice. Cancer Res Treat. 2014 Jan;46(1):2-18.

Raab O. Z. Biol. 1900;39:524–546.

Ramasamy TS, Ayob AZ, Myint HH, Thiagarajah S, Amini F. Targeting colorectal cancer stem cells using curcumin and curcumin analogues: insights into the mechanism of the therapeutic efficacy. Cancer Cell Int. 2015 Oct 9;15:96.

Rhodes DR, Sanda MG, Otte AP, Chinnaiyan AM, Rubin MA. Multiplex biomarker approach for determining risk of prostate-specific antigen-defined recurrence of prostate cancer. J Natl Cancer Inst. 2003 May 7;95(9):661-8.

Robinson DR1, Wu YM, Kalyana-Sundaram S, Cao X, Lonigro RJ, Sung YS, Chen CL, Zhang L, Wang R, Su F, Iyer MK, Roychowdhury S, Siddiqui J, Pienta KJ, Kunju LP, Talpaz M, Mosquera JM, Singer S, Schuetze SM, Antonescu CR, Chinnaiyan AM. Identification of recurrent NAB2-STAT6 gene fusions in solitary fibrous tumor by integrative sequencing. Nat Genet. 2013 Feb;45(2):180-5.

Sak K. Chemotherapy and dietary phytochemical agents. Chemother Res Pract. 2012;2012:282570.

Sarkar FH and Li YW: Targeting multiple signal pathways by chemopreventive agents for cancer prevention and therapy. Acta Pharmacol Sin 28: 1305-1315, 2007.

Schneider C, Gordon ON, Edwards RL, Luis PB. Degradation of Curcumin: From Mechanism to Biological Implications. J Agric Food Chem. 2015 Sep 9;63(35): 7606-14.

Semenza GL. HIF-1: upstream and downstream of cancer metabolism. Curr Opin Genet Dev. 2010 Feb;20(1):51-6.

Semenza GL. Tumor metabolism: cancer cells give and take lactate. J Clin Invest. 2008 Dec;118(12):3835-7.

Shankar S, Davis R, Singh KP, Kurzrock R, Ross DD, Srivastava RK. Suberoylanilide hydroxamic acid (Zolinza/vorinostat) sensitizes TRAIL-resistant breast cancer cells orthotopically implanted in BALB/c nude mice. Mol Cancer Ther. 2009 Jun;8(6): 1596-605.

Szaciłowski K, Macyk W, Drzewiecka-Matuszek A, Brindell M, Stochel G. Bioinorganic photochemistry: frontiers and mechanisms. Chem Rev. 2005 Jun; 105(6):2647-94.

Thiery JP, Morgan M. Breast cancer progression with a Twist. Nat Med. 2004 Aug; 10(8):777-8.

Thomas DA, Massagué J. TGF-beta directly targets cytotoxic T cell functions during tumor evasion of immune surveillance. Cancer Cell. 2005 Nov;8(5):369-80.

Vesuna F, Lisok A, Kimble B, Raman V. Twist modulates breast cancer stem cells by transcriptional regulation of CD24 expression. Neoplasia. 2009 Dec;11(12): 1318-28.

Wahlström B, Blennow G. A study on the fate of curcumin in the rat. Acta Pharmacol Toxicol. 1978 Aug;43(2):86-92.

Wang Q, Qu C, Xie F, Chen L, Liu L, Liang X, Wu X, Wang P, Meng Z. Curcumin suppresses epithelial-to-mesenchymal transition and metastasis of pancreatic cancer cells by inhibiting cancer-associated fibroblasts. Am J Cancer Res. 2017 Jan 1;7(1):125-133.

Serri C, Argirò M, Piras L, Mita DG, Saija A, Mita L, Forte M, Giarra S, Biondi M, Crispi S, Mayol L. Nano-precipitated curcumin loaded particles: effect of carrier size and drug complexation with (2-hydroxypropyl)-β-cyclodextrin on their biological performances. Int J Pharm. 2017 Mar 30;520(1-2):21-28.

Shengpeng Wang, Miao Tan, Zhangfeng Zhong, Meiwan Chen, and Yitao Wang. Nanotechnologies for Curcumin: An Ancient Puzzler Meets Modern Solutions. Journal of Nanomaterials Volume 2011 (2011), Article ID 723178, 8 pages

Spagnuolo RD, Brich S, Bozzi F, Conca E, Castelli C, Tazzari M, Maestro R, Brenca M, Gualeni AV, Gloghini A, Stacchiotti S, Pierotti MA, Pilotti S, Negri T. Sunitinib-induced morpho-functional changes and drug effectiveness in malignant solitary fibrous tumours. Oncotarget. 2016 Jul 19;7(29):45015-45026.

Stacchiotti S, Negri T, Libertini M, Palassini E, Marrari A, De Troia B, Gronchi A, Dei Tos AP, Morosi C, Messina A, Pilotti S, Casali PG. Sunitinib in solitary fibrous tumor. Ann Oncol. 2012;23:3171–9.

Stacchiotti S, Libertini M, Negri T, Palassini E, Gronchi A, Fatigoni S, Poletti P, Vincenzi B, Dei Tos AP, Mariani L, Pilotti S, Casali PG: Response to chemotherapy of solitary fibrous tumour: A restrospective study. Eur J Cancer 2013 April 5, pii:S0959-8049(13):00220-00227.

Spikes JD. The historical development of ideas on applications of photosensitized reactions in the health science. In Primary photo-process in biology and Medicine; Bensasson RV, Jori G, Land EJ, Truscott TG Eds; Springer: Boston, MA, USA, 1985; pp209-227.

Tang M, Larson-Meyer DE, Liebman M. Effect of cinnamon and turmeric on urinary oxalate excretion, plasma lipids, and plasma glucosein healthy subjects. Am J Clin Nutr. 2008 May;87(5):1262-7.

Thannickal VJ and Fanburg BL: Reactive oxygen species in cell signaling. Am J Physiol Lung Cell Mol Physiol 279: L1005-L1028, 2000.

Wei T , Chen C, Liu J, Liu C, Posocco P, Liu X, Cheng Q, Huo S, Liang Z, Fermeglia M, Pricl S, Liang XJ, Rocchi P, Peng L. Anticancer drug nanomicelles formed by self-assembling amphiphilic dendrimer to combat cancer drug resistance. Proc Natl Acad Sci U S A. 2015 Mar 10;112(10):2978-83.

Wellner U, Schubert J, Burk UC, Schmalhofer O, Zhu F, Sonntag A, Waldvogel B, Vannier C, Darling D, zur Hausen A, Brunton VG, Morton J, Sansom O, Schüler J, Stemmler MP, Herzberger C, Hopt U, Keck T, Brabletz S, Brabletz T. The EMT-activator ZEB1 promotes tumorigenicity by repressing stemness-inhibiting microRNAs. Nat Cell Biol. 2009 Dec;11(12):1487-95.

Mu X, Brynien D, Weiss KR. The HDAC inhibitor Vorinostat diminishes the in vitro metastatic behavior of Osteosarcoma cells. Biomed Res Int. 2015;2015:290368.

Yallapu MM, Jaggi M, Chauhan SC. Curcumin nanoformulations: a future nanomedicine for cancer. Drug Discov Today. 2012 Jan;17(1-2):71-80.

Yallapu (A) MM, Othman SF, Curtis ET, Bauer NA, Chauhan N, Kumar D, Jaggi M, Chauhan SC. Curcumin-loaded magnetic nanoparticles for breast cancer therapeutics and imaging applications. Int J Nanomedicine. 2012;7:1761-79.

Yamaguchi H, Hung MC. Regulation and Role of EZH2 in Cancer. Cancer Res Treat. 2014 Jul;46(3):209-22.

Yang KY, Lin LC, Tseng TY, Wang SC, Tsai TH. Oral bioavailability of curcumin in rat and the herbal analysis from Curcuma longa by LC-MS/MS. J Chromatogr B Analyt Technol Biomed Life Sci. 2007 Jun 15;853(1-2):183-9.

Yang X, Pursell B, Lu S, Chang TK, Mercurio AM. Regulation of beta 4-integrin expression by epigenetic modifications in the mammary gland and during the epithelial-to-mesenchymal transition. J Cell Sci. 2009 Jul 15;122(Pt 14):2473-80.

Yin JJ, Liu J, Ehrenshaft M, Roberts JE, Fu PP, Mason RP, et al. Phototoxicity of nano titanium dioxides in HaCaT keratinocytes--generation of reactive oxygen species and cell damage. Toxicol Appl Pharmacol. 2012; 263: 81-8.

Yoo CB, Jones PA. Epigenetic therapy of cancer: past, present and future. Nat Rev Drug Discov. 2006 Jan;5(1):37-50. Review. Erratum in: Nat Rev Drug Discov. 2006 Feb;5(2):121.

Zhang S, Schafer-Hales K, Khuri FR, Zhou W, Vertino PM, Marcus AI. The tumor suppressor LKB1 regulates lung cancer cell polarity by mediating cdc42 recruitment and activity. Cancer Res. 2008 Feb 1;68(3):740-8

Acknowledgements

First and foremost I want to thank my chief, Dr. Silvana Pilotti. It has been an honor to be her first Ph.D. student. She has taught me, both consciously and unconsciously, how translational research would be done. I appreciate all her contributions of time, ideas, and funding (:-) to make my Ph.D. experience productive and stimulating. The joy and enthusiasm she has for her research was contagious and motivational for me, even during tough times in the Ph.D. pursuit. I am also thankful for the excellent example she has provided as a successful woman in a "men's world".

The members of Laboratory of Molecular Pathology group have contributed immensely to my personal and professional time at Istituto Nazionale Tumori in Milan. The group has been a source of friendships as well as good advice and collaboration. I am especially grateful for the fun group of LPMS members, who have tolerate me every day, especially in those days of madness: Antonio and Nicholandia, thank you! The thing that made me go crazy was the locked PC in the most disadvantaged moments. Then, I started screaming: 'Antonioooooooooo! Nicholaaaas! Help meeee!' They hate me, I know it!

I would like to acknowledge honorary group member Luca Varisniaus, who was here as 'infiltrated' and with the other two men he spent his time joking on me: it was very funny at all!

Furthermore, I have to thank my tutor, Dott.ssa Elena Tamborini, who helped me during my Ph.D. project (till the end!). Thank you for all!

I am also grateful to Adalberto's group which gave me a very huge help in nanomicelles encapsulation. I could not do any experiment without their help: essential! They have always found time to carry on my experiments with their one, for all the three days of curcumin-nanomicelles preparation.

The time spent to get the Ph.D. was definitely less heavy and stressful thanks to the presence of a classmate that over time became a trusted friend: thanks to Katia for the support! Everything started during the first winterschool, when I asked her for the Units WIFI password. Fate had made me meet another "biologist" like me, with the same idea of translational research! At least, we shared good-times together during the carbon nanotubes presentations! Thank you for having made me fall in love with Trieste, the city where I feel at home! I would also like to thank her cats (Otto in particular) who have hosted me without assaulting me during night!;-P. Moreover, I am particularly in debt with Katia. She proposed me to work together on PDT experiments, combining my nanomicelles with her laser to defeat cancer and the terrible bacteria!

I must thank ICGEB institute for the hospitality and in particular Dr. Serena Zacchigna, thanks to whom I have been able to carry out PDT experiments. I have obtained very interesting results which have enriched my Ph.D. thesis.

I must thank my "non-biologist" friends that always joked with me on curcumin! Alessandro: thank you for have tolerated me when I was angry, mad, demoralized and when I stuffed you with information about curcumin; you know you're such a brother to me and you're doing very well! Lorenzo "the neuroscientist": I have adored our scientifically relevant talks; thank you for correcting my thesis, but above all, for all the Swiss chocolate you provided me to overcome all stressful situations! Francesca (+Shevuzland) and Simone: I want to thank you for constant moral support and friendship. Be invited to dinner and find a jar of curcumin as your placeholder is not for everyone! Moreover, receiving messages whenever an article of curcumin came out, or when a curcumin dish was cooked was very funny!! Curcumin is the future! Friends, you are great!

Lastly, I would like to thank my family for all their love and encouragement. For my parents who raised me with a love of science and supported me in all my pursuits (Mummy and Dad I promise you: this is my last degree! no more graduation gifts will be required!!)

Thank you!